



HAL
open science

Evaluation of plug-in hybrid vehicles in realworld conditions

Philippe Degeilh, Vivien Prevost, Joseph Kermani, Roland Dauphin

► **To cite this version:**

Philippe Degeilh, Vivien Prevost, Joseph Kermani, Roland Dauphin. Evaluation of plug-in hybrid vehicles in realworld conditions. 10/22, Concawe. 2022. hal-03901013

HAL Id: hal-03901013

<https://ifp.hal.science/hal-03901013>

Submitted on 15 Dec 2022

HAL is a multi-disciplinary open access archive for the deposit and dissemination of scientific research documents, whether they are published or not. The documents may come from teaching and research institutions in France or abroad, or from public or private research centers.

L'archive ouverte pluridisciplinaire **HAL**, est destinée au dépôt et à la diffusion de documents scientifiques de niveau recherche, publiés ou non, émanant des établissements d'enseignement et de recherche français ou étrangers, des laboratoires publics ou privés.

Copyright

Report

Report no. 10/22

Evaluation of plug-in hybrid vehicles in real- world conditions



Evaluation of plug-in hybrid vehicles in real-world conditions

This report was prepared by:

Philippe Degeilh, Vivien Prevost, Joseph Kermani (IFP Energies nouvelles)

Under the supervision of Roland Dauphin (Concawe Science Executive)

Fuels@concawe.eu

At the request of:

- Concawe Fuels and Emissions Management Group (FEMG)
- Refining into the Energy Transition Management Group (RETMG)
- Special Task Force on Fuels for Gasoline Engines (FE/STF-20)
- Special Task Force on Fuels for Diesel Engines (FE/STF-25)

We thank for their contribution:

- Members of FE/STF-20
- Members of FE/STF-25
- Members of FEMG
- Members of RETMG
- Members of the secretariat

Reproduction permitted with due acknowledgement

ABSTRACT

Assessing the real-world energetic performance and emissions of Plug-in Hybrid Vehicles (PHEVs) is complex. First, because of the complexity of the powertrain itself, pairing thermal and electric propulsion. Second, because their evaluation results are extremely sensitive to their usage while driving (e.g. trip distance) and before driving (e.g. recharging behaviour). In this context, the present study aims at delivering energy consumptions and GHG emissions data of the PHEVs in real-world conditions and as a function of their use cases.

The study is based on an extensive experimental campaign. Two Euro 6d PHEVs were selected to allow a back-to-back comparison between petrol and diesel internal combustion engines. The first purpose of the test campaign is to evaluate and compare the energy consumptions (in terms of electricity and fuel), the CO₂ and pollutant emissions of different vehicle configurations: charged PHEVs vs non-charged PHEV; non-charged PHEV vs non-plug-in hybrid electric vehicles (HEV); Diesel vs gasoline; traditional fossil-based fuels vs renewable fuels, etc. These vehicles were tested in a first step on a chassis dynamometer to accurately control and reproduce experimental conditions allowing the different configurations to be compared and to allow the implementation of advanced measurement systems (engine-out and tailpipe emissions of both regulated and non-regulated pollutants, energy consumptions, AdBlue consumption). In a second step, the vehicles were tested on-road to allow a comparison of the measurements made in the laboratory and assess their representativeness. All the driving cycles performed, either in lab or on-road, were RDE-compliant. Both PHEVs tested show low regulated emissions (well below Euro 6d limits) and unregulated pollutant emissions in the range of Euro 7 proposals¹. Compared to the gasoline PHEV, in charge sustaining (CS) mode, the Diesel PHEV shows a 20.5% reduction in tank-to-wheels (TtW) greenhouse gases (GHG) emission, and a reduction of regulated pollutant emissions. On the gasoline PHEV under the operating conditions tested in this program, switching from a standard E10 fuel (mostly fossil-based) to a 100% renewable gasoline blended with 20% v/v of ethanol (E20) fuel has no significant impact on the pollutant tailpipe emissions, or on the TtW CO₂ emissions. However, it implies a higher volumetric fuel consumption (+4.5%), linked to the higher oxygen content in E20 (hence the lower energy density). For the Diesel PHEV under the operating conditions tested in this program, switching from a standard B7 fuel (mostly fossil-based) to a 100% renewable HVO fuel also has no significant impact on the pollutant tailpipe emissions. In charge sustaining mode, it decreases by 2% the TtW CO₂ emissions, and increases by +8,4% the volumetric fuel consumption, due to the fuels physico-chemical properties (resp. CO₂ emission factor and energy density).

These experimental measurements allowed the calibration of energy simulation models of both vehicles, using Simcenter Amesim™ software and its IFP-Drive library. The simulator was calibrated to fit roller test bench results, real road measurements, and climatic cell data. For the latter, elementary thermal models of Heating, Ventilation and Air Conditioning (HVAC) and battery conditioning were added to the vehicle simulator to fit with overconsumption and electrical range decrease due to cold or warm ambient conditions. Regarding the other powertrain components, their parametrization relied on a dedicated tool that generates efficiency maps based on engine/motor/battery general description. Special attention was paid to the on-line hybrid control strategy, so that the simulated vehicle behavior remains accurate for various types of driving, including the harshest ones, while still fitting with both electric and fuel consumptions. As this simulator modelled properly the available experimental data, a comprehensive

¹ According to CLOVE proposal made at the AGVES meeting. The measured emissions are regularly below the proposed limits, and sometimes above.

range of real-world uses was forecasted over a wide Design of Experiments (DoE). This DoE spans vehicle configurations, battery capacity, outside temperature, and driving profiles extracted from IFPEN's clustered trips database. The huge amount of results was then synthesized through an analytical method, since it would be too heavy to re-simulate and generalize day to day patterns.

Finally, a mathematical method of weighting each of the simulated use-cases according to their representativeness of real use was proposed, based on usage statistics in terms of daily distance travelled and temperature. The study is carried out for a wide range of battery sizing and recharging frequency, thus making it possible to determine the weighted average energetic performance and emissions of PHEVs according to these two key parameters, determined respectively by the original equipment manufacturers (OEMs) and the end user. Considering the technology sensitivity to real use conditions and considering the statistical conditions of use in Europe (temperature and daily mileage), this approach allows to quantify the weighted average energetic performance (share of electric drive, fuel and electricity consumption) and TtW CO₂ emissions of PHEVs depending on their battery sizing and recharging frequency. It shows that frequent recharging of PHEVs is a necessary condition for a high electric drive rate: **recharging every day a gasoline PHEV having a battery of 15 kWh leads to an average fuel consumption of 2.25 L/100km and a share of electric drive (utility factor, UF) of 77 %, whilst recharging it every 3 days leads to a fuel consumption of 4.85 L/100km (+116 %) and a UF of 48 % (-29 points)**. By comparison, the non-rechargeable gasoline HEV with a 2kWh battery evaluated under the same conditions shows an average fuel consumption of 7.3 L/100km and a UF of 24%. **Compared to this reference HEV, the gasoline 15kWh PHEV vehicle allows a consumption reduction of 69% if it is recharged every day and a reduction of 34% if it is recharged every three days**. Furthermore, it is observed that **the first kilowatt-hours of battery capacity are the most effective in electrifying the PHEVs**: for instance, adding another 15 kWh of battery capacity to the vehicle, leading to a 30 kWh PHEV, would increase by only 10 points the utility factor, from 77 % to 87 %, if recharged every day; instead, the same 15 kWh battery capacity could have electrified 77% of the mileage of another PHEV, which is more efficient if the total amount of available batteries is constrained².

The assessment of life cycle GHG emissions of PHEVs, adding the vehicle production emissions and the Well-To-Tank (WtT) emissions of energy carriers are not covered in this report, and will be addressed in a further study.

² Ehsan Shafiei, Roland Dauphin, Marta Yugo, Optimal electrification level of passenger cars in Europe in a battery-constrained future, Transportation Research Part D: Transport and Environment, Volume 102, 2022, 103132, ISSN 1361-9209, <https://doi.org/10.1016/j.trd.2021.103132>

KEYWORDS

Plug-in Electric Vehicle, Utility Factor, CO₂ emissions, Pollutant emissions, Fuel consumption, Electricity consumption, Renewable fuels, Chassis-dyno tests, on-road tests, Simulation, Use cases

INTERNET

This report is available as an Adobe pdf file on the Concawe website (www.concawe.org).

NOTE

Considerable efforts have been made to assure the accuracy and reliability of the information contained in this publication. However, neither Concawe nor any company participating in Concawe can accept liability for any loss, damage or injury whatsoever resulting from the use of this information.

This report does not necessarily represent the views of any company participating in Concawe.

CONTENTS		Page
1.	INTRODUCTION	1
1.1.	CONTEXT AND MOTIVATION	1
1.2.	OBJECTIVES	3
1.3.	STRUCTURE OF THE STUDY AND OF THE REPORT	3
2.	EXPERIMENTAL CAMPAIGN	4
2.1.	OBJECTIVES OF THE PROTOCOL	4
2.2.	SELECTED VEHICLES AND MAIN SPECIFICATIONS	4
2.3.	SELECTED FUELS AND MAIN SPECIFICATIONS	5
2.4.	EXPERIMENTAL CAMPAIGN IN LABORATORY (CHASSIS DYNO)	6
2.4.1.	Vehicle instrumentation and measurement systems	6
2.4.2.	RDE test cycle reproduced on chassis dyno	9
2.4.3.	Road load	12
2.4.4.	Tests operated on laboratory	13
2.4.5.	Results of laboratory test campaign	15
2.4.5.1.	Volumetric Fuel Consumption	15
2.4.5.2.	Electrical Consumption and Utility Factor	17
2.4.5.3.	Carbon Dioxide emissions	20
2.4.5.4.	Total GHG emissions, including CH ₄ and N ₂ O emissions (Engine-out and Tailpipe Emissions)	21
2.4.5.5.	Oxides of Nitrogen (NO _x) engine-out and tailpipe emissions	25
2.4.5.6.	Particulate Mass and Particle Number engine-out and tailpipe emissions	26
2.4.5.7.	Carbon Monoxide engine-out and tailpipe emissions	32
2.4.5.8.	Hydrocarbons engine-out and tailpipe emissions	34
2.4.5.9.	Ammonia (Engine-out and Tailpipe Emissions)	36
2.5.	EXPERIMENTAL CAMPAIGN ON-ROAD	39
2.5.1.	Vehicle instrumentation and measurement systems	39
2.5.2.	RDE cycle on-road	40
2.5.3.	Tests operated on-road	41
2.5.4.	Results of on-road test campaign	42
2.5.4.1.	Carbon Dioxide emissions	42
2.5.4.2.	Volumetric Fuel Consumption	43
2.5.4.3.	Electrical Consumption and Utility Factor	44
2.5.4.4.	Oxides of Nitrogen (NO _x) emissions	46
2.5.4.5.	Particle Number emissions	47
2.5.4.6.	Carbon Monoxide emissions	48
2.6.	EXPERIMENTAL SUMMARY	49
3.	SIMULATION WORK	53
3.1.	SIMULATION PLATFORM SET UP	54
3.1.1.	Simulation platform description	54
3.1.2.	Components calibration	55
3.1.2.1.	Road laws	55
3.1.2.2.	Transmission	56
3.1.2.3.	Engines	56
3.1.2.4.	Electric Motor	58
3.1.2.5.	Battery	59
3.1.2.6.	Outside temperature effect auxiliaries	61
3.1.3.	Powertrain energy management laws	64
3.1.3.1.	Online hybrid strategy	64
3.1.3.2.	Driving conditions adaptation	65
3.1.4.	Simulator validation	68
3.1.4.1.	Detailed energy consumptions balances	68
3.1.4.2.	Road law selection	71

3.2.	PROJECTION OVER COMPREHENSIVE RANGE OF CASES	72
3.2.1.	Simulations Design of Experiment	72
3.2.1.1.	IFPEN's Clustered cycles projection base	72
3.2.1.2.	PHEV depletion modes	74
3.2.1.3.	Vehicles configurations	76
3.2.1.4.	DoE overview	76
3.2.2.	Analytical model rendering	76
3.2.2.1.	Results linearization principle	77
3.2.2.2.	Temperature deviations assessment	79
3.2.2.3.	Coefficients results	80
3.2.2.4.	Mathematical Implementation	81
3.2.2.5.	Mathematical model validation with physical simulation	84
3.3.	SUMMARY OVER GENERALIZED USAGE	85
3.3.1.	Capturing the sensitivity of technologies: Assessment of results on a large matrix	85
3.3.2.	Statistics of use: Representativeness of each use case	86
3.3.3.	Weighted average outputs	90
3.3.4.	Sensitivity to ambient temperature and daily mileage distributions	92
3.3.5.	Discussion of results	95
4.	CONCLUSION AND OUTLOOK	99
5.	GLOSSARY	101
6.	APPENDIX - DETAILED FUEL PROPERTIES	103
6.1.	B7	103
6.2.	E10	105
6.3.	100% RENEWABLE PARAFFINIC DIESEL	107
6.4.	100% RENEWABLE E20	109
7.	APPENDIX - RELATIVE GAPS BETWEEN TESTED CONFIGURATIONS	112
7.1.	CONFIGURATION RELATIVE DIFFERENCES IN % FOR CHARGE DEPLETING MODE ON TOTAL RDE CYCLE	112
7.2.	CONFIGURATION RELATIVE DIFFERENCES IN % FOR CHARGE SUSTAINING MODE ON TOTAL RDE CYCLE	115
8.	APPENDIX - ANALYTICAL MODEL COEFFICIENTS	118
8.1.	ENERGY CONSUMPTION	118
8.2.	UTILITY FACTORS	119
8.3.	TEMPERATURE DEVIATION PROGRESSION	120

1. INTRODUCTION

1.1. CONTEXT AND MOTIVATION

Transport related GHG emissions represent approximately a quarter of EU GHG emissions. In the context of targeting carbon neutrality in 2050 as set by the EU Green Deal, reducing transport related GHG emissions represents both an important stake and challenge.

The present study focuses on passenger cars only. When considering each vehicle individually, there are several ways to consider their GHG emissions:

- The Tank-to-Wheel (TtW) approach focuses only on the tailpipe emissions.
- The Well-to-Wheel (WtW) approach is more complete and considers the GHG emissions related to the production of the energy carriers.
- The Life Cycle Assessment (LCA) approach is holistic and also considers the GHG emissions related to the production of capital goods that are necessary to the transport system (e.g. vehicles, infrastructures of the energy system, etc.).

Obviously, the LCA approach is the most satisfying as it is the most relevant to climate related issues. Nevertheless, the TtW and WtW approaches should also be considered simultaneously because they are currently regulated in Europe (TtW for the vehicles; WtT with combustion for the fuels). For example, a solution that would have a high performance in the LCA scope, but a bad performance in the TtW scope would probably face big barriers to its development in the EU market.

In this context, Plug-in Hybrid Electric Vehicles (PHEVs) represent an interesting option as they seem to address the challenges with low GHG emissions at each stage (TtW, WtW and LCA). Furthermore, they can relieve some of the pressure on the implementation of fast charging infrastructures for Battery Electric Vehicles (BEVs) so as to make their rollout feasible in a shorter timeframe. However, it is believed that the assessments currently available in the literature may require some updates:

- TtW: the OEMs are committed to reduce the TtW CO₂ emissions of passenger cars (in gCO₂/km) by 37.5%³ in 2030 compared to a 2021 starting points. A 55% reduction compared to 1990 levels is proposed in the fit-for-55 package⁴. It is highly likely that, to reach this target, a high amount of electrification will be necessary, including PHEVs as they generally give CO₂ emissions in the range of ~30 gCO₂/km. As of today, these TtW CO₂ emissions are assessed based on the Worldwide Harmonized Light Vehicles Test Procedure (WLTP). The WLTP does not necessarily consider the real-world emissions of the vehicle, which could affect PHEV credibility in the future:
 - Some PHEVs are purchased due to tax incentives but are rarely plugged in (especially company cars)⁵;

³CO₂ emission performance standards for cars and vans, Regulation (EU) 2019/631

⁴[https://www.europarl.europa.eu/RegData/etudes/BRIE/2022/698920/EPRS_BRI\(2022\)698920_EN.pdf](https://www.europarl.europa.eu/RegData/etudes/BRIE/2022/698920/EPRS_BRI(2022)698920_EN.pdf)

⁵https://www.fleeteurope.com/en/new-energies/europe/features/plug-hybrids-watch-fuel-bill?a=DQU04&t%5B0%5D=PHEV%20Insights&t%5B1%5D=PHEV&t%5B2%5D=Plug-in%20hybrid&t%5B3%5D=Telematics&curl=1&utm_source=Fleet+Europe+Newsletter&utm_campaign=ae86bbac5b-EMAIL_CAMPAIGN_2020_03_05_02_06&utm_medium=email&utm_term=0_4128e0d88f-ae86bbac5b-65473135
https://www.fleeteurope.com/en/new-energies/europe/features/dont-go-plug-hybrids-without-considering-telematics-first?t%5B0%5D=PHEV%20Insights&t%5B1%5D=PHEV&t%5B2%5D=Plug-in%20hybrid&t%5B3%5D=Telematics&curl=1&utm_source=Fleet+Europe+Newsletter&utm_campaign=0a9c6f5a00-EMAIL_CAMPAIGN_2020_03_25_04_05&utm_medium=email&utm_term=0_4128e0d88f-0a9c6f5a00-65473135
<https://www.telegraph.co.uk/news/2020/02/05/revealed-plug-in-hybrid-cars-emit-three-times-co2-real-world/>
<https://ev-database.uk/cheatsheet/fuel-consumption-plugin-hybrid>

- Some journeys are much longer than the WLTC over which the CO₂ emissions are assessed. Therefore, it is possible that in some cases, the Internal Combustion Engine (ICE) runs for a larger proportion of the total distance travelled than expected in the regulation. According to German statistical studies⁶, only 2 % of daily trips are longer than 100 km, but they account for 26 % of the mileage driven. Similarly, in France, only 1.3 % of the trips are longer than 80 km, but account for 40 % of the total mileage (approximately. 6000 km/y)⁷, including around 50 % of them travelled by car. Therefore, these “rare but long trips” may have a significant impact on the real-world fuel consumption and TtW emissions of PHEVs, which should be assessed properly.
- The PHEV has a higher weight than a conventional HEV or pure thermal vehicle - a downside for fuel consumption and CO₂ emissions if not charged.
- WtW and LCA: several WtW and LCA studies, such as those led by Ricardo⁸ or by IFPEN^{9,10} rank the PHEV among the best solutions in terms of CO₂ emissions. This is especially true if they use renewable fuels. In some very favourable cases, PHEVs can even have lower CO₂ emissions than BEVs over their life cycle as their battery is smaller - this will of course be highly dependent on the driver’s behaviour in charging the vehicle as well as the carbon intensity of the energy sources. If they have encouraging outcomes for PHEV, these studies do not answer the question of the real ratio of EV drive from PHEVs (raised above, also called “Utility Factor”, UF), which may be a limiting factor to the applicability of their conclusions.

If it is understood that PHEVs fuelled by renewable fuels and low carbon electricity are an interesting option in terms of CO₂ emissions over their life cycle, this technical option also offers the opportunity to reduce the consumption of liquid fuels. This is particularly interesting in the frame of the outcomes of Concawe’s work published by FuelsEurope¹¹, which mentions that liquid fuels for road transportation could be 100% low-carbon by 2050, but with a consumption of liquid fuels that would be approximately one third compared to today’s level to be compliant with the 1.5 TECH scenario from “A Clean Planet for All”. Hence, to make PHEVs fuelled by renewable fuels a viable solution in the long term, they have to prove that they can compete with a third of the consumption of liquid fuels as a first approximation (and still comply with this in real-world operation).

In addition to CO₂ emissions and energy consumption, air quality is also an important factor for road transportation. PHEVs are often seen as an asset for air quality as they allow electric drive in the cities. However, the intermittent electric-drive of PHEVs (and hybrids in general) can present additional challenges for tailpipe emissions control due to multiple exhaust aftertreatment heating phases during a

⁶ Infras, DLR, IVT und infras360 (2018) : Mobilität in Deutschland (im Auftrag des BMVI)

⁷ https://www.statistiques.developpement-durable.gouv.fr/sites/default/files/2018-11/La_mobilite_des_Francais_ENTD_2008_revue_cle7b7471.pdf

⁸ Determining the environmental impacts of conventional and alternatively fuelled vehicles through Life Cycle Assessment - Final stakeholder meeting - January 2020

⁹ [https://www.ifpenergiesnouvelles.fr/sites/ifpen.fr/files/inline-images/Innovation%20et%20industrie/Analyse%20du%20cycle%20de%20vie%20\(ACV\)/Rapport_ACV%20GNV_version%20finale.pdf](https://www.ifpenergiesnouvelles.fr/sites/ifpen.fr/files/inline-images/Innovation%20et%20industrie/Analyse%20du%20cycle%20de%20vie%20(ACV)/Rapport_ACV%20GNV_version%20finale.pdf)

¹⁰ <https://www.ifpenergiesnouvelles.fr/sites/ifpen.fr/files/inline-images/NEWSROOM/Communiqu%C3%A9%20de%20presse/projet-e4t-bilan-impact-electrification-2018.pdf>

¹¹ <https://www.fuels europe.eu/clean-fuels-for-all/>

drive cycle - which are not necessarily well monitored in the current vehicle homologation process.

1.2. OBJECTIVES

In this context, the aim of this study is to assess the energetic performance and emissions of state-of-the-art PHEVs in real-world conditions. More specifically, this study intends to:

- 1- Provide TtW data allowing life-cycle assessment of PHEVs in real-world conditions. This includes:
 - Average electricity consumption (kWh/km), fuel consumption (L/km and MJ/km) and TtW CO₂ emissions (g/km), and a comparison with the values obtained with a non-plug-in HEV.
 - Average electric drive ratio (utility factor, km/km)
 - And spans the following conditions:
 - Sensitivity cases around the different behaviours of the driver regarding recharging.
 - Sensitivity cases around the battery size and range.
 - Sensitivity cases around the fuel used (e.g. fossil fuel vs. low carbon renewable fuel).
 - Sensitivity cases around the carbon intensity of the electricity mix (not part of this study, will be handled separately).
- 2- Provide data on pollutants emissions of PHEVs in real-world conditions and determine if:
 - They are relevant solutions to improve air quality.
 - The aftertreatment system efficiently manages the particularities of PHEV drive.

1.3. STRUCTURE OF THE STUDY AND OF THE REPORT

CO₂ emissions, regulated and non-regulated pollutant emissions, as well as the electrical services offered (all-electric range and utility factor) will thus be assessed according to the conditions of use of the vehicles (type of driving, fuel property, recharging frequency, etc.). To this end:

- An experimental campaign was carried out on a chassis dynamometer and on-road on two state-of-the-art PHEVs. This is detailed in chapter 2 of this report.
- A simulation campaign based on these measurements made it possible to extend the findings to more extensive usage scenarios. Finally, paired with large-scale usage statistics, it made it possible to establish the average behavior of PHEVs according to parameters such as the recharging frequency and the battery capacity. This is explained in chapter 3 of the report.

2. EXPERIMENTAL CAMPAIGN

2.1. OBJECTIVES OF THE PROTOCOL

The objective of the study is to evaluate the energy and emissions performance of the latest generation PHEVs under real-world conditions. The test protocol therefore focused on real-world driving emissions (RDE). In more detail, the analysis aims to compare:

- Diesel vs. gasoline - one vehicle with a diesel engine and the other a gasoline engine.
- Standard vs. renewable fuels - B7 vs. HVO and E10 vs. E20.
- Full battery mode (charge depleting mode (CD)) vs. empty battery (charge sustaining mode (CS)).
- PHEV vs. HEV - on a comparison with an equivalent non-rechargeable HEV vehicle (by artificially varying the battery weight of the vehicle on the chassis dyno - see section 2.4.3 for more details).

Most of the experimental campaign is carried out on roller test bed, to maximise the repeatability and comparability between all the configurations tested. On-road tests are then conducted to validate the behaviour and comparison seen in the first experimental part.

Exhaustive measurement equipment is used to assess, CO₂ emissions, regulated and non-regulated pollutants emissions (both engine-out and tailpipe), energy consumptions (both fuel and electricity) as well as the electrical services offered (all-electric range and utility factor).

2.2. SELECTED VEHICLES AND MAIN SPECIFICATIONS

As one of the goals of the study is to compare a gasoline PHEV with a Diesel one in a similar configuration, the vehicles selection narrowed to a pair of Mercedes C300de (Diesel) and C300e (gasoline). These two vehicles have the same electrical characteristics (battery, electric machine, architecture), and the powertrain of these two vehicles differ only by the thermal engine. In addition, the two gasoline and Diesel thermal engines offer similar driveability (torque and power).

Additionally, this selection of vehicles allowed to access a database previously built by IFPEN on these vehicles in other testing conditions (other driving cycles, other climate conditions, etc.). This additional database showed to be extremely useful when calibrating and validating the vehicles simulators (see Chapter 3).

Table 1 Main specifications of selected vehicles

	C300e EQ Power	C300de EQ Power
Regulation	Euro 6d-temp	
Fuel type	Petrol	Diesel
Test mass [kg]	1885	1970
WLTP CO ₂ [g/km]	CS ¹² : 146 Weighted ¹³ : 31	CS: 140 Weighted: 30.5
Thermal Engine	2.0L 4cyl 155 kW turbo Direct injection	2.0L 4cyl 143 kW turbo Direct injection
Transmission	9-speed automatic transmission	
Battery	13.5 kWh 365V	
Electric motor	90 kW	
Hybridization	P2 parallel hybrid architecture	
Aftertreatment system	2*Three Way Catalyst (TWC) close coupled + Gasoline Particulate Filter (GPF) underfloor	Diesel Oxidation Catalyst (DOC) + Selective Catalyst Reduction Filter (SCRF) + Selective Catalyst Reductor (SCR) close coupled
Mileage [km]	4000	14000


Figure 1 Picture of the tested Mercedes C300de EQ Power

2.3. SELECTED FUELS AND MAIN SPECIFICATIONS

For each vehicle, two fuels were used:

- A standard fuel, traditionally used for vehicle homologation purpose, and complying with the specifications of the mainstream commercial fuels (EN590 and EN228).
- A 100% renewable biofuel, either complying with an alternative fuel specification (paraffinic Diesel, EN15940) or with a possible foreseen specification for E20¹⁴. It is important to highlight that the vehicles are not

¹² In charge sustaining mode, i.e. empty battery at start of test.

¹³ Weighted between charge depleting mode (i.e. full battery at start of test) and charge sustaining mode, according to the current regulation.

¹⁴ As there exist no specification for E20 today (discussions only starting at CEN level), the authors assumed that a fuel complying with all the EN228 except the oxygen content would be sensible.

homologated with these fuels, and that these fuels are tested for research purpose only. Long-term compliance with these fuels would require further research work. In this instance:

- The 100% renewable paraffinic Diesel is a hydrotreated vegetable oil (HVO).
- The 100% renewable E20 is produced using fermentation and an alcohol-to-gasoline process, using grains, residues and wastes as feedstock, and reduces GHG emissions by 66% compared to a fossil according to the supplier. A C14 analysis performed on the fuel confirmed its biogenic origin.

Table 2 Main characteristics of selected fuels (detailed properties provided in the appendix)

Property	Method	Standard		Renewable	
		EN590	EN228-E10	100% renewable paraffinic fuel (HVO) EN15940 compliant	100% renewable gasoline including 20% ethanol EN228 compliant except for oxygenate content
Density [kg/L]	EN ISO 12185	0.834	0.748	0.764	0.762
Lower Heating Value (m) [MJ/kg]	ASTM D 240/ASTM D3338 mod/GC calculated	42.13	41.40	44.16	39.78
Carbon content [%m/m]	ASTM D 5291/ASTM D3343 mod/GC calculated	85.8	83.1	84.62	79.4
Hydrogen content [%m/m]	ASTM D 5291/ASTM D3343/GC calculated	13.5	13.4	15.38	13.4
Oxygen content [%m/m]	MO238LA2008/EN 14078/GC calculated	0.7	3.5	0	7.2
Total aromatics	EN 12916/IP 391 mod/NF M 07-086/EN ISO 22854	22.2 %m/m	26.7 %v/v	0.1 %m/m	28.7 %v/v
Cetane number / RON-MON [-]	EN ISO 5165/5164/5163/ASTM D6890	52.5	97.0-85.9	78.2	99.4-88.0
Final boiling point [°C]	EN ISO 3405/ASTM D86	354.1	180.2	302.5	201.7

2.4. EXPERIMENTAL CAMPAIGN IN LABORATORY (CHASSIS DYNO)

2.4.1. Vehicle instrumentation and measurement systems

Table 3 details the equipment used on each vehicle during the roller test bed campaign. The measurements spanned engine-out and tailpipe regulated and

unregulated emissions, CO₂ (and more generally GHG) emissions, fuel and electrical consumption, and some temperatures.

The devices for measuring regulated emissions are part of the permanent equipment of the test bench: CO₂, NO / NO₂, CO, HC, PM and PN. The measurements of THC, CH₄, CO, CO₂, and NO_x are carried out by a Horiba MEXA 7000 analyzer. The particles in mass are determined by CVS and samples on filter and weightings. The particles in number (with a diameter greater than 10 nm) are determined by an SPCS (IFPEN chassis dyno has been updated to anticipate the future official measurement down to 10nm). An additional particle counter CPC-100 was implemented for counting particles greater than 23 nm, so that simultaneous counting of particles between 10 and 23 nm is possible. Finally, the measurements of NO, NO₂, N₂O and NH₃ are measured by a Horiba QCL (MEXA-ONE-QL-NX) analyzer.

The use of a gas analyzer induces gas sampling that can have an impact on the vehicle's aftertreatment system. Artificial flows are induced when the engine is turned off and can cause changes in temperature and gas composition conditions. These phenomena can then influence the thermal deactivation dynamics of the catalysts or modify the storage of oxygen in the catalyst blocks. These impacts are greater in the case of PHEVs, with long engine-off phases. To avoid these effects and to limit the intrusiveness of gas sampling on the vehicle's behavior, the sampling rates of the gas analyzers are cut off when the engine speed is below its idle speed.

Table 3 Chassis Dyno Hardware

	Measurement
Engine-out	Raw sample - HORIBA MEXA (CO ₂ , CO, NO _x , NO, NO ₂ , CH ₄ , THC, NMHC)
	HORIBA QCL (NH ₃ , N ₂ O, NO, NO ₂)
	CPC-100 (PN23)
	SPCS 110 (PN10)
Tailpipe	CVS - HORIBA MEXA (CO ₂ , CO, NO _x , NO, NO ₂ , CH ₄ , THC, NMHC)
	HORIBA QCL (NH ₃ , N ₂ O, NO, NO ₂)
	CPC-100 (PN23)
	SCPS 110 (PN10)
	PM by filter weighting DMS500 (particle size distribution)
Fuel consumption	Carbon balance on tailpipe emissions
Electrical consumption	HIOKI 3390 (current clamp on high-voltage (HV) direct current (DC) cable between battery and inverter Current clamp on low-voltage (LV) battery)
Aftertreatment system	AdBlue consumption when urea SCR is used thanks to instrumentation of the injector control signals (number of pulses and Ti), urea Pressure and a characterization of the injector
Temperature	Engine-out TWC or DOC inlet DPF or GPF inlet and outlet Sump Coolant
Additional bench measurements	Exhaust flow Ambient temperature, pressure, and humidity Roller power Vehicle speed Engine speed



Figure 2 Picture of the chassis dyno setup with the tested vehicle

2.4.2. RDE test cycle reproduced on chassis dyno

The cycle operated at the test bench was derived from a previous RDE test driven on-road and compliant with the latest RDE requirements.

Figure 3 depicts the vehicle speed in function of distance driven with Roller test bed phases and RDE phases (urban, rural and motorway). RDE phases are induced by the RDE regulation. The cycle is cut in 3 categories based on the vehicle speed: the urban phase gathered the events where the vehicle speed is lower than 60 km/h (included), the rural phase between 60km/h and 90km/h (included) and the motorway phase above 90km/h.

The roller bench phases are driven by the equipment capabilities, in this case, the volume of the sampling bags. The volume of the gas trapped can be reduced to the sampling duration because of the constant volume sampling (CVS) system. On the equipment used for the PHEV testing, the sampling bags could be used for a maximum of 1322 seconds. As the RDE cycle total duration is approximately of 5600 seconds, the choice made was to use 6 bags. The first bag is focused on the beginning of the test, the firsts kilometres, the second phase is mainly composed of urban conditions, the third one with mainly rural condition, the fourth phase is mainly urban, the fifth one mainly motorway and the last (sixth) phase is also mainly urban conditions.

The RDE trip is also defined by its driveability. To assess and categorise the driving behaviour, two main indicators are used: the 95th percentile of $v \cdot a_{pos}$, i.e. the 95th percentile of vehicle speed x (acceleration $\geq 0.1 \text{ m/s}^2$) for each RDE phase, and the Relative Positive Acceleration (RPA), i.e. the sum of vehicle speed x (acceleration $\geq 0.1 \text{ m/s}^2$) / distance driven (in km) for each RDE phase. Those indicators are constrained by the RDE regulation.

Figure 4 and Figure 5 shows those driveability indicators 95th percentile of $v \cdot a_{pos}$ and RPA respectively in relation to the RDE boundaries. Table 4 details the RDE indicators for the reference test driven during the study compared to the RDE limits.

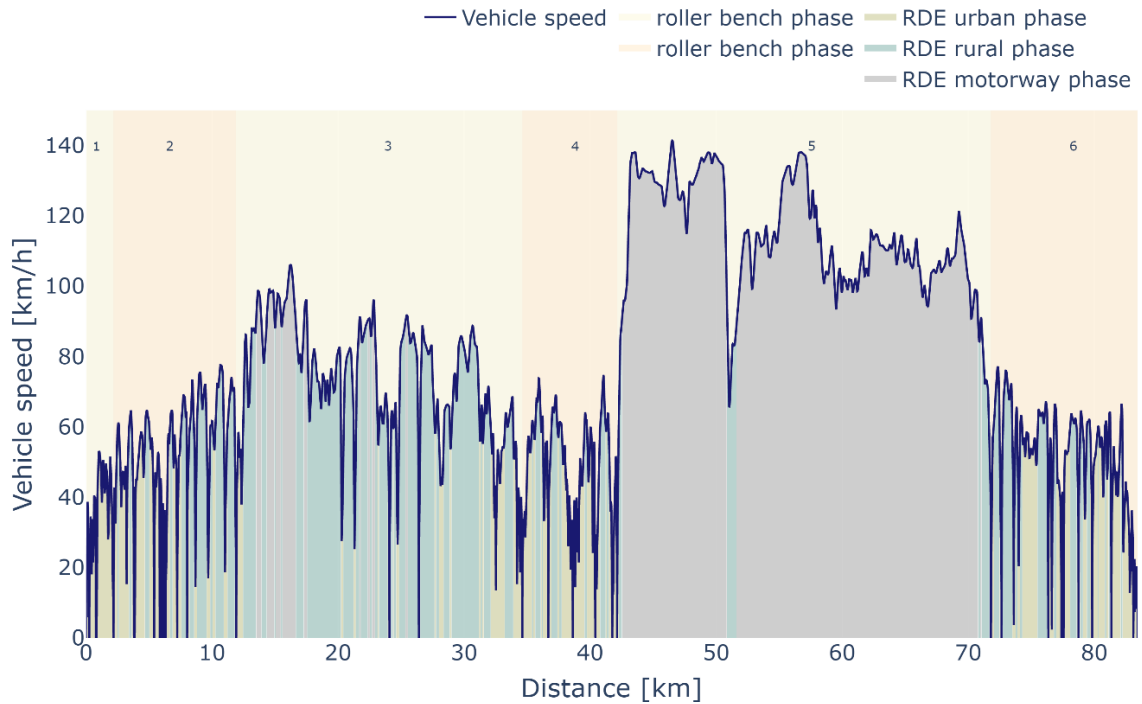


Figure 3 Vehicle speed profile with chassis dyno phase and RDE cut (urban, rural, motorway)

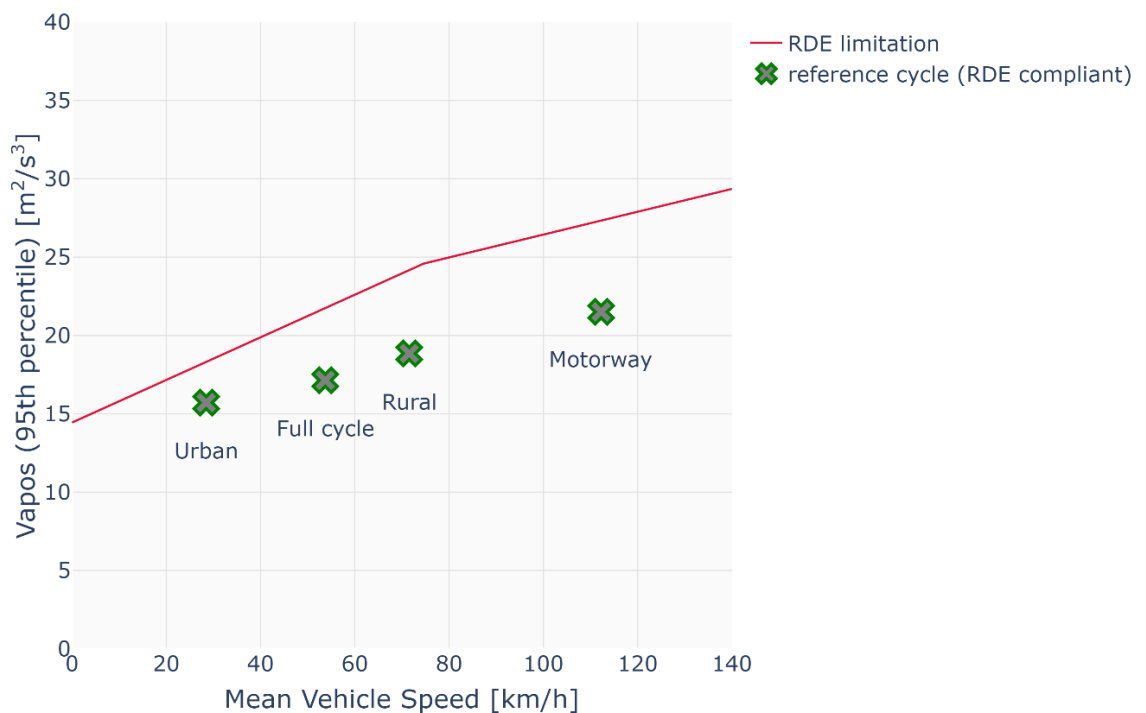


Figure 4 VA_{pos} on RDE reference cycle on roller test bench, by urban, rural, motorway phases and over total cycle, compared to RDE maximum boundary.

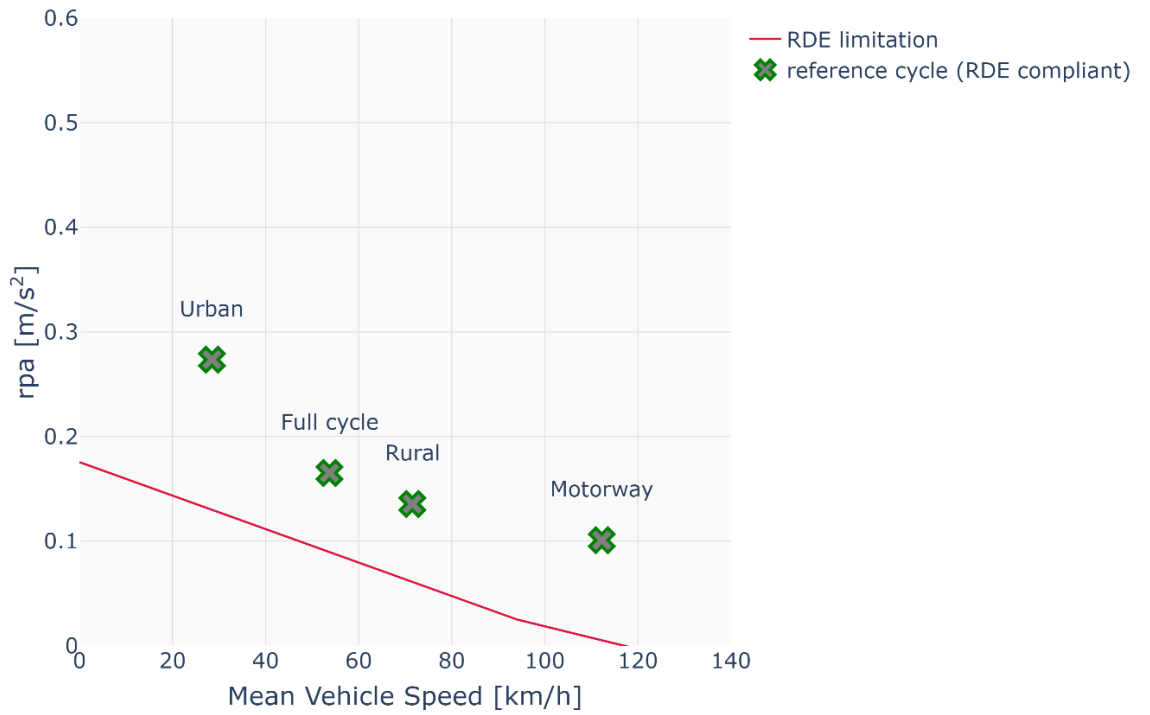


Figure 5 Relative Positive Acceleration on RDE reference cycle on roller test bench, by urban, rural, motorway phases and over total cycle, compared to RDE minimum boundary.

Table 4 RDE compliance

	Limit	Cycle
Trip duration [min]	[90, 120]	93
Total distance [km]	48 <	83.4
cold start stop time [s]	< 90	52
cold start mean speed [km/h]	[15, 40]	23.7
cold start max speed [km/h]	60	53
urban share [%]	[19, 44]	30.8
urban distance [km]	16<	25.7
urban mean speed [km/h]	[15, 40]	28.5
urban rpa [#]	150 < (WP3), 100 < (WP4)	1125
urban cumulated positive altitude [m/100km]	< 1200	560
urban stop time share [%]	[6, 30]	13.7
stop duration (max) [s]	< 300	69
stop number (>10s) [#]	2 <	27
rural share [%]	[23, 43]	31.9
rural distance [km]	16<	26.7
rural rpa [#]	150 < (WP3), 100 < (WP4)	488
motorway share [%]	[23, 43]	37.2
motorway distance [km]	16<	31.1
high speed > 100 duration [min]	5 <	13
high speed 145 share [%]	< 3	0
motorway rpa [#]	150 < (WP3), 100 < (WP4)	325
motorway maximum speed [km/h]	[110, 160]	141
total cumulated positive altitude [m/100km]	< 1200	620
elevation difference [m]	[-100, 100]	0
elevation max [m]	< 700	180

2.4.3. Road load

Road laws are needed to assess the energy required to propel the vehicle. The driving resistance force is given through a speed polynomial based on masses and dimensionless coefficients registered in the next table for all vehicle configurations.

$$F_{\text{wheel}} = \text{Inertia} \cdot g \cdot (F_0 + F_1 \cdot v) + F_2 \cdot v^2$$

Table 5 shows the road load coefficients used at the test bed. Those coefficients are issued from C300e certification coefficients in Vehicle Low configuration. They were chosen because they are closer to real masses and show less difference between Diesel and gasoline. The choice of a unique set of coefficients was made to simplify the comparison.

In order to simulate the resistance behaviour of a Not off-vehicle chargeable hybrid electric vehicle (NOVC-HEV, later referred as “HEV”) compared to an off-vehicle chargeable hybrid electric vehicle (OVC-HEV, later referred as “PHEV”), a market research was performed with vehicle models that are commercialised in both HEV configuration and PHEV configuration. The difference between the vehicle mass was assessed around 120 kg. This hypothesis was also validated by the estimation of the mass the components of the HEV and the PHEV, i.e. mainly a gap due to a reduced battery size and no on-board charging equipment. The hypothesis that externally both PHEV and HEV are identical lead to the use of the same F0, F1 and F2 road load coefficients.

Table 5 Vehicle Road Laws

	PHEV Diesel	HEV Diesel	PHEV Gasoline	HEV Gasoline
inertia [kg]	1970	1850	1885	1765
F0 [N]			134.8	
F1 [N/(km/h)]			0.561	
F2 [N/(km/h) ²]			0.02762	

2.4.4. Tests operated on laboratory

Both vehicles are tested with 2 fuels, standard and renewable, and three testing conditions, charged (CD - Charge Depleting), uncharged (CS - Charge Sustaining) and also uncharged using a reduced weight (CS HEV) to simulate the configuration of a hypothetical (non-plug-in) hybrid electric vehicle. Each test was repeated three times to assess and ensure good repeatability.

To avoid biases due to the timeline of tests and configuration changes, the proposed test matrix is based upon 3 main test blocks with the standard fuels and 3 blocks performed with the renewable fuels. An extra test block was added for further evaluation of the renewable fuels with a battery conditioning that is uncharged (CS).

Also, in the test matrix, a configuration was chosen as reference to monitor the repeatability of the vehicle during the test campaign.

Tests identified as invalid at the time of running were repeated in-sequence whereas those identified later as non-conforming were repeated in a position in the sequence subject to the constraint of avoiding successive tests on the same configuration. The actual test order deviated from the planned test order due to operational requirements. Table 6 shows the initial test matrix.

Table 6 Test matrix on roller test bench

	Vehicle	Fuel	Battery	MASS	Repeat
Block 1	C300de	EN590	CD	PHEV	1
	C300e	E10	CD	PHEV	1
	C300e	E10	CS	PHEV	1
	C300de	EN590	CS	PHEV	1
	C300de	EN590	CS	HEV	1
	C300e	E10	CS	HEV	1
	C300de	EN590	CD	PHEV	2
	C300e	E10	CD	PHEV	2
Block 2	C300de	EN15940	CD	PHEV	1
	C300e	E20	CD	PHEV	1
Block 3	C300e	E10	CS	PHEV	2
	C300de	EN590	CS	PHEV	2
	C300de	EN590	CS	HEV	2
	C300e	E10	CS	HEV	2
	C300de	EN590	CD	PHEV	3
	C300e	E10	CD	PHEV	3
Block 4	C300de	EN15940	CD	PHEV	2
	C300e	E20	CD	PHEV	2
Block 5	C300e	E10	CS	HEV	3
	C300de	EN590	CS	HEV	3
	C300de	EN590	CS	PHEV	3
	C300e	E10	CS	PHEV	3
	C300de	EN590	CD	PHEV	4
	C300e	E10	CD	PHEV	4
Block 6	C300de	EN15940	CD	PHEV	3
	C300e	E20	CD	PHEV	3
Extra	C300e	E20	CS	PHEV	1
	C300de	EN15940	CS	PHEV	1
	C300de	EN15940	CS	PHEV	2
	C300e	E20	CS	PHEV	2

The Diesel vehicle tested had realized a DPF regeneration that needed some extra test to recreate the soot cake. The test where the regeneration occurred as well as the conditioning tests that followed were omitted from the analysis¹⁵.

¹⁵ According to the current regulation, a test where a DPF regeneration occurs is non-valid. However, a test performed right after the DPF regeneration, when the soot cake is not fully recreated, is valid. The reason why we decided to omit these results from the analysis is related to repeatability issues: tests performed right after DPF regeneration generally have higher particulate emissions, which is detrimental to repeatability. In the context of this study, whose purpose is to compare different vehicles and fuels configurations, a good repeatability was needed, which led to omit these tests which would have looked like outliers and would have limited the extent of the conclusions regarding the comparison of the configurations.

The statistical analysis was carried out on all remaining data declared valid by the test facility. Statistical outlier testing was performed, and no significant outliers were identified for further omission following this.

2.4.5. Results of laboratory test campaign

Key results from the RDE tests performed on the chassis dyno are described in this section and the full results are tabulated in *Table 9*, *Table 10*, *Table 11* and Appendix 7. Where shown on charts, error bars denote the 68 % confidence intervals (i.e. +/- the standard deviation).

The table Appendix 7.1 summarizes the relative differences in percentage between the tested configurations. Those percentages are reminded in the following sections of the report.

In the following figures using the format of *Figure 6* in this section, the comparisons between the average values obtained on the RDE cycle for the different configurations are shown as follows:

- E10 vs E20 (used in the gasoline PHEV) vs B7 vs HVO (used in the Diesel PHEV).
- In the following configurations: Charge Depleting mode (CD), Charge Sustaining mode (CS) and HEV CS mode.

2.4.5.1. Volumetric Fuel Consumption

Figure 6 shows the evolution of fuel consumption in all the tested configurations. The volumetric fuel consumption is calculated thanks to the fuel properties, the CO₂, HC and CO emissions in mass.

The Diesel PHEV using B7 shows lower volumetric fuel consumption compared to the gasoline PHEV using E10: -20.1% in CD and -26.7% in CS. This finding is consistent with the literature and explained by the better efficiency of compression ignition engines and by the higher density of B7 compared to E10, leading to a higher energy density by volume.

Regarding CS tests, it is needed to assess behaviour that are comparable with a state of charge (SOC) of the battery identical at the beginning and at the end of the test (iso SOC). To this end, a correction factor is computed. If the variation of energy stored in the battery had to be produced by the combustion engine:

$$\Delta E_{elec} [Wh] = \eta_{elec} \times \eta_{thermal} \times \Delta E_{fuel} [Wh]$$

Where,

- ΔE_{elec} is the variation of electrical energy stored in the battery during the test.
- η_{elec} is the mean electrical efficiency (from the shaft to the battery). Based on the calibrated simulators, it is set to 77% (motor 87%, inverter 90%, battery 98%).
- $\eta_{thermal}$ is the mean thermal efficiency (from the fuel to the shaft). Based on the calibrated simulators, it is set to 35% for Diesel and 33% for gasoline.
- ΔE_{fuel} is the theoretical delta of fuel energy needed to produce ΔE_{elec} .

Therefore,

$$\Delta E_{fuel} [Wh] = \frac{\Delta E_{elec}}{\eta_{thermal} \times \eta_{elec}} = \frac{(SOC_{CS,end} - SOC_{CS,ini}) \times Battery\ capacity [Wh]}{\eta_{thermal} \times \eta_{elec}}$$

Furthermore, the thermal energy consumption measured over the cycle is:

$$E_{fuel} [Wh] = FC [L] \times Fuel\ density \left[\frac{g}{L} \right] \times Fuel\ LHV \left[\frac{kJ}{kg} \right] \times \frac{1}{3.6}$$

Finally, the correction factor is determined as follows, along with the corrected consumption and CO₂ emission values:

$$Correction\ factor = 1 - \frac{\Delta E_{fuel}}{E_{fuel}}$$

$$FC_{corrected} \left[\frac{L}{100km} \right] = Correction\ factor \times FC \left[\frac{L}{100km} \right]$$

$$CO_{2corrected} \left[\frac{g}{km} \right] = Correction\ factor \times CO_2 \left[\frac{g}{km} \right]$$

Thus, if the vehicle performs a partial recharge of the battery during the CS test, its fuel consumption will be corrected downwards. Conversely, if it uses energy from the battery and partially discharges it during this CS test, its consumption will be corrected upwards¹⁶.

Once this correction applied (*Figure 7*), the gap between the gasoline PHEV using E10 and the Diesel PHEV using B7 in CS increases from -26,7% to -32.6%. The explanation is that the Diesel vehicle showed a higher partial battery recharge than the gasoline vehicle during the CS tests.

Switching to renewable fuels leads to a higher volumetric fuel consumption, both for the gasoline and the diesel vehicles: + 4.5 % for E20 compared to E10 in CS and + 8.4 % for HVO compared to B7 in CS, after applying the correction to return to iso-SOC. This is due to the lower energy density by volume of these renewable fuels: a lower density for HVO compared to B7 (in spite of a higher energy density by mass) and a higher oxygen content for E20 compared to E10.

No significant impact of the HEV versus PHEV configuration was detected for either the Diesel or gasoline vehicle. This is a rather surprising result given that one would normally expect a significantly lighter vehicle (-120 kg) to result in lower energy consumption. Quite logically, the HEV vehicle with 120kg less weight needs less energy for the same driving cycle: it consumes 0.53 kWh/100km less positive energy at the wheel compared to the PHEV vehicle. On the other hand, on hybrid vehicles in general, part of the kinetic energy delivered to the vehicle is recovered during regenerative braking. Thus, the PHEV vehicle, with its 120kg more, recovers 0.22 kWh/100km more to its battery compared to the HEV vehicle. This compensation explains why vehicles with regenerative braking (HEV, PHEV, BEV) are therefore less sensitive to mass variations compared to conventional vehicles. However, it does not explain the total lack of mass sensitivity established experimentally.

¹⁶ Another methodology consists in carrying out several CS tests in initial SOC conditions around the maintenance threshold, but sufficiently different to allow the direct determination of a correlation coefficient between the SOC variation and the consumption on cycle (coefficient called K_{CO2}). This methodology is the one recommended by the WLTP protocol but has not been applied here because all the CS tests carried out have SOC variations that are too close.

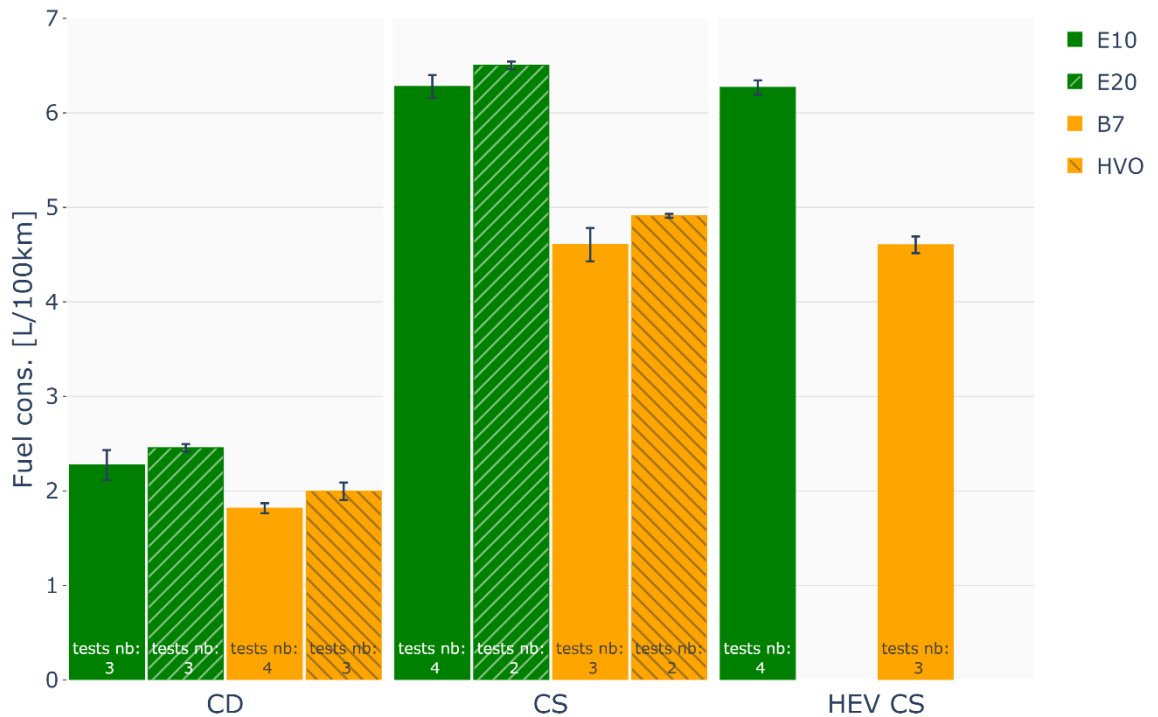


Figure 6 Comparison of Volumetric Fuel Consumption [L/100km] measured on RDE cycles on chassis dyno for each fuel and mode.

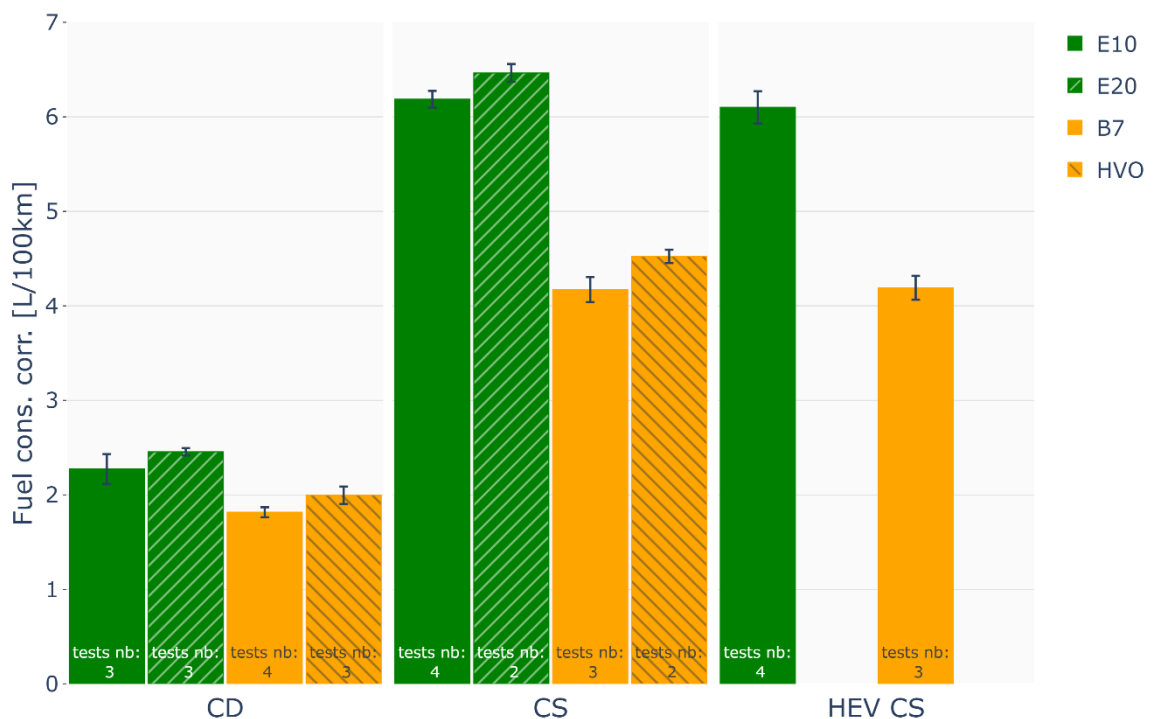


Figure 7 Comparison of corrected Volumetric Fuel Consumption [L/100km] measured on RDE cycles on chassis dyno for each fuel and mode.

2.4.5.2. Electrical Consumption and Utility Factor

Figure 8 illustrates the net electrical energy consumed for each configuration on the RDE cycles. Concerning this consumption of electrical energy, it is particularly relevant to focus on consumption in charge depleting mode. Indeed, electrical

consumption in charge sustaining mode is only the result of marginal variations of SOC between the start and the end of the cycle. These consumptions have no concrete reality, insofar as there is no external electrical energy to consume in this mode which is, by definition, a mode of maintaining the charge level. Moreover, these "parasitic" consumptions are reduced to zero by determining the corrected fuel consumptions and CO₂ emissions in CS, as detailed in the previous paragraph.

Thus, regarding the CD cases, the Diesel PHEV fuelled with B7 consumes 9.4% less electrical energy than the gasoline PHEV fuelled with E10. As the battery, i.e. the electric energy tank, is identical between the two models, this means that the SOC at the end of the RDE in the case of the B7 PHEV CD is systematically higher than for the E10 PHEV CD RDE. The difference can be explained by a difference of calibration on the electric versus thermal use between the petrol and Diesel PHEV, specifically around the motorway driving. The Diesel vehicle seems to use its thermal engine sooner reducing the use of electricity, also at the end of the driving, the battery of the Diesel vehicle seems to recharge more, explaining the reduced net electrical consumption compared to the gasoline one (see *Figure 9*). This could also be explained by a difference of behaviour between the two vehicles induced by their history as they are second-hand vehicles. Switching from standard (E10 and B7) to renewable fuels (E20 and HVO) has no significant impact on the CD electrical consumption.

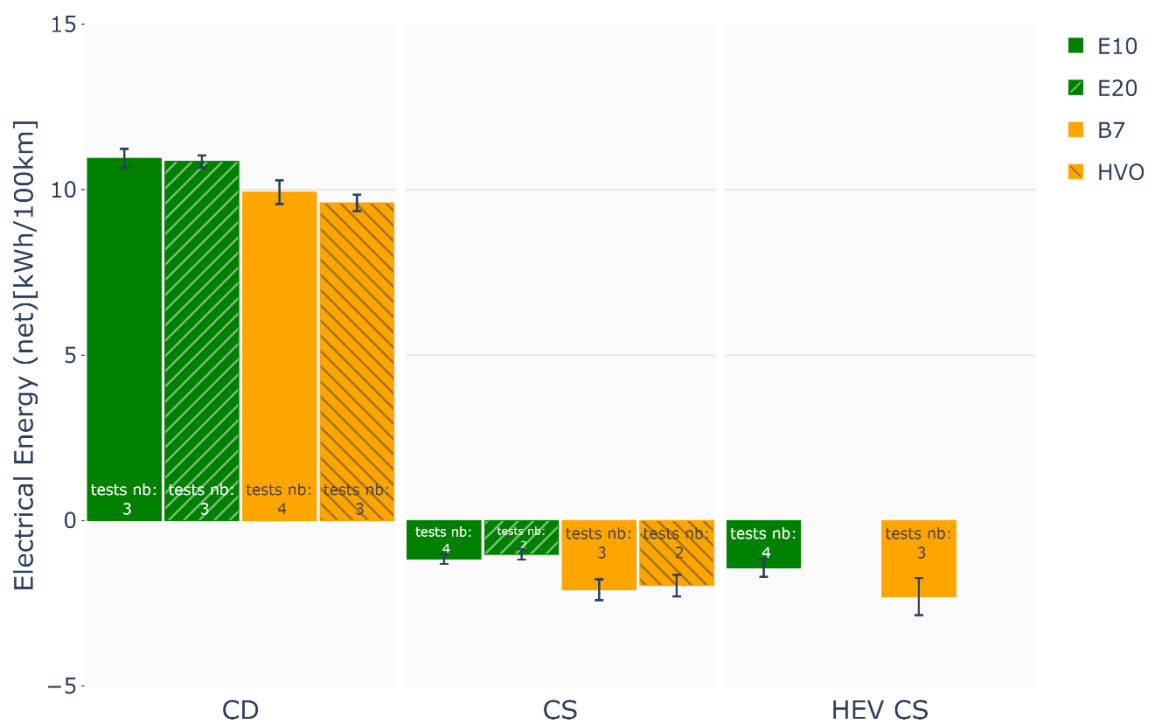


Figure 8 Comparison of Electrical consumption [kWh/100km] measured on RDE cycles on chassis dyno for each fuel and mode.

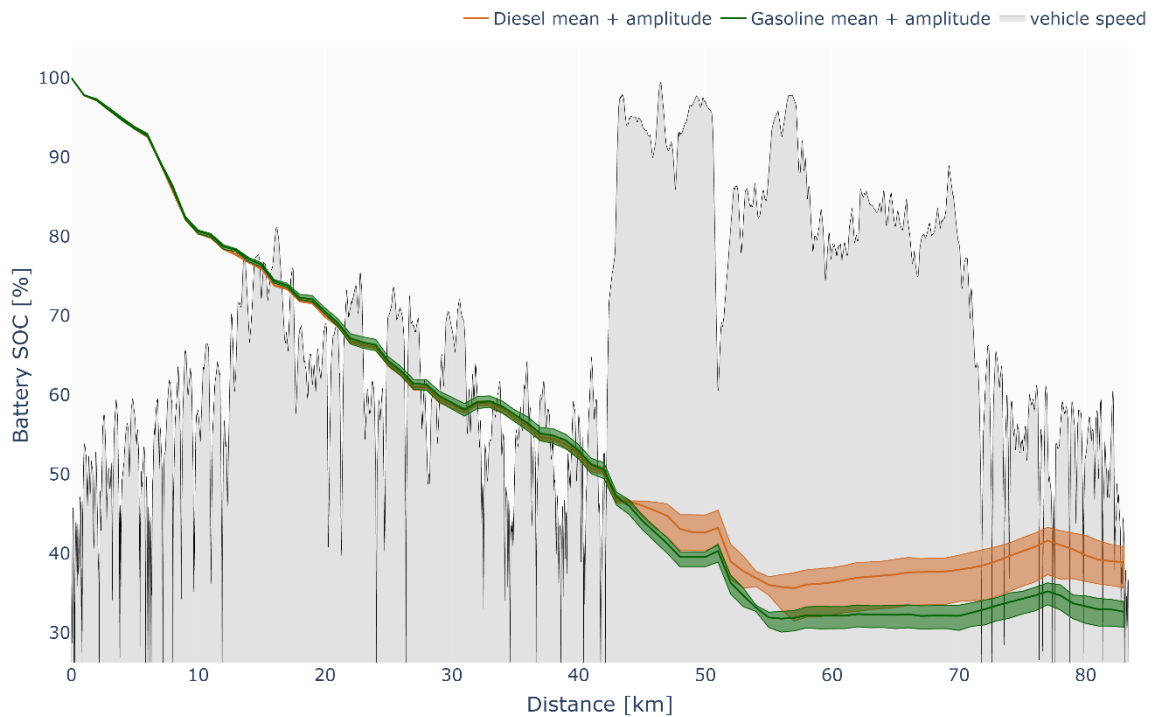


Figure 9 Comparison of Battery State of Charge [%] in depleting mode on RDE cycles on chassis dyno for B7 and E10.

Figure 10 depicts the utility factors, i.e., the percentage of distance driven in all-electric mode. The Diesel PHEV fuelled with B7 shows 8.8% lower electric driving mode in CD and 20.7% less in CS compared to E10. This behaviour can be linked to a difference of calibration between the Petrol and Diesel PHEV, as the thermal engine efficiency may differ and the fuel properties are in favour of the Diesel vehicle, the electric usage may decrease. This behaviour is consistent with the analysis made on the electrical consumption. Switching from standard (E10 and B7) to renewable fuels (E20 and HVO) has no significant impact on the UF, neither in CS nor CD. Likewise, HEV demonstrated UF similar to PHEV ones in CS, for both the gasoline and the Diesel vehicle.

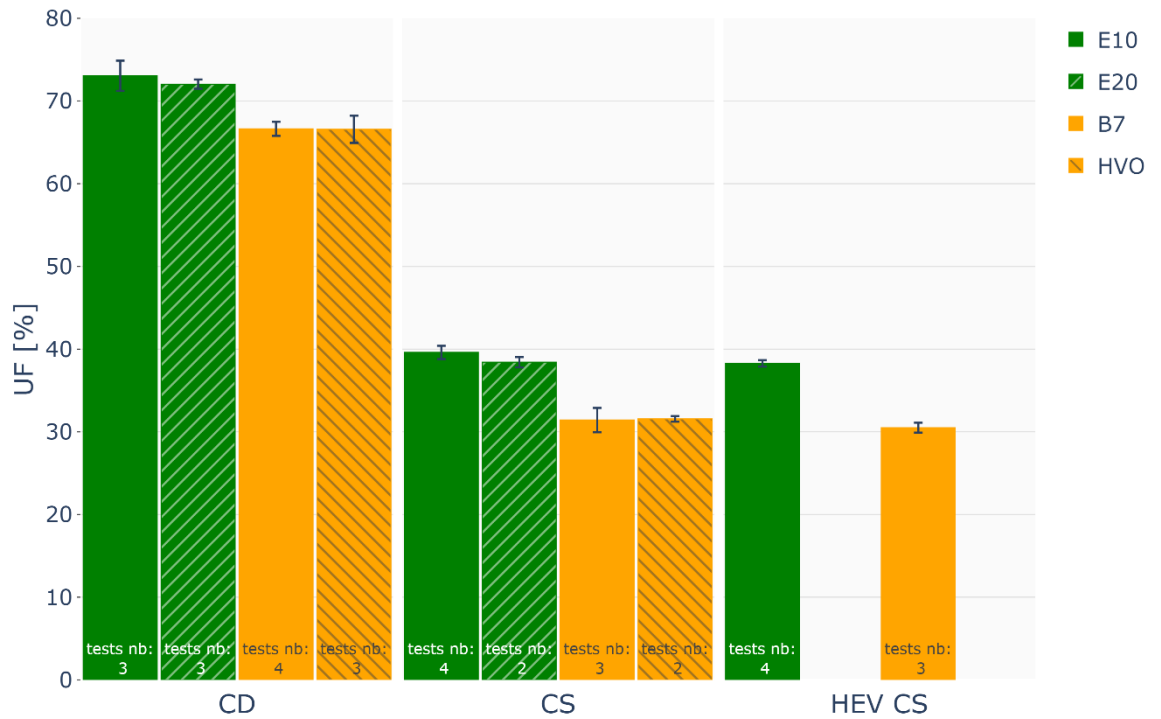


Figure 10 Comparison of Utility factor [%] measured on RDE cycles on chassis dyno for each fuel and mode.

2.4.5.3. Carbon Dioxide emissions

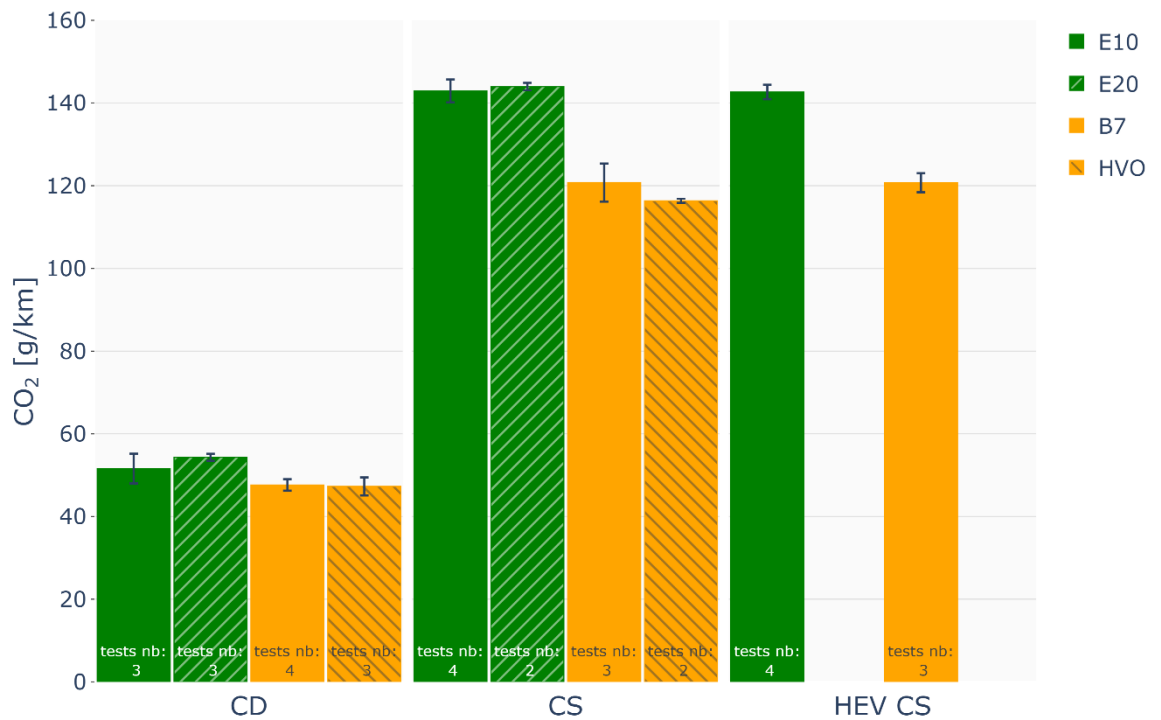


Figure 11 Comparison of tailpipe CO₂ emissions [g/km] measured on RDE cycles on chassis dyno for each fuel and mode.

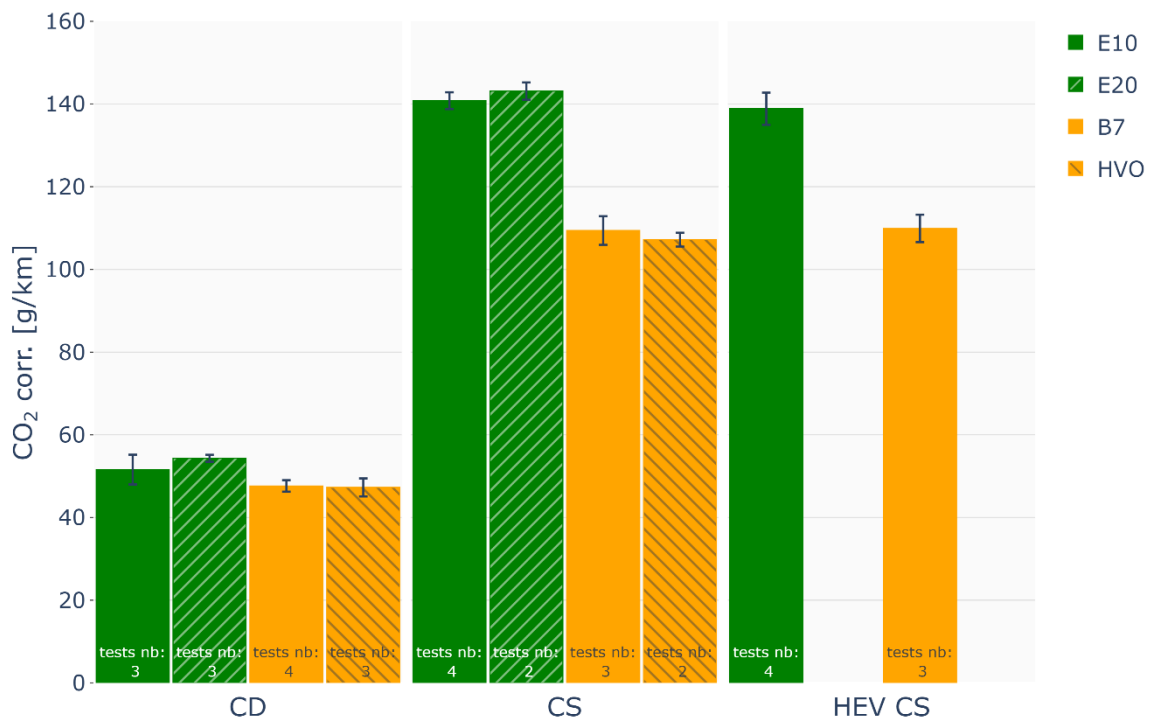


Figure 12 Comparison of corrected tailpipe CO₂ emissions [g/km] measured on RDE cycles on chassis dyno for each fuel and mode.

Tailpipe CO₂ emissions differences between E10, E20, B7 and HVO are shown in Figure 11. In charge sustaining mode, the Diesel technology shows a reduction of 15.5 % of CO₂ emissions (22.3 % when CO₂ is corrected to return to iso SOC CS condition) compared to the gasoline one. This is consistent with the statements made above on volumetric fuel consumption, and the CO₂ emission factors of the respective fuels.

Using renewable fuels, E20 does not significantly impact the CO₂ emissions compared to E10. On the contrary, HVO shows lower CO₂ emissions by 3.6 % (2.0 % when corrected) compared to B7 in charge sustaining mode, thanks to its lower CO₂ emission factor.

Reducing the mass of the vehicle, HEV mode, does not impact the CO₂ emissions, for gasoline, as well as for Diesel. As for the volumetric fuel consumption, it is a quite surprising result

2.4.5.4. Total GHG emissions, including CH₄ and N₂O emissions (Engine-out and Tailpipe Emissions)

As a reminder, CH₄ and N₂O are greenhouse gases having global warming potential (GWP) significantly higher than CO₂. Estimations from the fifth assessment report (AR5) of the IPCC (Intergovernmental Panel on Climate Change) define a GWP of 28 for CH₄ and 265 for N₂O for a hundred-year time horizon. Thus, despite emissions levels generally three orders of magnitude below CO₂ emissions, these emissions have to be considered for a proper assessment of TtW greenhouse gases emissions.

Adding non-regulated greenhouse gases leads to an increase of total GHG compared to CO₂ only by around 3% in Diesel and 0.8% in gasoline. The main contributor to this CO₂ equivalent increase is the N₂O, because of its high GWP and because almost no CH₄ is released at the tailpipe. As more N₂O is emitted by the Diesel PHEV, the -

22.3% CO₂ emissions gap that was quantified between gasoline and Diesel vehicles is reduced to -20.5% considering total GHG emissions.

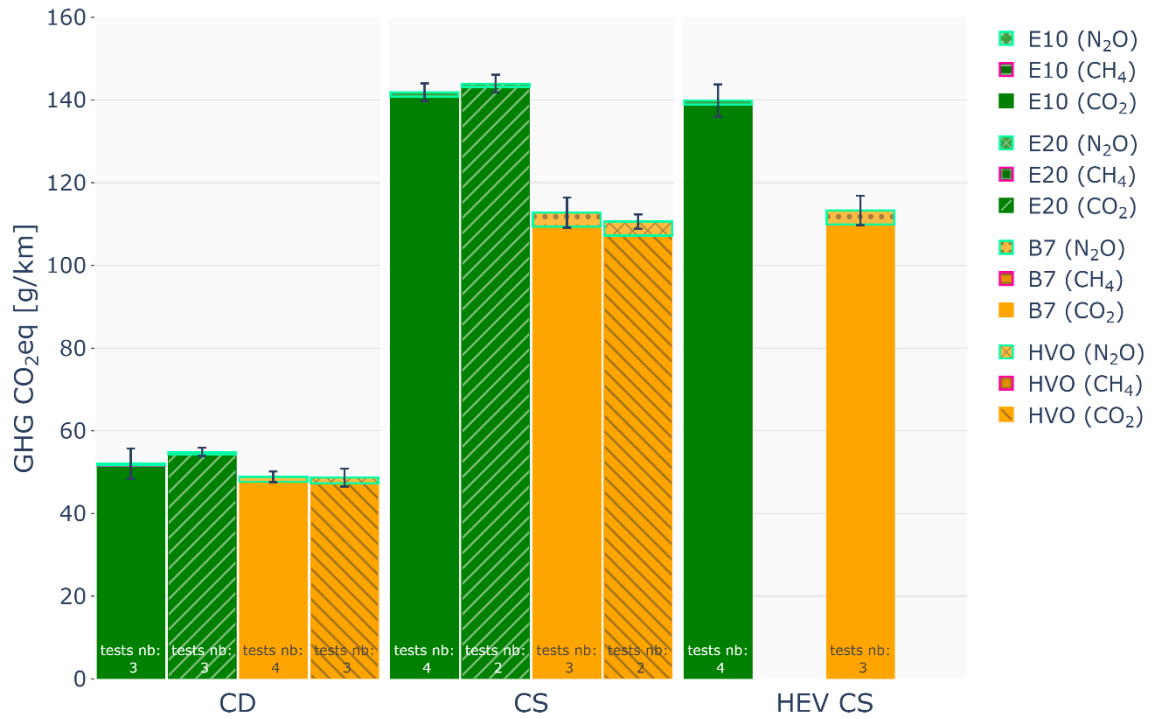


Figure 13 Comparison of tailpipe greenhouse gases emissions [g CO₂eq/km] measured on RDE cycles on chassis dyno for each fuel and mode.

Details of N₂O and CH₄ emissions, both engine-out and tailpipe, to underline the origin of these, are presented below.

Concerning tailpipe CH₄ emissions (*Figure 15*), both Diesel and gasoline vehicles show similarly low levels, around 0.3 mg/km, representing less than 10 mg of CO₂ equivalent / km. Engine-out (*Figure 14*), the gasoline engine emits significant amounts of CH₄ whereas levels of the Diesel one are low, around 1 mg/km. E20 demonstrates higher engine-out CH₄ emissions compared to E10, respectively +34% in CD and +31% in CS. This finding is similar to the one established for total HC (cf. paragraph 2.4.5.8). As mentioned before, these emissions are anyway converted by the after-treatment system since they are very low at the tailpipe.

Concerning engine-out N₂O emissions (*Figure 16*), E10 emissions are 217 % higher than B7 in CS mode but the observed trend is inverted at the tailpipe (*Figure 17*): the E10 tailpipe N₂O emissions are not increased by the aftertreatment system (AFTS), whereas B7 tailpipe N₂O emissions are sensibly impacted by the AFTS and are 3 times higher than E10 emissions. This is expected to be due to reactions occurring in the SCR. Even if the emissions levels seem low it represents up to 3 g of CO₂ equivalent / km (12 mg of N₂O / km).

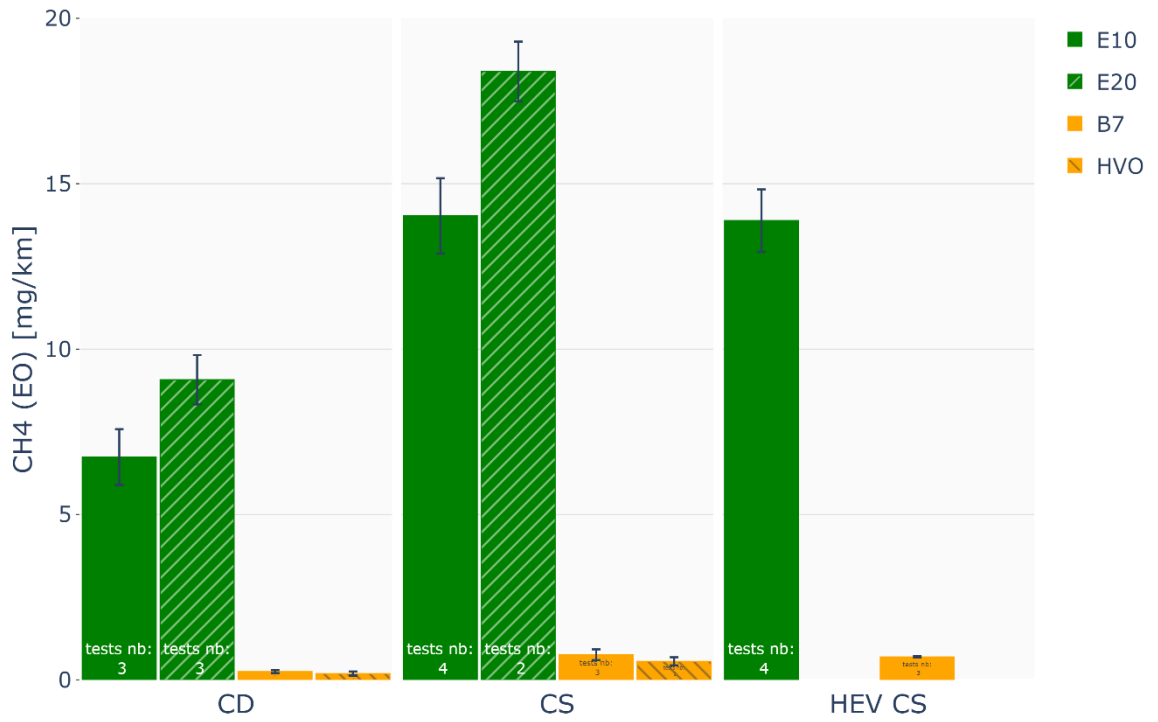


Figure 14 Comparison of engine-out CH₄ emissions [mg/km] measured on RDE cycles on chassis dyno for each fuel and mode.

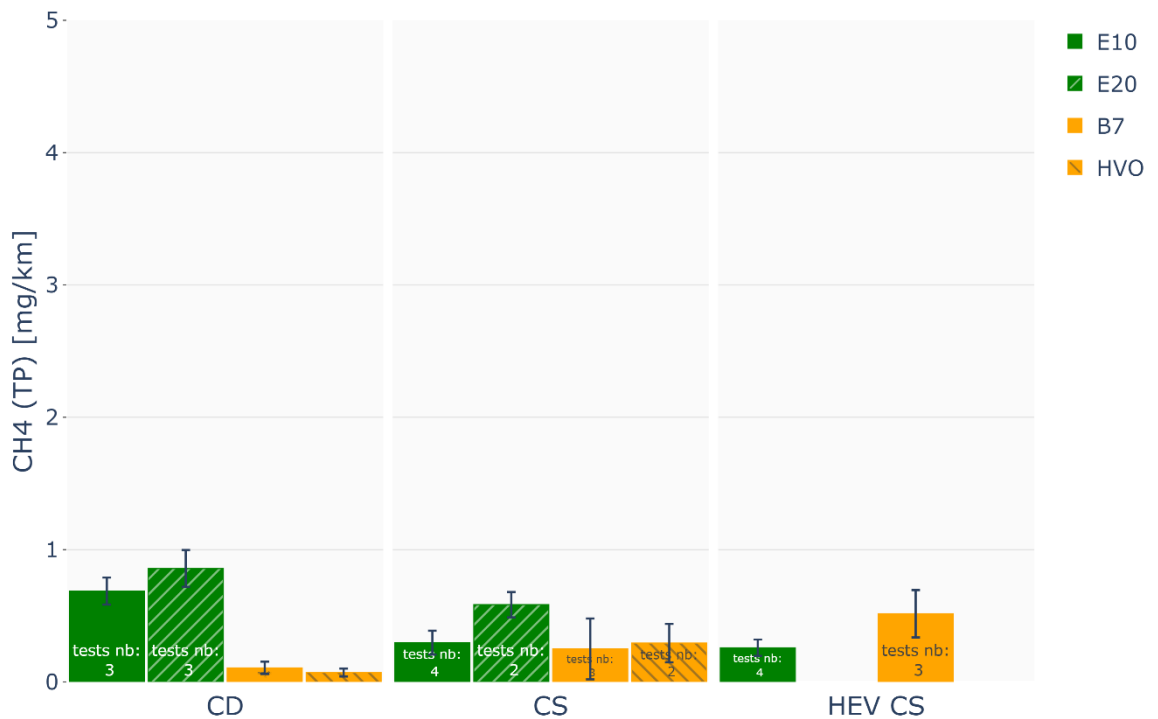


Figure 15 Comparison of tailpipe CH₄ emissions [mg/km] measured on RDE cycles on chassis dyno for each fuel and mode.

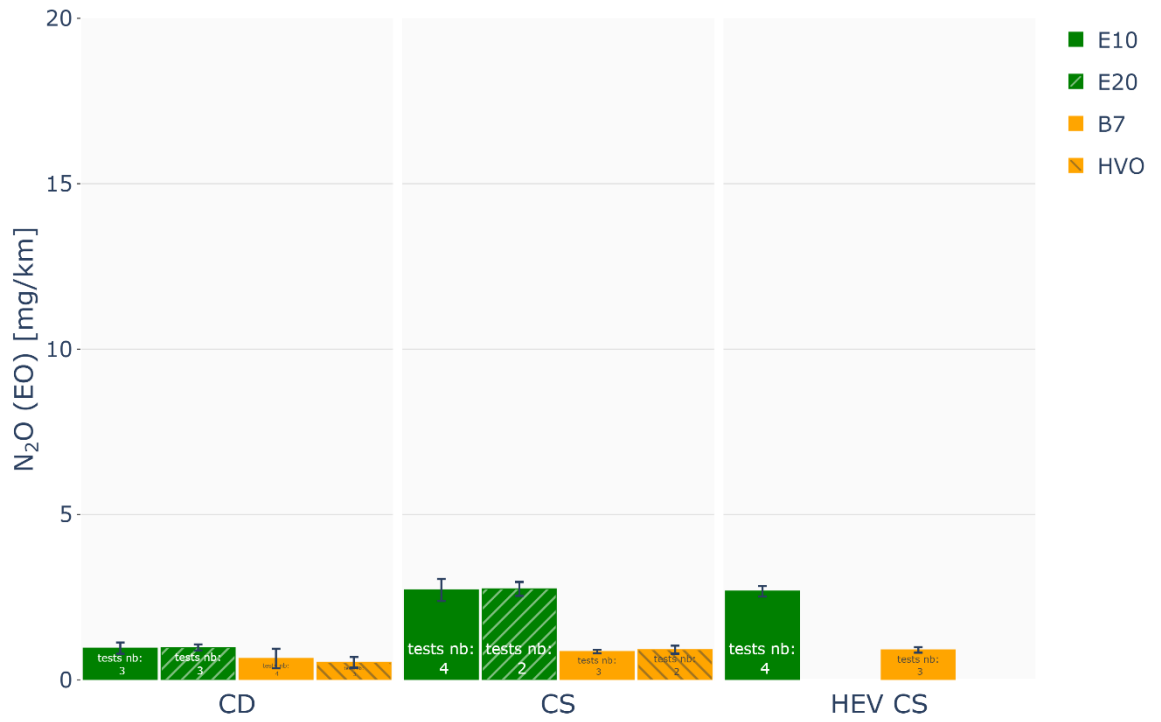


Figure 16 Comparison of engine-out N₂O emissions [mg/km] measured on RDE cycles on chassis dyno for each fuel and mode.

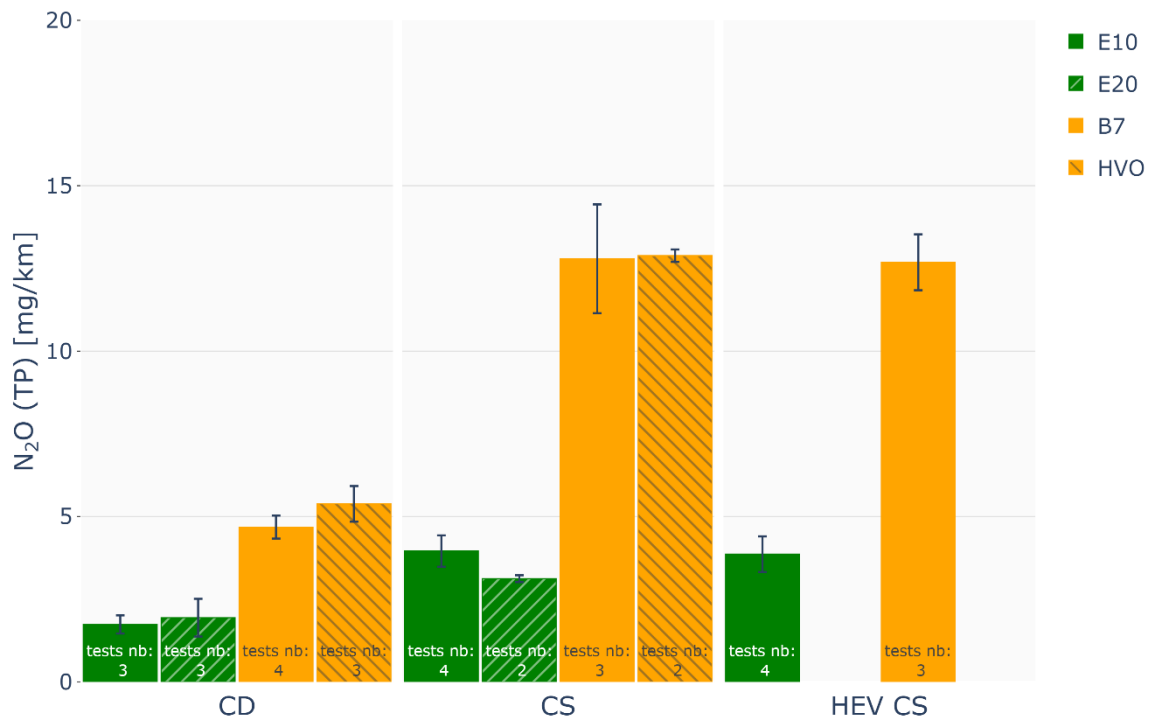


Figure 17 Comparison of tailpipe N₂O emissions [mg/km] measured on RDE cycles on chassis dyno for each fuel and mode.

2.4.5.5. Oxides of Nitrogen (NO_x) engine-out and tailpipe emissions

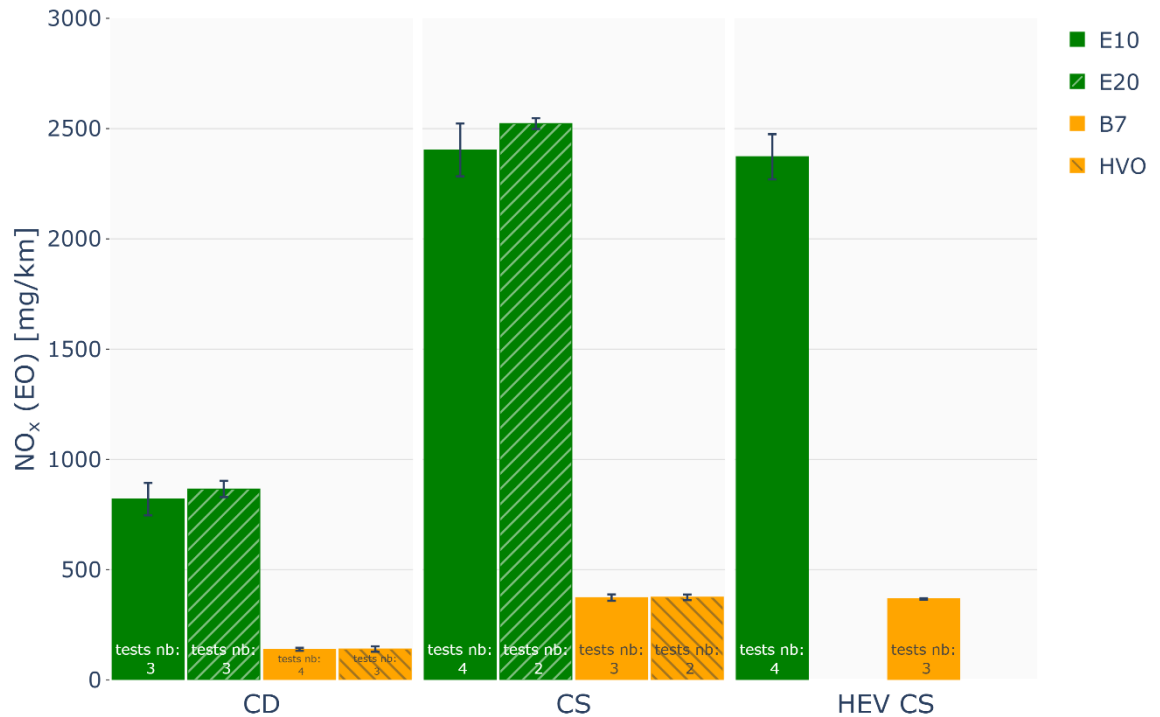


Figure 18 Comparison of engine-out NO_x emissions [mg/km] measured on RDE cycles on chassis dyno for each fuel and mode.

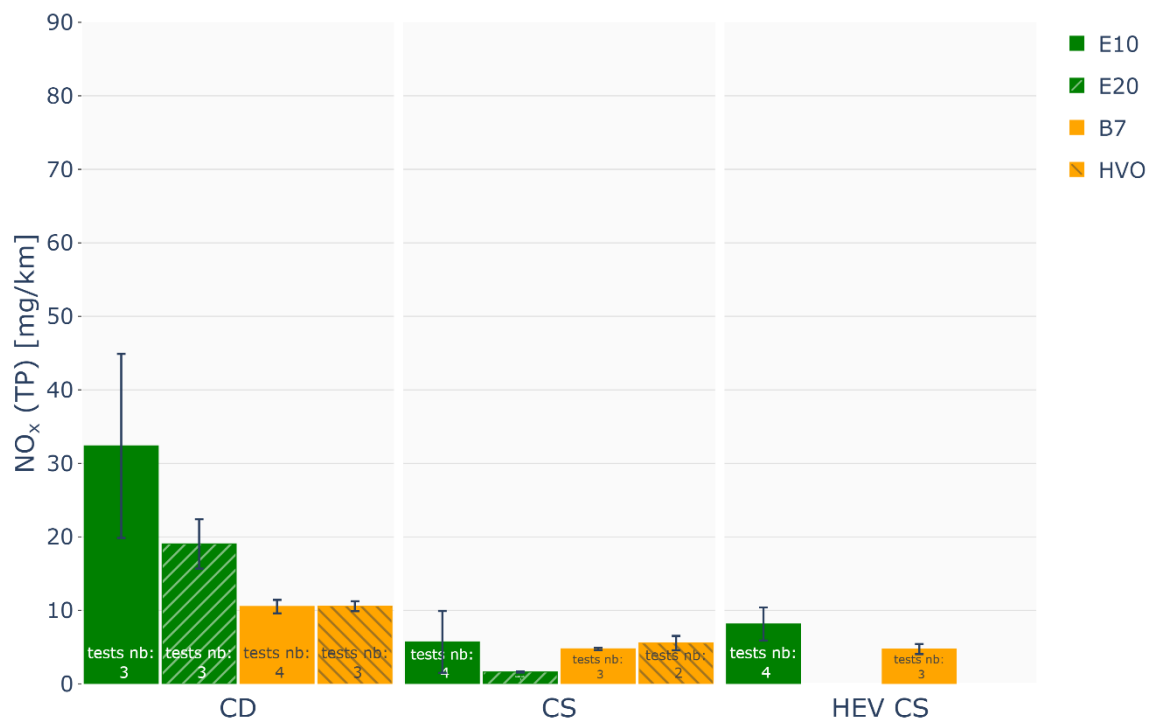


Figure 19 Comparison of tailpipe NO_x emissions [mg/km] measured on RDE cycles on chassis dyno for each fuel and mode.

As expected from the literature, the Diesel engine using EGR emits less engine-out NO_x than the stoichiometric gasoline one: around 80% less both in CS and CD (*Figure 18*). At the tailpipe (*Figure 19*), the first observation is that both B7 and E10 vehicles

have very low emissions level in CS mode, below 10 mg/km, bearing in mind that the Euro6d limits for NO_x emissions are 60 mg/km for gasoline and 80 mg/km for Diesel. In CD mode, the gasoline PHEV has higher NO_x emissions than the Diesel one, mostly due to the cold start of the engine during the motorway phase.

Switching to renewable fuels has no significant impact on the engine-out NO_x emission levels. At the tailpipe, HVO does not have a significant effect on NO_x emissions compared to B7, when E20 shows a reduction of tailpipe NO_x emissions compared to E10, both in CD and CS mode. Changing from PHEV to HEV has no significant impact neither on the engine-out and tailpipe NO_x emission levels.

As the very low NO_x tailpipe level could foreshadow, the NO_x AFTS, i.e., the three-way catalyst for the gasoline PHEV and the SCR for Diesel PHEV, demonstrates high conversion efficiencies, over 95% in CS mode, as shown in *Figure 20*. Despite higher engine-out NO_x emissions, E20 shows lower tailpipe NO_x compared to E10 in CD and in CS, de facto improving the AFTS conversion efficiency. HVO does not impact NO_x AFTS conversion efficiency compared to B7, nor does HEV compared to PHEV.

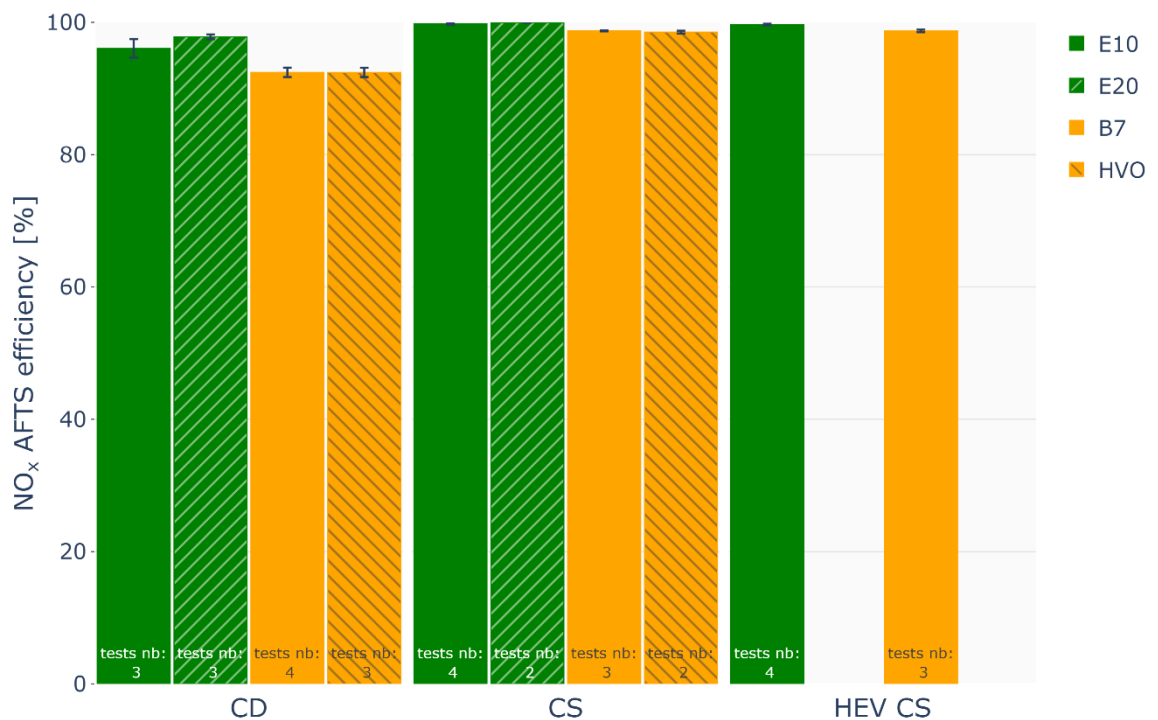


Figure 20 Comparison of NO_x AFTS conversion efficiency [%] measured on RDE cycles on chassis dyno for each fuel and mode.

2.4.5.6. Particulate Mass and Particle Number engine-out and tailpipe emissions

Engine-out particle emissions are globally higher for the Diesel PHEV compared to the gasoline PHEV, for both PN23 (*Figure 21*) and PN10 (*Figure 22*). This finding is in line with the well-known behaviour of Compression Ignited engine compared to Spark Ignited engines (diffusion flame vs premixed flame). The Diesel PHEV fuelled with B7 emits almost 200 times more PN23 engine-out compared to the gasoline PHEV fuelled with E10 in CS mode and around 50 times more for PN10. Compared to E10, E20 tends to increase by a factor of 4.4 engine-out PN23 and by 3.6 engine-out PN10 in CS mode.

At the tailpipe, and as expected from the literature, the gasoline PHEV emits more PN23 (*Figure 23*) or PN10 (*Figure 24*) than the Diesel PHEV. In CS mode, the gasoline

PHEV fuelled with E10 emits around 480% more particle compared to the Diesel PHEV fuelled with B7, regardless of the cut diameter considered at 10 or 23 nm. E20 or HVO have no significant impact on tailpipe PN23 or PN10 compared to E10 or B7, nor the HEV configuration compared to PHEV. In all the tested configurations, the tailpipe PN emissions are far below the Euro 6d limits.

Figure 25 and Figure 26 exhibit the PN filter efficiency, i.e., GPF for the gasoline PHEV and DPF for the Diesel PHEV. The DPF efficiencies are higher than the GPF ones, in agreement with the existing literature. HVO does not have a significant impact on the DPF efficiency, nor the HEV configuration for PN23 or PN10 filtration. As on the one hand, E20 tends to increase engine-out PN23 and PN10 compared to E10, and on the other hand, E20 tailpipe PN23 or PN10 are similar to E10 ones, the GPF filtration efficiencies with E20 are higher than with E10. HEV configuration does not impact the GPF filtration efficiency.

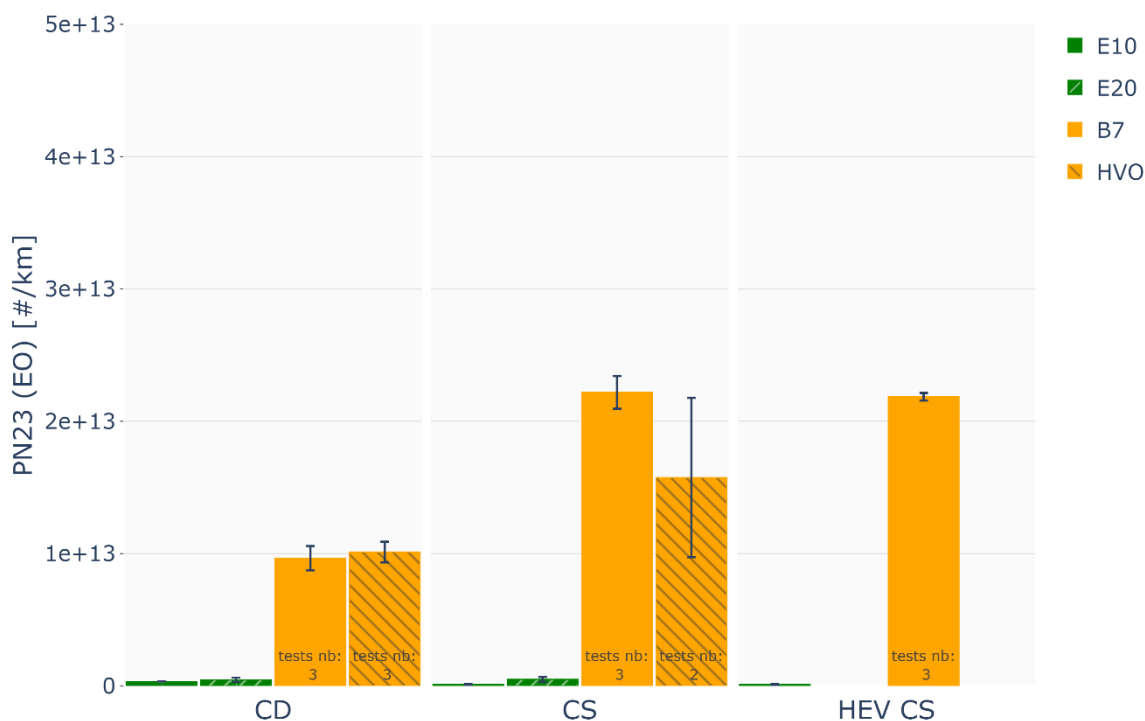


Figure 21 Comparison of engine-out PN23 emissions [#/km] measured on RDE cycles on chassis dyno for each fuel and mode.

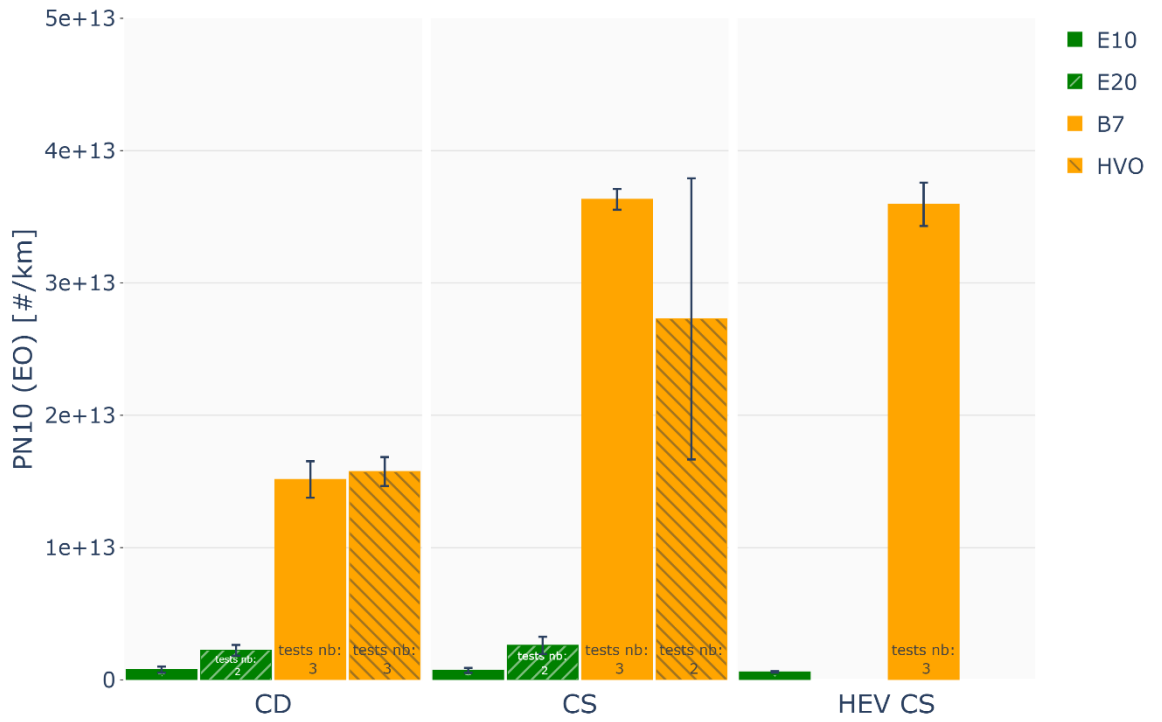


Figure 22 Comparison of engine-out PN10 emissions [#/km] measured on RDE cycles on chassis dyno for each fuel and mode.

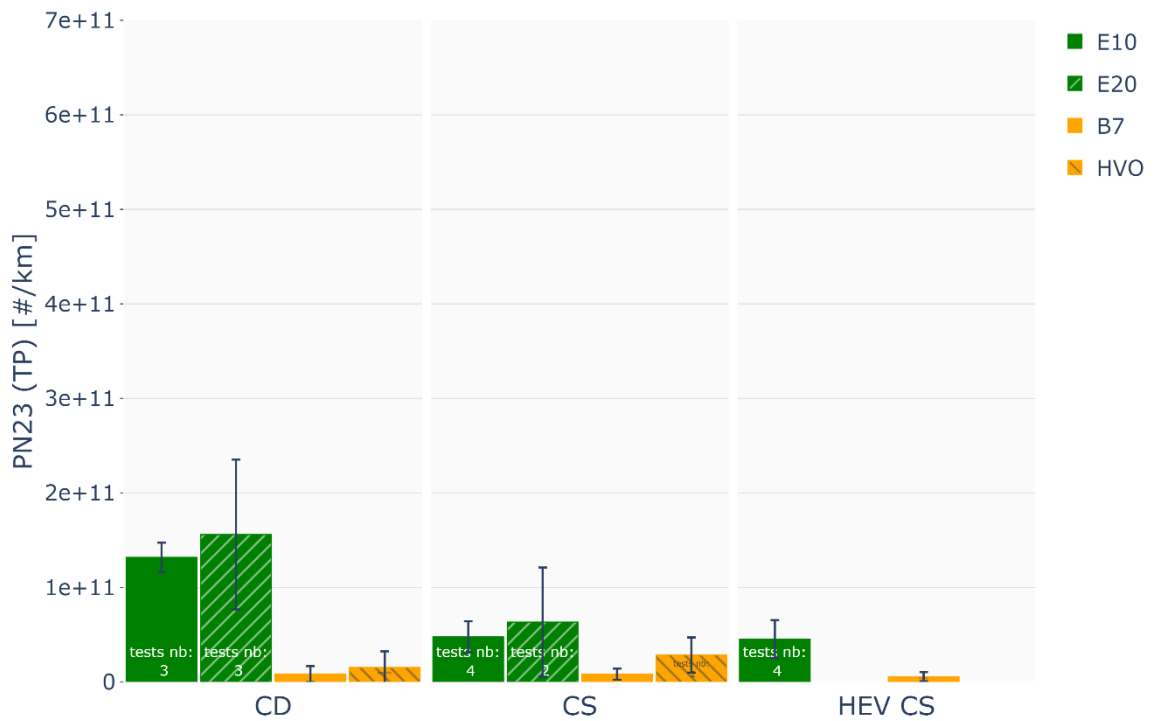


Figure 23 Comparison of tailpipe PN23 emissions [#/km] measured on RDE cycles on chassis dyno for each fuel and mode.

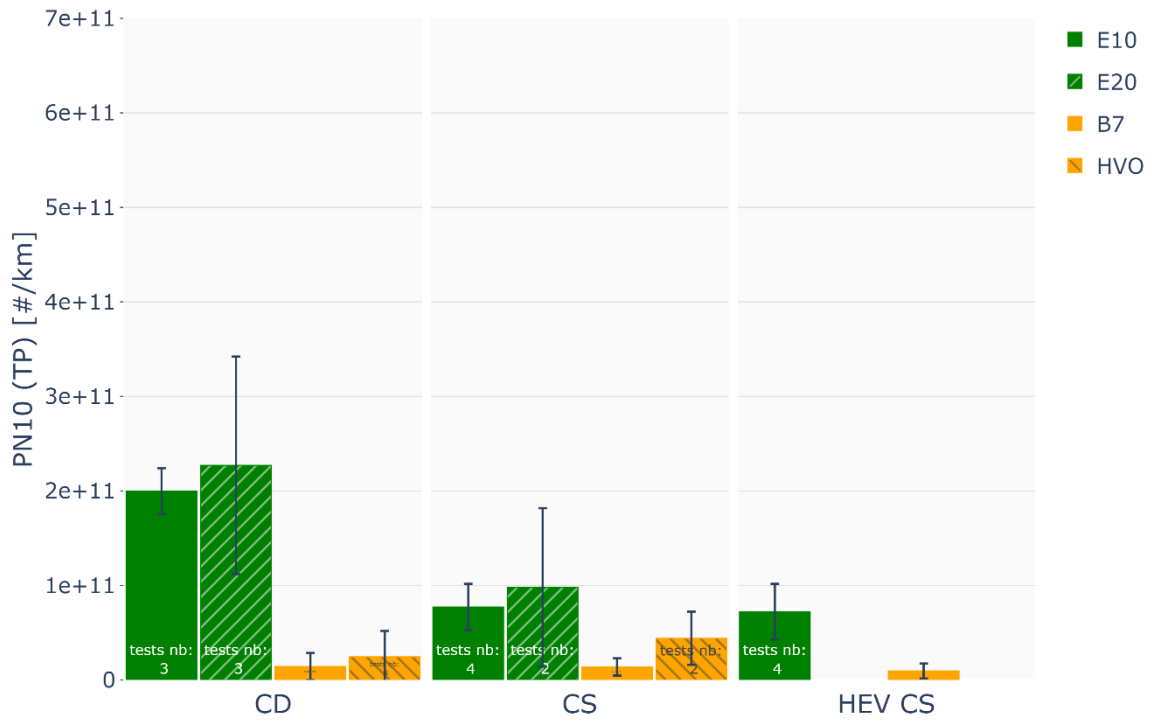


Figure 24 Comparison of tailpipe PN10 emissions [#/km] measured on RDE cycles on chassis dyno for each fuel and mode.

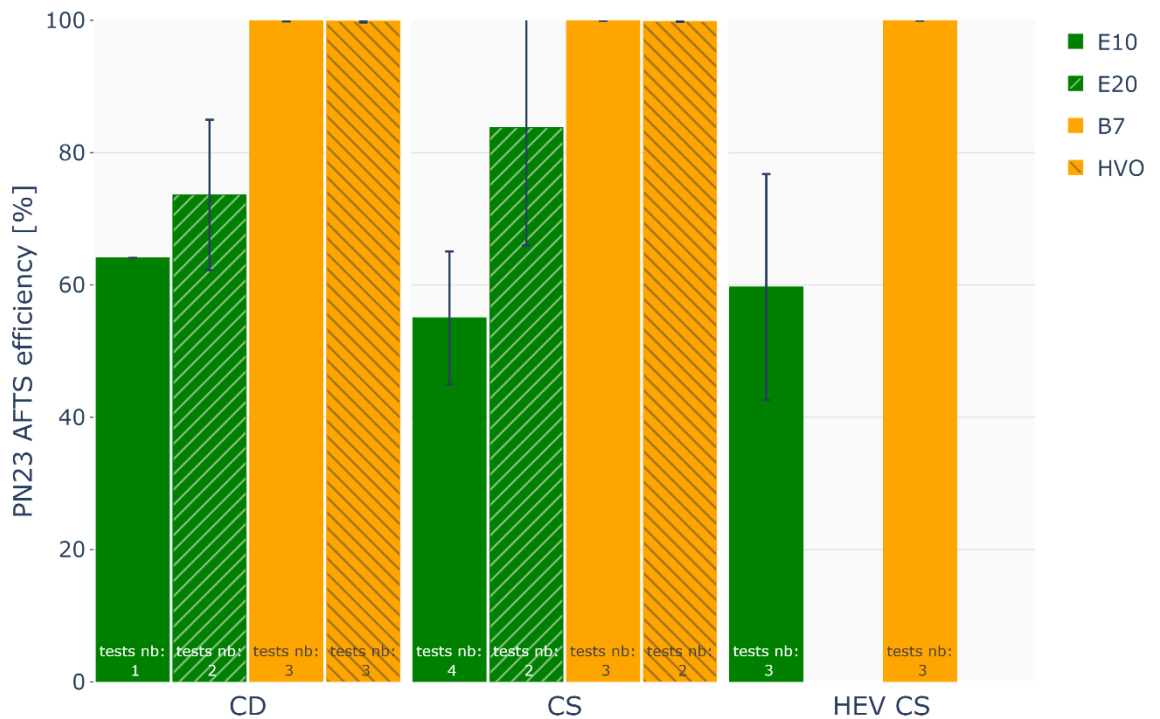


Figure 25 Comparison of PN23 efficiency [%] measured on RDE cycles on chassis dyno for each fuel and mode.

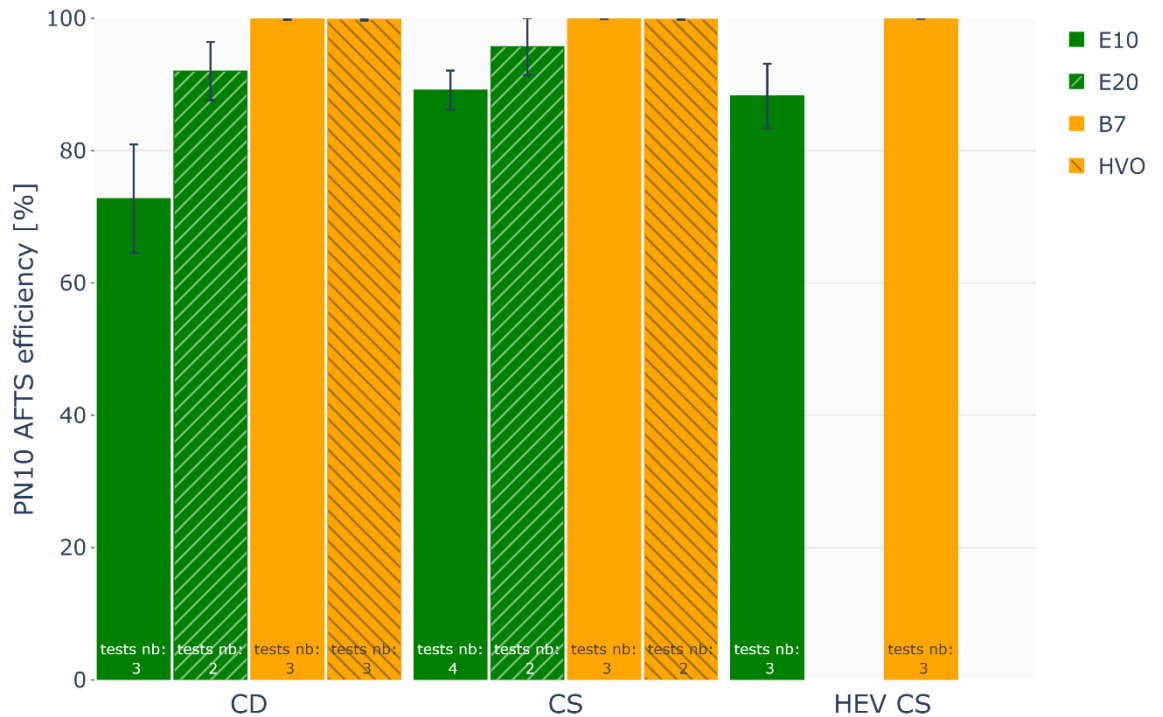


Figure 26 Comparison of PN10 efficiency [%] measured on RDE cycles on chassis dyno for each fuel and mode.

Figure 27 and Figure 28 shows DMS500 measurement results at the tailpipe for a representative cycle with B7 and E10 respectively. As shown previously, levels for E10 are higher than for B7. The DMS500 device makes it possible to evaluate the particle size distribution at each moment of the test. The particles have larger diameters for gasoline than for Diesel. This is due to the filtration technology used, and the sensitivity of engine performance to the back pressure of the gasoline powertrain which induces the need to manage a trade-off between filtration efficiency and fuel consumption. Also, B7 emissions are mainly located around the engine start. E10 emissions are higher at engine start and are sensitive to the driving behavior and enrichment phases (motorway insertion, around 3500s in Figure 28).

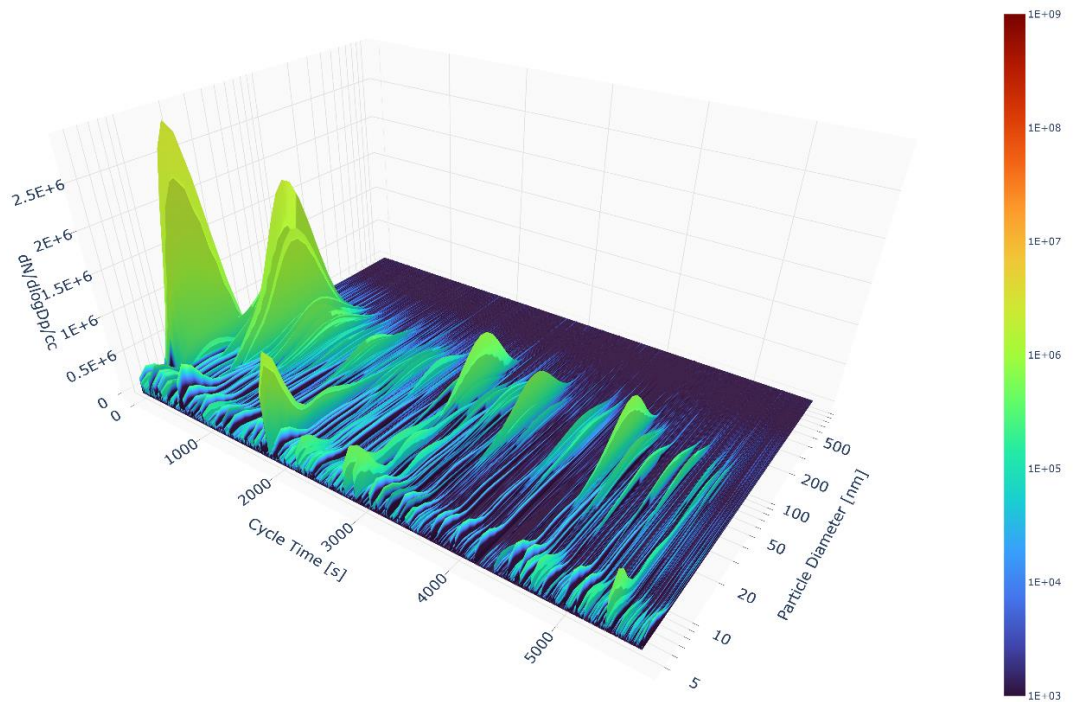


Figure 27 Spectrum of tailpipe PN emissions measured with DMS500 - RDE test cycle, roller test bench, CS mode, Diesel vehicle, B7

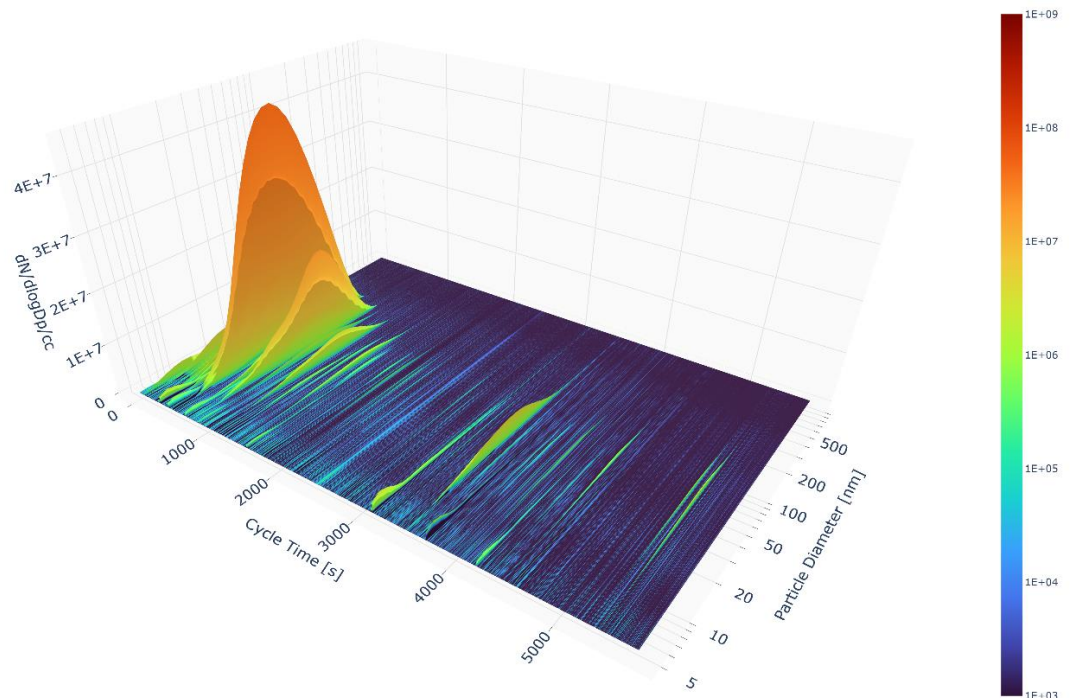


Figure 28 Spectrum of Tailpipe PN emissions measured with DMS500 - RDE test cycle, roller test bench, CS mode, gasoline vehicle, E10

Figure 29 shows PM emissions at the tailpipe. These values are to be compared with Euro 6d levels of 4.5 mg/km. Both vehicles show very low level of particulate matter in mass.

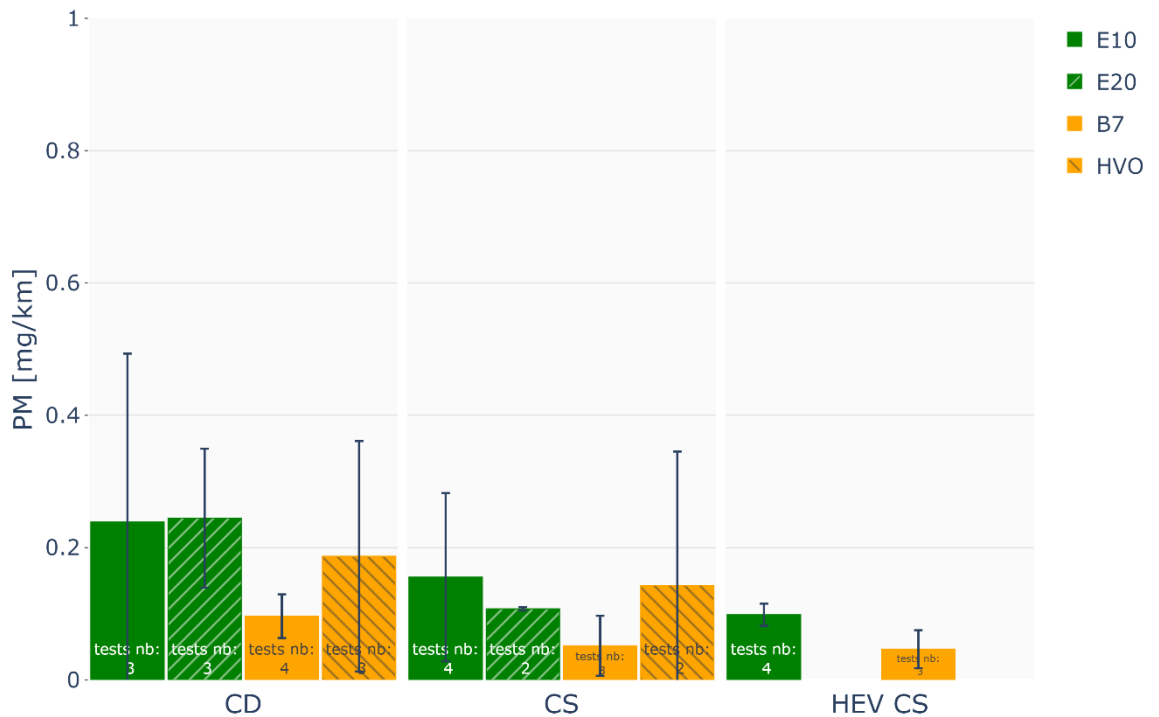


Figure 29 Comparison of tailpipe PM emissions [mg/km] measured on RDE cycles on chassis dyno for each fuel and mode.

2.4.5.7. Carbon Monoxide engine-out and tailpipe emissions

Concerning engine-out CO emissions (*Figure 30*), the Diesel PHEV fuelled with B7 emits 92% less than the gasoline PHEV fuelled with E10 in CS mode. E20 does not have any impact on CO engine-out emissions compared to E10, when HVO tends to reduce engine-out CO emissions by 24% compared to B7 in CS. HEV does not affect engine-out CO emissions, neither for gasoline nor for Diesel vehicles.

At the tailpipe (*Figure 31*), the first analysis for the CO levels is that the Diesel and gasoline PHEVs show very low emissions level in CS mode, below 60 mg/km for E10/E20 (compared to the Euro6d limit of 1000 mg/km), and below 10 mg/km for B7/HVO (compared to Euro6d limits of 500 mg/km). The tailpipe CO emissions of the gasoline PHEV fuelled with E10 are higher than those of the Diesel PHEV fuelled by B7, by around 300% in CS mode, with B7 emissions of less than 8mg/km. HVO tends to reduce by 59% the tailpipe CO emissions compared to B7 in CS whereas E20 increases tailpipe CO emissions by 113% compare to E10.

Figure 32 exhibits CO AFTS conversion efficiency, i.e., three-way catalyst for the gasoline PHEV and DOC for the Diesel PHEV. Three-way catalyst and DOC show similarly high conversion efficiencies. Neither E20, nor HVO, nor HEV configuration have any impact on the CO conversion efficiencies.

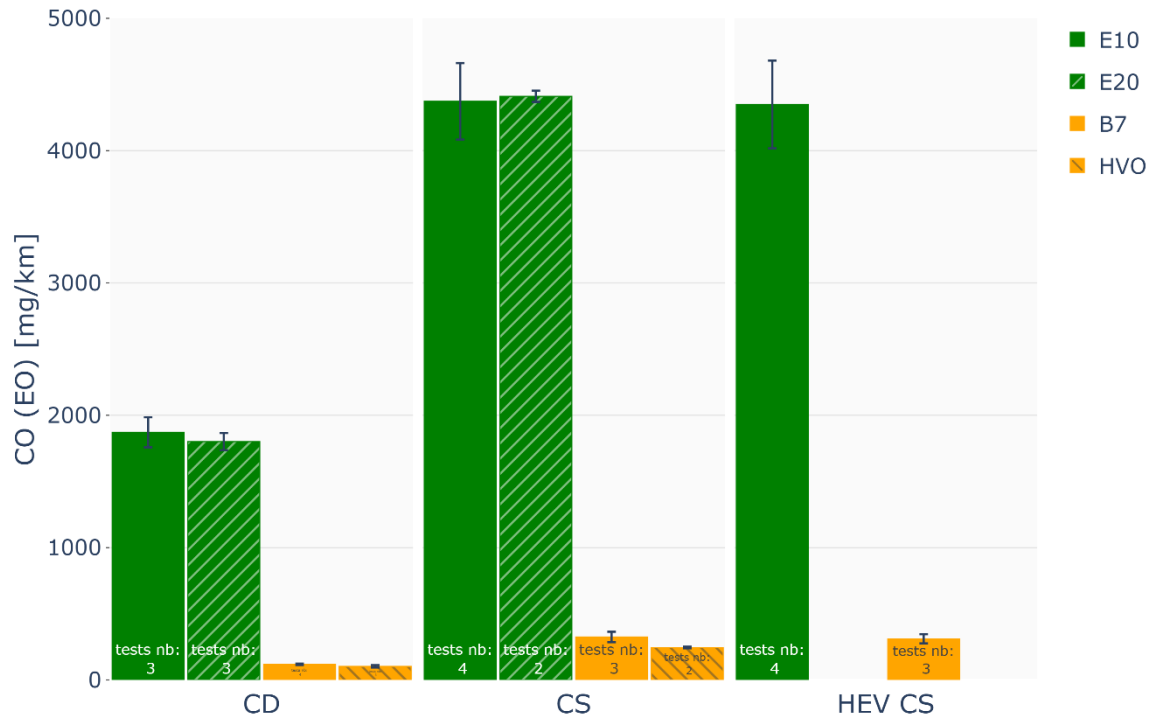


Figure 30 Comparison of engine-out CO emissions [mg/km] measured on RDE cycles on chassis dyno for each fuel and mode.

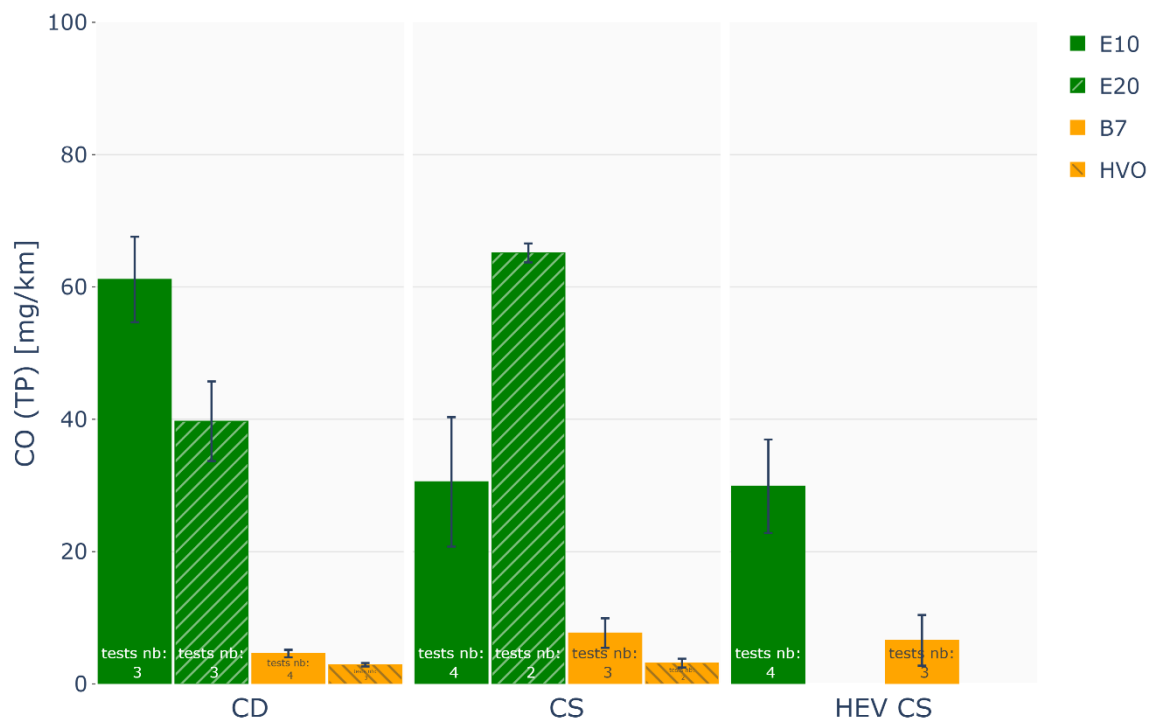


Figure 31 Comparison of tailpipe CO emissions [mg/km] measured on RDE cycles on chassis dyno for each fuel and mode.

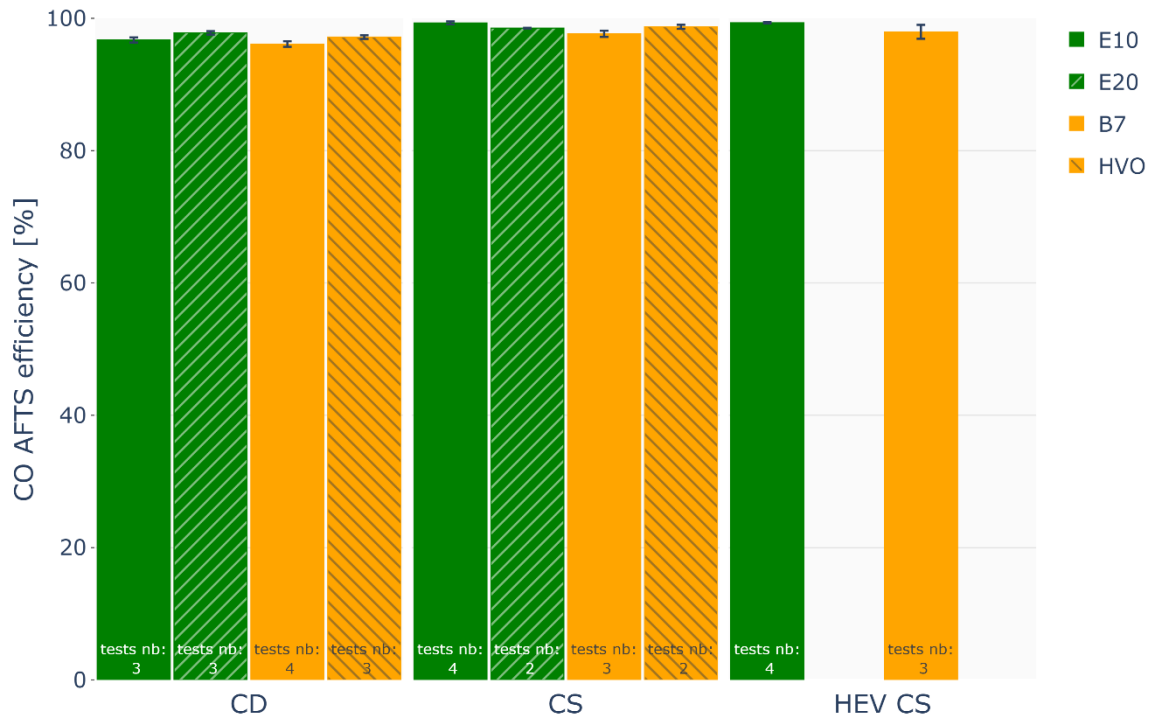


Figure 32 Comparison of CO AFTS conversion efficiency [%] measured on RDE cycles on chassis dyno for each fuel and mode.

2.4.5.8. Hydrocarbons engine-out and tailpipe emissions

Figure 33 depicts THC engine-out emissions. The Diesel PHEV fuelled with B7 shows 89 % lower engine-out THC emissions compared to the gasoline PHEV fuelled with E10 in CS. E20 shows 45 % higher engine-out THC emissions compared to E10 in CS. HVO (compared to B7) and HEV (compared to PHEV) configuration have no significant effect on the engine-out THC emissions.

Figure 34 shows the THC tailpipe emissions. Very low tailpipe THC emissions performed by the gasoline PHEV and the Diesel PHEV are observed, below 10 mg/km in both fuel type, compared to a Euro 6d limit of 100 mg/km for gasoline vehicles and 90 mg/km (170-80) for Diesel vehicles. The tailpipe THC emissions of the Diesel PHEV fuelled with B7 are 80 % lower than the ones of the gasoline PHEV fuelled with E10 in CS.

Figure 35 exhibits THC AFTS conversion efficiency, i.e., three-way catalyst for the gasoline PHEV and DOC for the Diesel PHEV. Both technologies show similar conversion efficiencies, above 95 % in CS. Neither E20 (compared to E10), nor HVO (compared to B7), nor HEV (compared to PHEV) configuration have any impact on the THC conversion efficiencies.

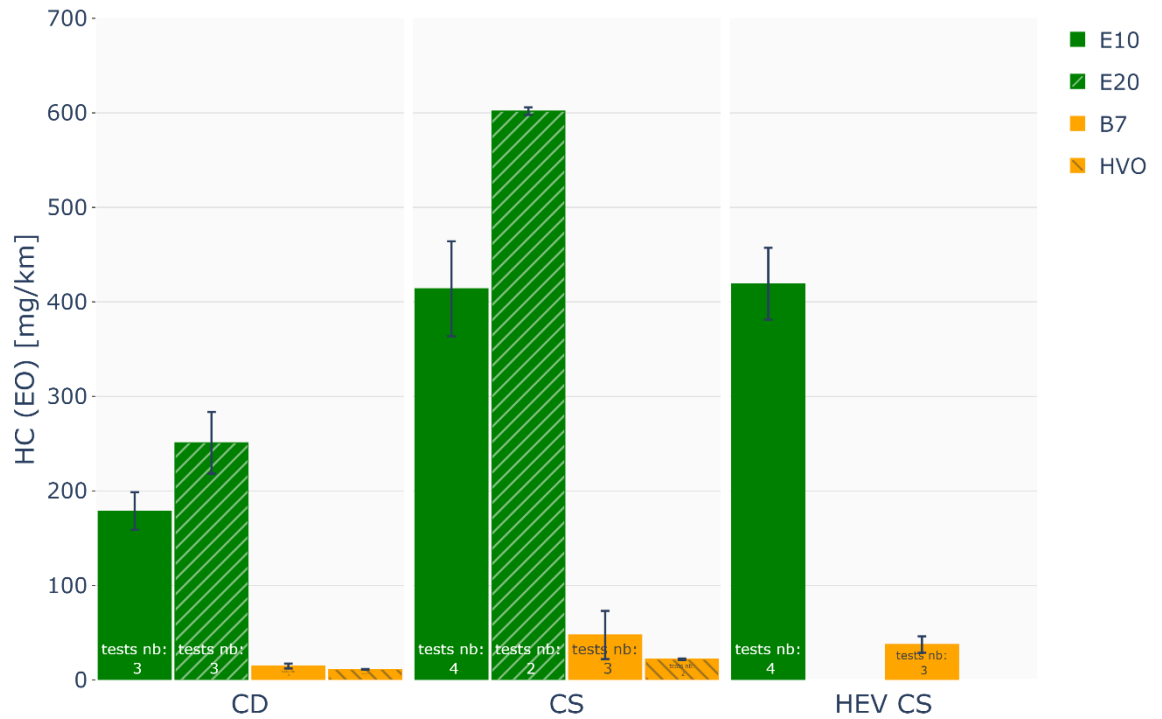


Figure 33 Comparison of engine-out THC emissions [mg/km] measured on RDE cycles on chassis dyno for each fuel and mode.

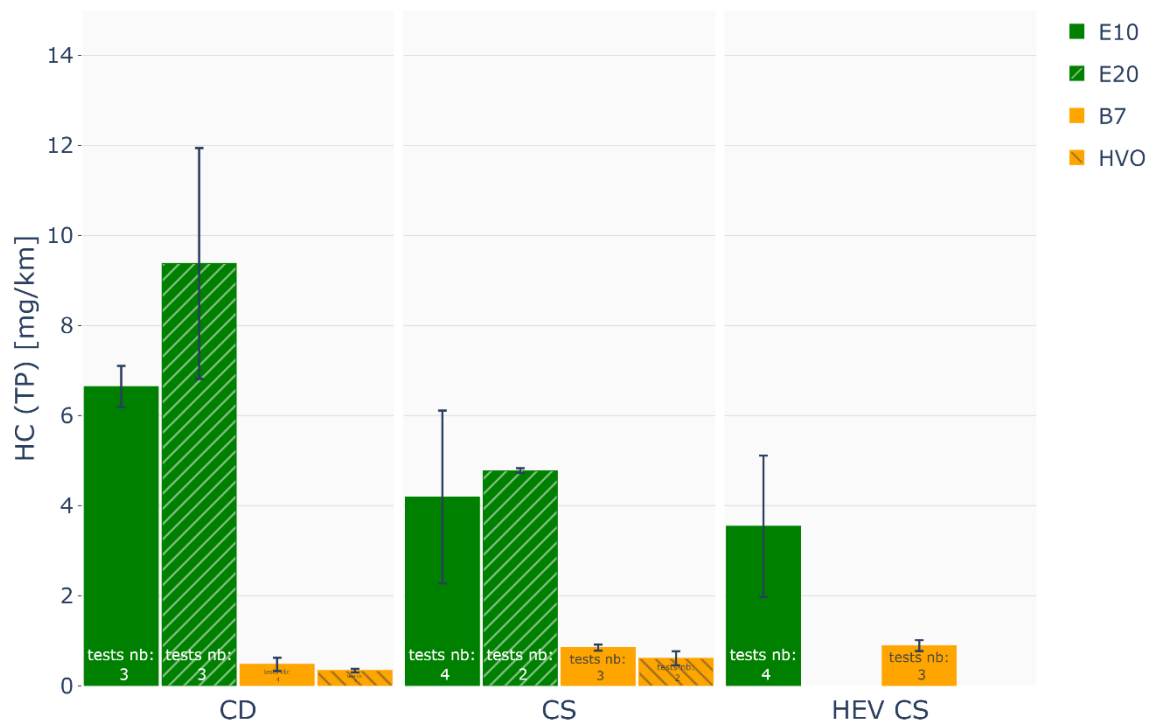


Figure 34 Comparison of tailpipe THC emissions [mg/km] measured on RDE cycles on chassis dyno for each fuel and mode.

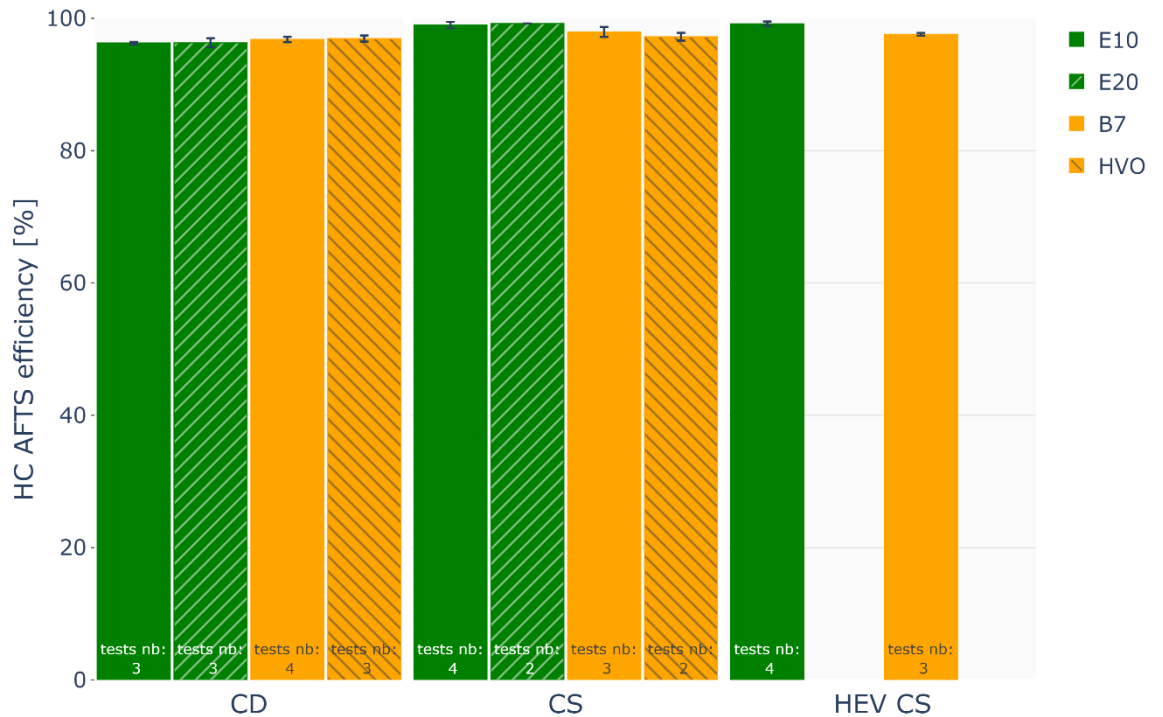


Figure 35 Comparison of THC AFTS efficiency [%] measured on RDE cycles on chassis dyno for each fuel and mode.

2.4.5.9. Ammonia (Engine-out and Tailpipe Emissions)

Figure 36 and Figure 37 illustrate respectively engine-out and tailpipe NH_3 emissions. As expected, no NH_3 is emitted at the engine-out of both the gasoline PHEV and the Diesel PHEV. At the tailpipe, the Diesel PHEV shows an increase of the NH_3 released, due to the NO_x after treatment technology that is urea-based. Most of the NH_3 is released during the motorway phase of the RDE, as the urea injector instrumentation confirms (cf. Figure 38). The typical behaviour observed is that NH_3 slip occurs when a threshold of temperature, and probably gas hourly space velocity (GHSV) is crossed. Those conditions are met when driving on motorway.

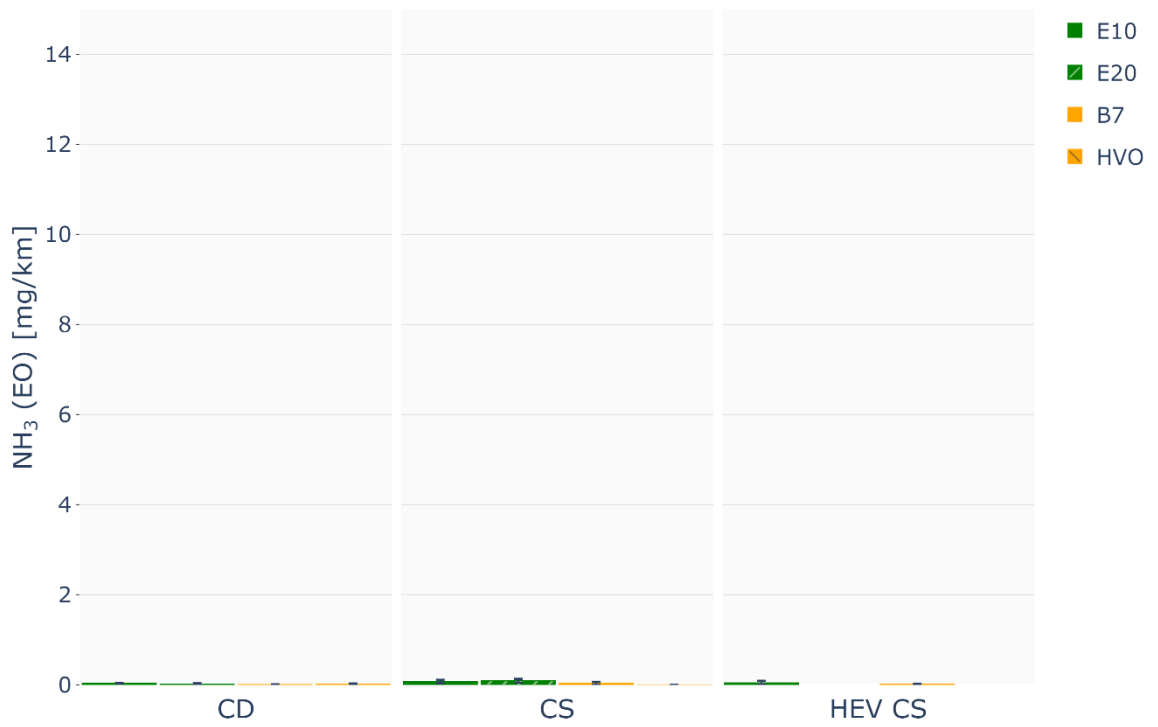


Figure 36 Comparison of Engine-out NH₃ emissions [mg/km] measured on RDE cycles on chassis dyno for each fuel and mode.

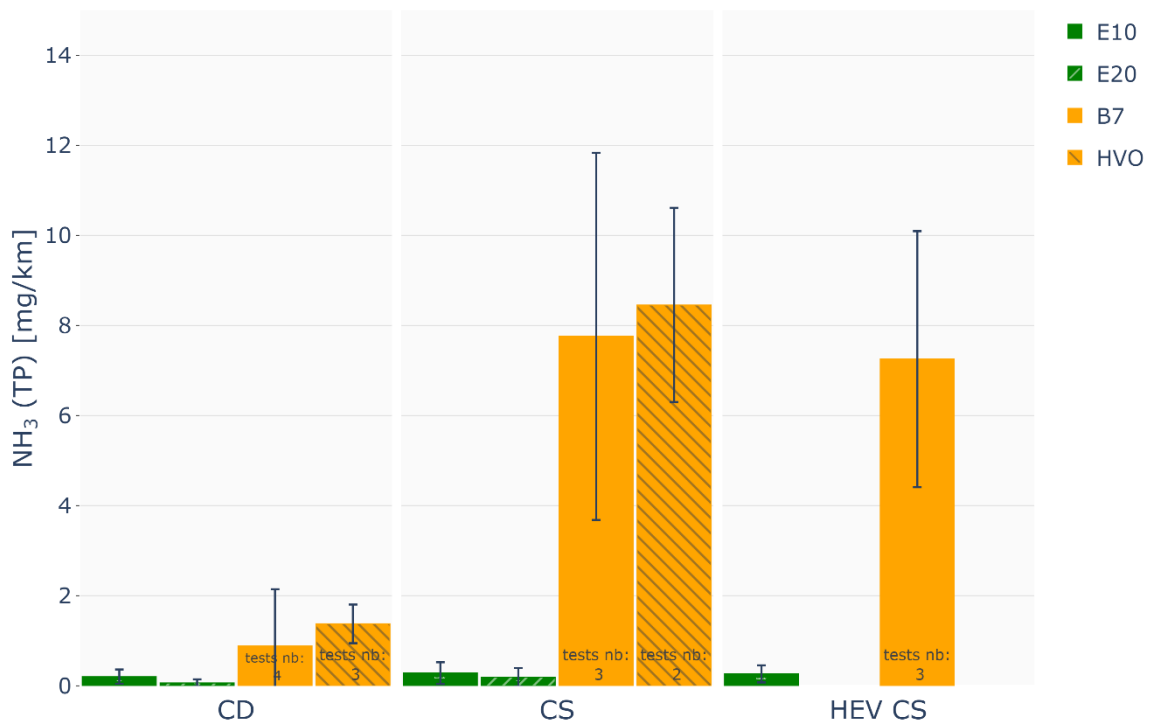


Figure 37 Comparison of Tailpipe NH₃ emissions [mg/km] measured on RDE cycles on chassis dyno for each fuel and mode.

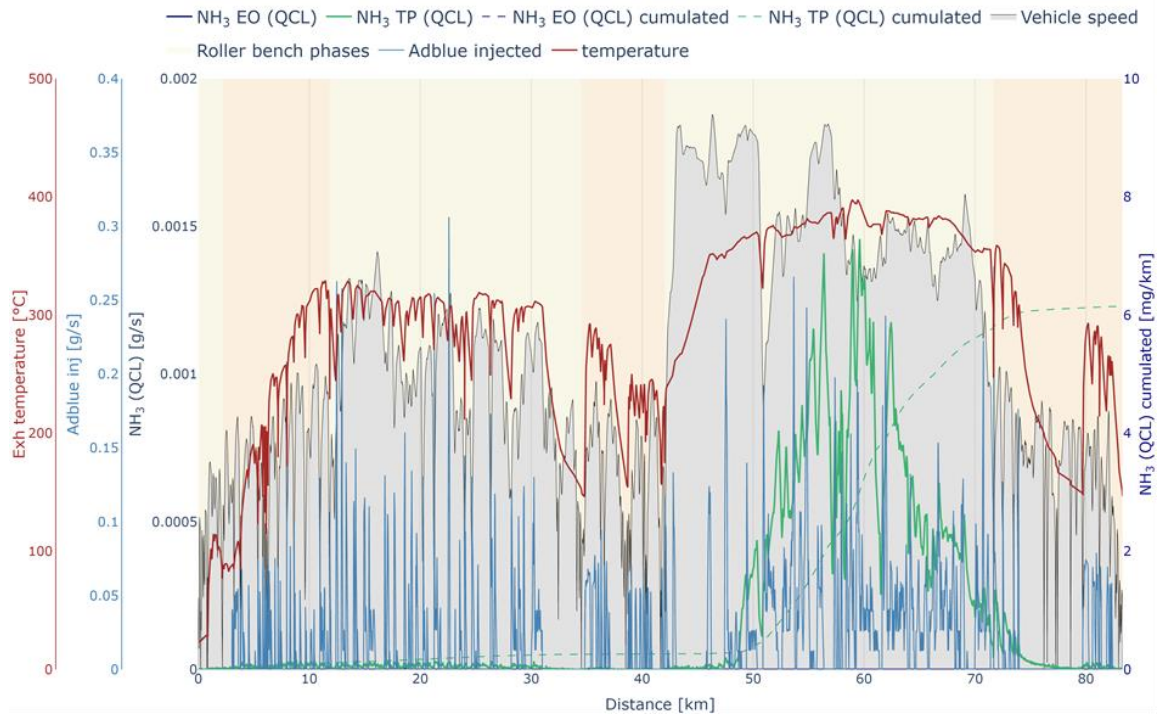


Figure 38 Distance-based evolution of AdBlue injection, exhaust gas temperature and NH₃ emissions (EO and TP) along an RDE cycle.

2.5. EXPERIMENTAL CAMPAIGN ON-ROAD

2.5.1. Vehicle instrumentation and measurement systems

Part of the instrumentation is similar to what was used during the chassis dyno tests: measurement of the battery output current, on-board diagnostic (OBD) information, urea consumption for the Diesel vehicle. Regarding the pollutants and greenhouse gases emissions, their measurement was performed with a portable emissions measurement system (PEMS) as detailed in Table 7.

Table 7 On-road vehicle instrumentation and measurement systems

	Measure
Tailpipe	HORIBA OBS-ONE GS (CO ₂ , CO, NO _x , NO, NO ₂)
	HORIBA OBS-ONE PN (PN23)
Fuel consumption	Carbon balance on tailpipe emissions
Electrical consumption	HIOKI 3390 (current clamp on HV DC cable between battery and inverter Current clamp on LV battery)
AFTS	AdBlue consumption when urea SCR is used thanks to instrumentation of the injector control signals (number of pulses and Ti), urea Pressure and a characterization of the injector
Temperature	Engine-out 3WC/DOC inlet DPF/GPF inlet and outlet Sump Coolant
Additional measurements	Exhaust Flow Meter (EFM) Ambient temperature, pressure and humidity (PEMS weather station) Vehicle speed (from PEMS Global Positioning System (GPS)) Engine speed



Figure 39 Vehicle setup for on-road tests, with PEMS equipment

2.5.2. RDE cycle on-road

Even if the itinerary is the same as the driving cycle performed at the chassis dyno, the speed profile as well as the aggressiveness indicator differs from what was performed at the test bed due to traffic and driveability factors (see *Figure 40*, *Figure 41* and **Error! Reference source not found.**). Only RDE compliant tests were kept in the analysis presented in the following.



Figure 40 Vehicle speed profiles measured during on-road tests compared to the RDE cycle performed on the chassis dyno

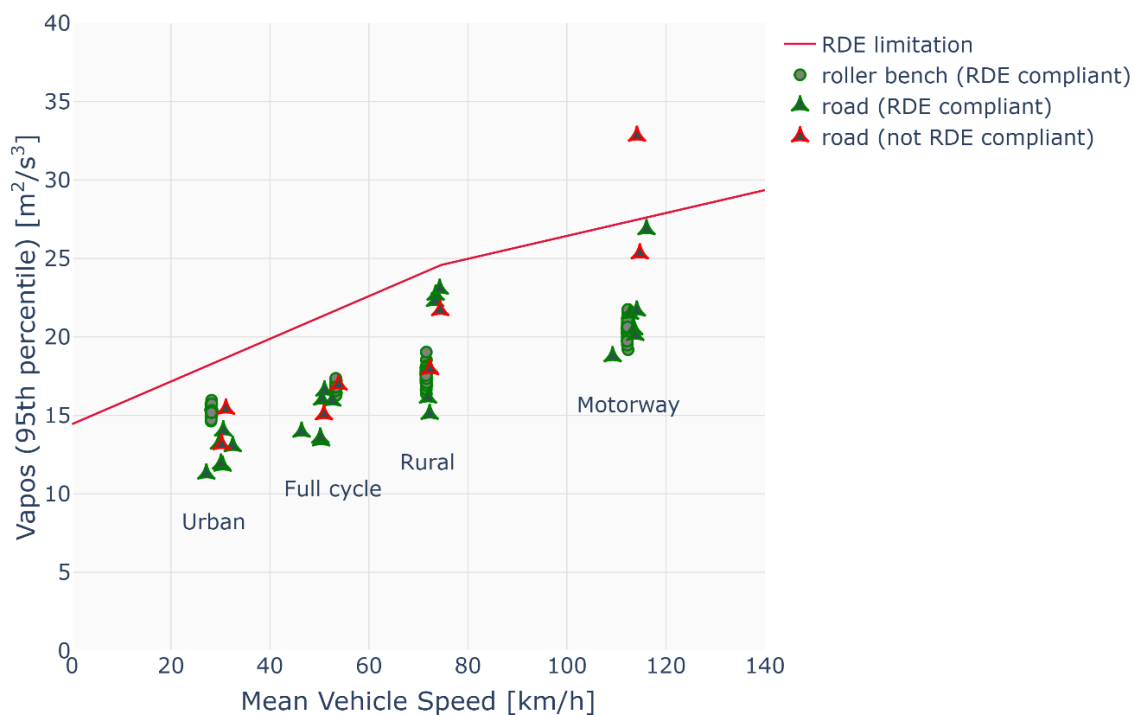


Figure 41 VA_{pos} measured during on-road-tests compared to RDE boundaries

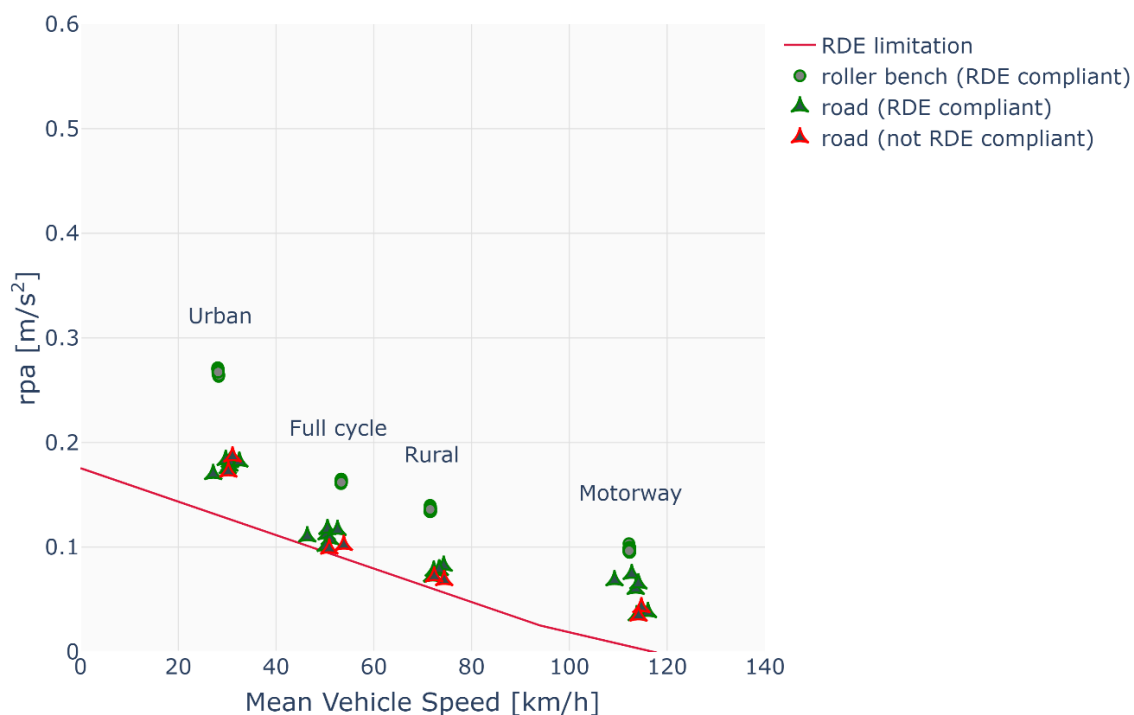


Figure 42 Relative Positive Acceleration measured during on-road tests compared to RDE boundaries

2.5.3. Tests operated on-road

As the Table 8 describes, only one repetition was made for the 2 battery modes with the reference fuel. As the RDE compliance condition was not always respected

and some hardware failed, the final test matrix was different from the one below and was finally populated with more tests and more repeats.

Table 8 Test matrix for on-road tests

Vehicle	Fuel	Battery	MASS	Repeat
C300de	EN590	CD	PHEV	1
C300e	E10	CD	PHEV	1
C300e	E10	CS	PHEV	1
C300de	EN590	CS	PHEV	1

2.5.4. Results of on-road test campaign

The key results from the RDE performed on-road are described in this section and are compared to the test performed at the roller test bed. The full results are tabulated in the Appendix. Where shown on charts, error bars denote the 68% confidence intervals (i.e. \pm the standard deviation).

Even though only one test per configuration was expected for the road tests, some tests that were not fully valid (e.g. one measurement missing among the full set of measurements) were included in the analysis when sensible to improve the statistical relevance of the results.

2.5.4.1. Carbon Dioxide emissions

Figure 43 depicts the emissions of CO₂ on-road compared to the emissions measured on the roller test bed with the same vehicle under close conditions. Higher CO₂ emissions, about +17% for B7 PHEV in CS (+28.9% when corrected) and +13% for E10 PHEV in CS (+13.5% when corrected), are observed for the on-road tests despite milder driving conditions. These gaps will be assessed more in-depth in Chapter 3 thanks to the models that were calibrated with all the data. A discrepancy between the “real” road law and the roller test bed road law seems to explain the stated difference on CO₂ emissions. More explanation on this evaluation is given in paragraph 3.1.4.2.

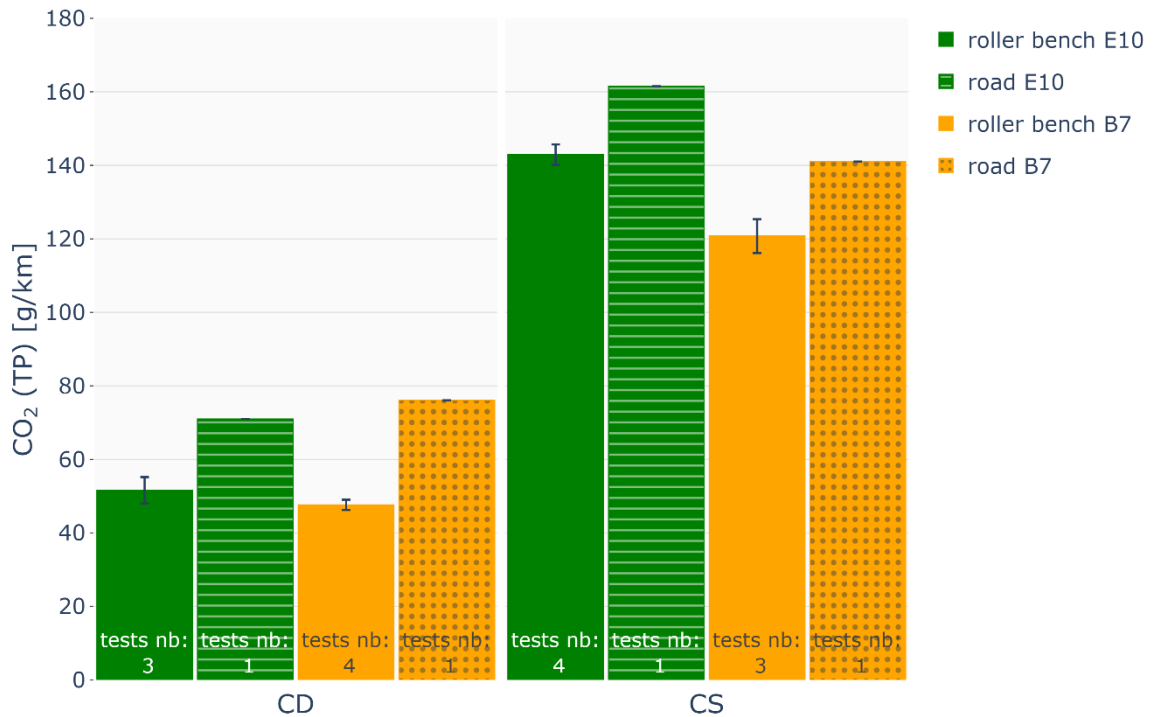


Figure 43 Comparison of tailpipe CO₂ emissions [g/km] measured on RDE on-road and chassis dyno tests for each fuel and mode.

2.5.4.2. Volumetric Fuel Consumption

Figure 44 illustrates the volumetric fuel consumption that is computed from the carbon balance, i.e., the CO₂, HC and CO emissions. The trends are therefore similar to the CO₂ emissions, i.e. the fuel consumption is higher on-road than on the chassis dyno, with 17% higher fuel consumption for B7 PHEV in CS mode (29.1% when corrected) and 13% for E10 PHEV in CS mode (13.6% when corrected).

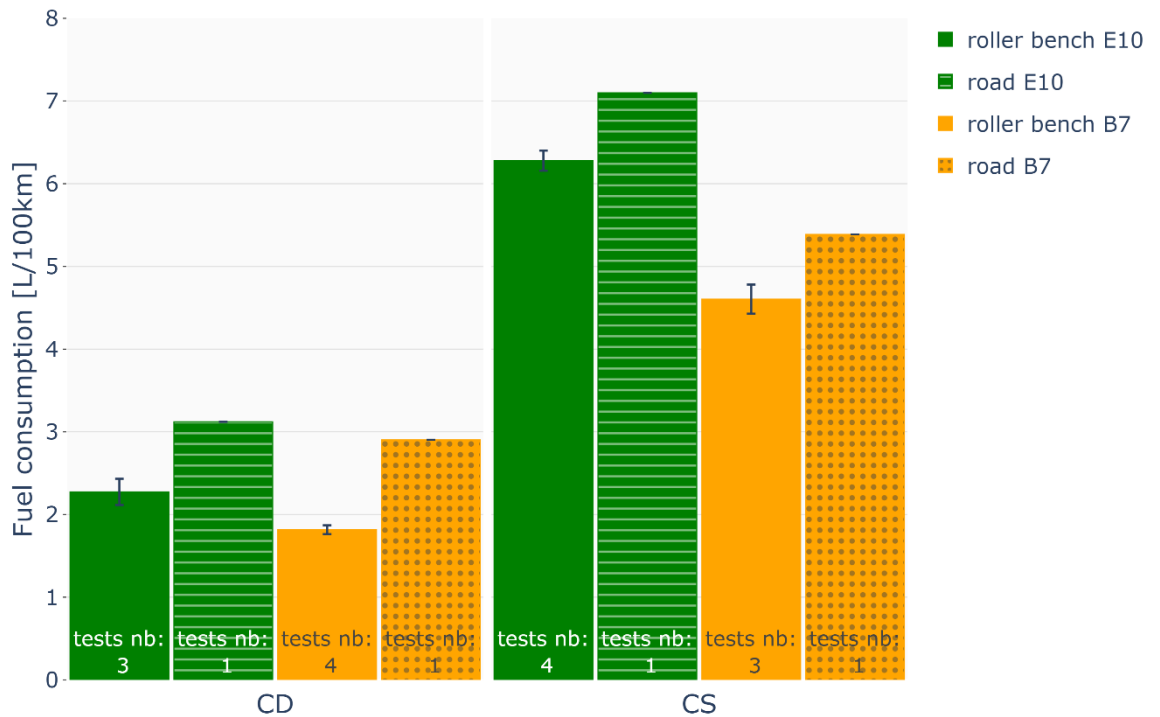


Figure 44 Comparison of volumetric fuel consumption [L/100km] measured on RDE on-road and chassis dyno tests for each fuel and mode.

2.5.4.3. Electrical Consumption and Utility Factor

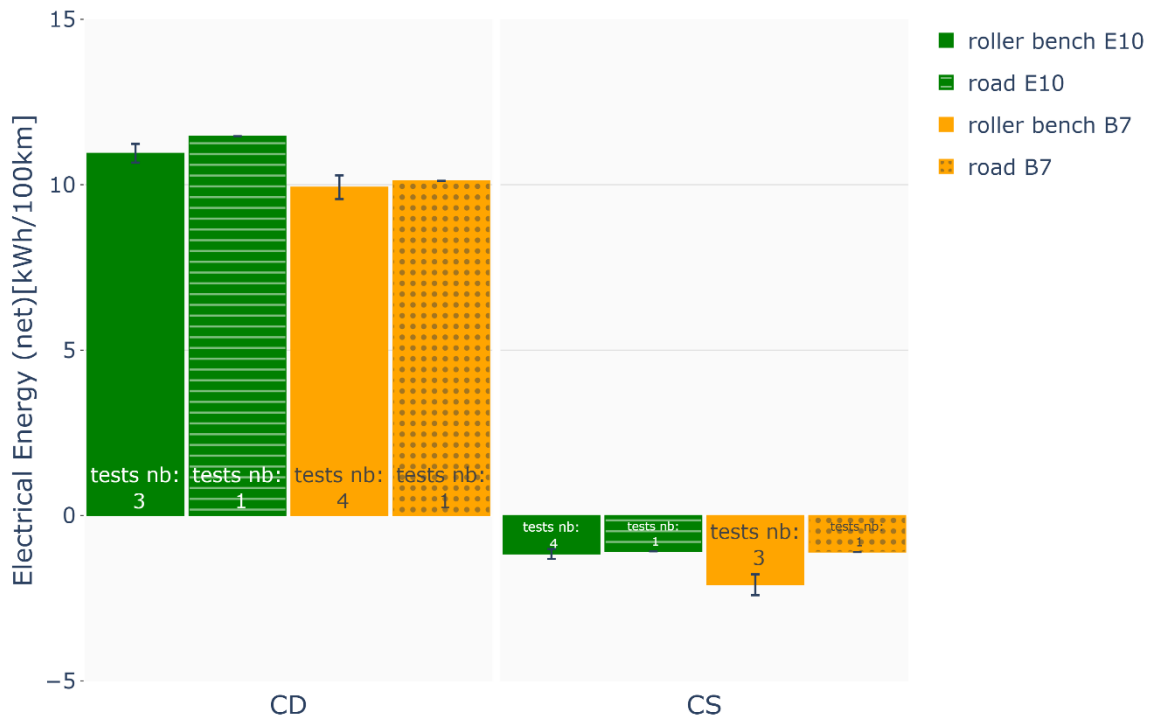


Figure 45 Comparison of electrical consumption [kWh/100km] measured on RDE on-road and chassis dyno tests for each fuel and mode.

Figure 45 shows the electrical energy consumption over the entire RDE. Figure 47 exhibits the utility factor. The aforementioned assumption that the “road” road law is more demanding than the “bench” road law seems to be verified, as a lower UF with a higher electrical energy consumed means higher energy used over the whole

driving cycle. For the Diesel PHEV, the lower electrical energy and UF, as stated in paragraph 2.4.5.2, can be explained by a better efficiency of the thermal engine moving the sweet spot optimization compared to the gasoline PHEV, and still improving the CO₂ emissions.

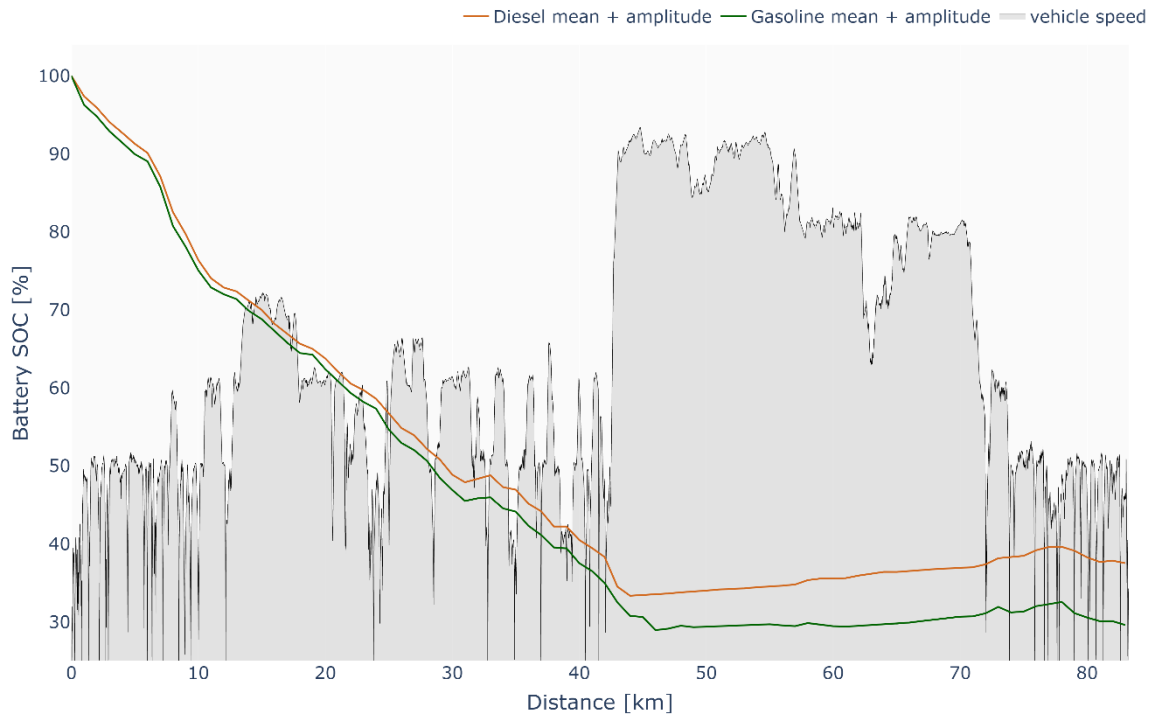


Figure 46 Illustration of the battery SOC [%] evolution on road test in charge depleting mode

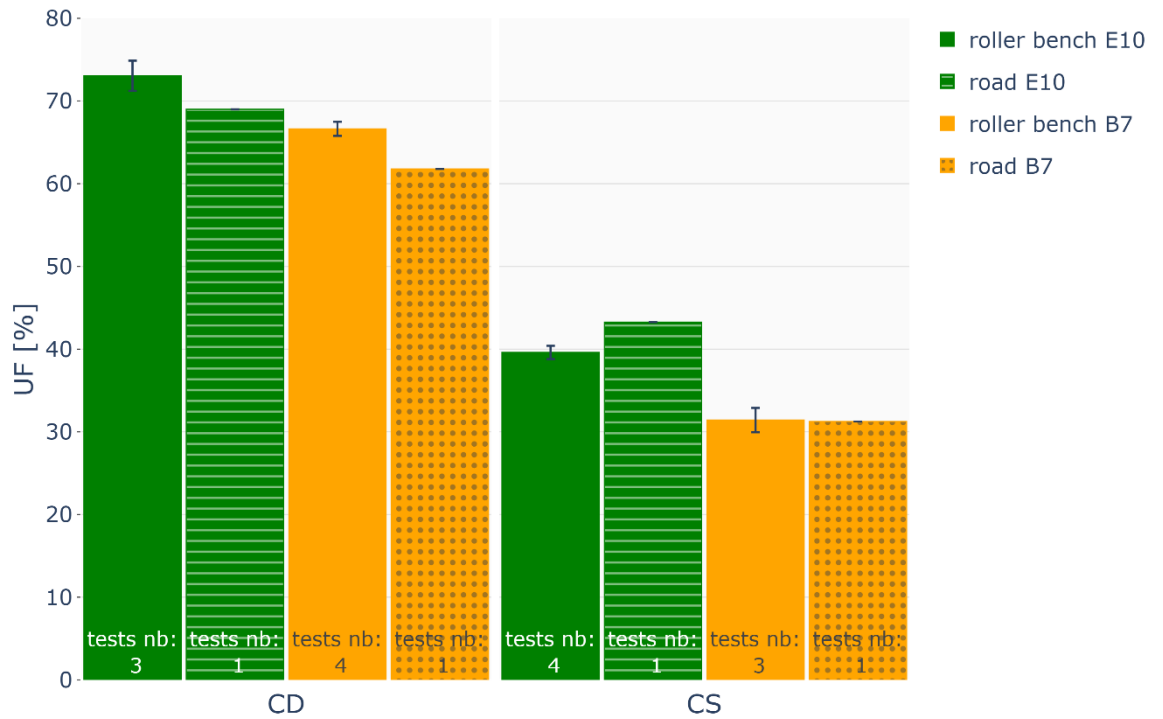


Figure 47 Comparison of Utility Factor [%] measured on RDE on-road and chassis dyno tests for each fuel and mode.

2.5.4.4. Oxides of Nitrogen (NO_x) emissions

Figure 48 shows the emissions of NO_x. The difference between on-road tests and roller test bed tests can be explained by the difference in terms of driveability, modifying the number of accelerations and their level hence the peaks of NO_x during the cycle. Even with those differences, the levels of NO_x emissions remain low.

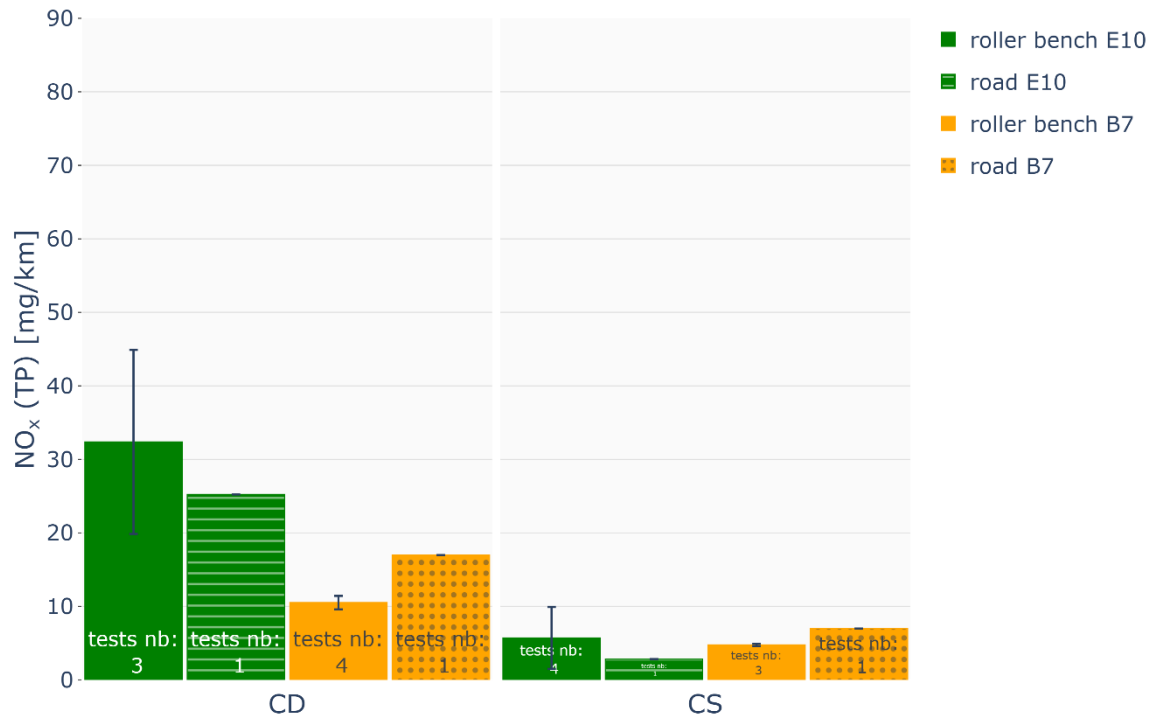


Figure 48 Comparison of tailpipe NOx emissions [mg/km] measured on RDE on-road and chassis dyno tests for each fuel and mode.

2.5.4.5. Particle Number emissions

Figure 49 depicts the PN23 emissions. The same observation as for the NOx emissions can explain what is observed on the PN23 emissions. For the gasoline PHEV in CD mode, a difference in the moment when the engine starts can lead to a big difference in PN emissions due to high peaks of PN emissions right after the engine starts.

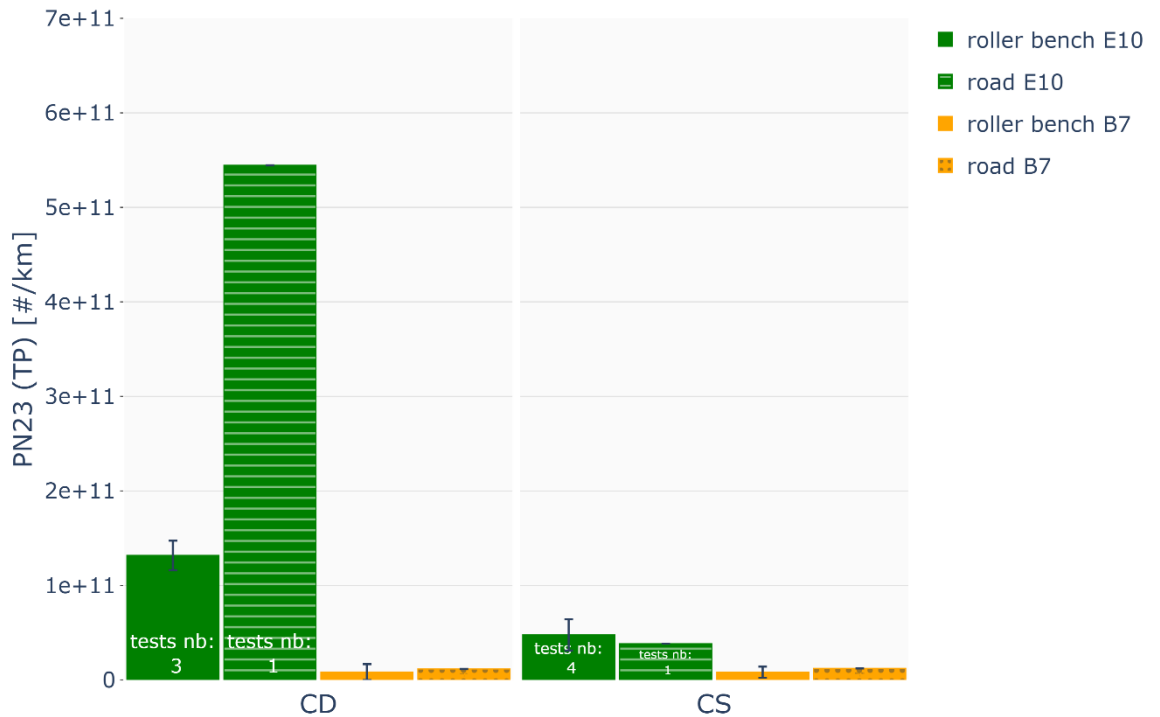


Figure 49 Comparison of tailpipe PN23 emissions [#/km] measured on RDE on-road and chassis dyno tests for each fuel and mode.

2.5.4.6. Carbon Monoxide emissions

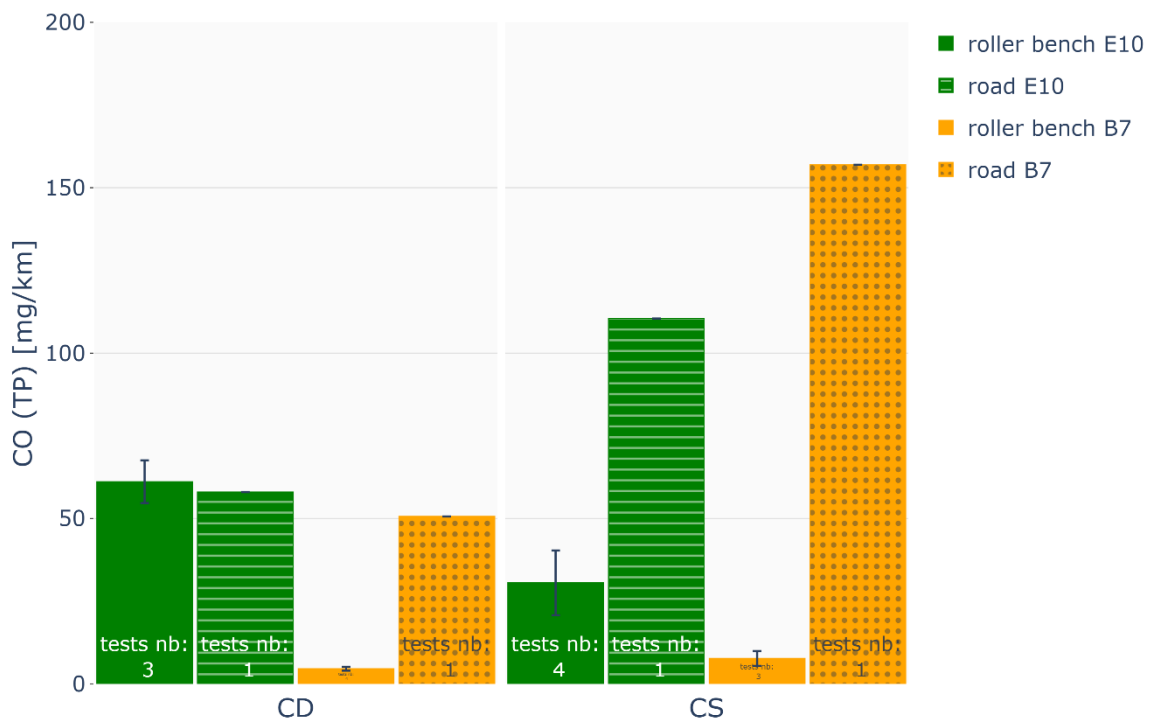


Figure 50 Comparison of tailpipe CO emissions [mg/km] measured on RDE on-road and chassis dyno tests for each fuel and mode.

Figure 50 shows the emissions of CO at the tailpipe. The trend that emerges is that “on-road” CO are higher than CO emissions measured in laboratory conditions. Still

the level remains low compared to the Euro6d levels. This can be due to a difference of AFTS efficiency and/or differences of the load profile.

2.6. EXPERIMENTAL SUMMARY

Two Euro 6d PHEVs were selected to allow a relevant comparison between gasoline and Diesel internal combustion engines. These vehicles were tested on a chassis dynamometer and on-road, both with standard and renewable fuels, in charge depleting and charge sustaining mode.

Concerning pollutants, the two PHEVs show low regulated (well below Euro 6d limits) and non-regulated (in the range of Euro 7 proposals) pollutant emissions. The Diesel PHEV allows, compared to the gasoline one, a reduction of TtW CO₂ emissions of up to 22.3% (and a reduction of 20.5% of TtW GHG emissions) in charge sustaining mode, and a reduction of pollutant emissions except for NH₃ and N₂O. The distance where the vehicle switched to CS mode on the RDE driven (i.e. the all-electric range) was around 54 km, close to the 57km homologated on WLTP.

Regarding the gasoline PHEV, switching from a standard E10 fuel to a 100% renewable E20 fuel does not have a significant impact on the pollutant tailpipe emissions under the conditions of this study, neither on TtW CO₂ emissions. However, it implies a higher volumetric fuel consumption (+4.5% on CS). With the Diesel PHEV, switching from a standard B7 fuel to a 100% renewable HVO fuel does not have any significant effect on the pollutant tailpipe emissions under the tested conditions. It decreases by 2.0% the TtW CO₂ emissions and increases the volumetric fuel consumption by 8.4% on CS.

Reducing the mass of the vehicle surprisingly does not impact the consumption neither the pollutant emissions: despite weighing 120 kg less, the HEV configuration presents results in emissions and energy consumption very close to the PHEV configuration in CS mode.

The measurements performed on-road show higher fuel consumption and CO₂ emissions. In CS mode, the Diesel vehicle showed a 29% higher fuel consumption and CO₂ emissions on the road compared to the laboratory tests. The gasoline vehicle showed a difference of 13.6%. This gap was investigated using the calibrated simulator and thus explained with a different road law between the roller test bed and the on-road (cf. details in chapter 3).

Table 9, and *Table 11* below summarizes the mean results observed on these two vehicles for all the configuration tested on both roller test bed and on-road tests. Additional tables specifying the relative differences between each configuration are also provided in the Appendix.

All this data, from RDE driving in the laboratory and on-road, fed the simulation work detailed in the next chapter, which aims at extending the findings to more varied conditions and to identify average results representative of use cases and statistically representative use.

Table 9 Energy mean values

	FC	FC corr*	CO₂	CO₂ corr*	GHG	GHG corr*	UF	EC	EC+	EC-
	<i>L/100km</i>	<i>L/100km</i>	<i>g/km</i>	<i>g/km</i>	<i>g CO₂eq /km</i>	<i>g CO₂eq /km</i>	<i>%</i>	<i>kWh/100km</i>	<i>kWh/100km</i>	<i>kWh/100km</i>
			CVS		CVS CO ₂ + N ₂ O + CH ₄	CVS corr* CO ₂ + N ₂ O + CH ₄				

C300 de	Chassis dyno	B7	PHEV	CD	1.8	1.8	48	48	49	49	67	10	16	-6
			CS	4.6	4.2	121	109	124	113	31	-2	5	-7	
		HEV	CS	4.6	4.2	121	110	124	113	30	-2	5	-7	
	HVO	PHEV	CD	2.0	2.0	47	47	49	49	67	10	15	-6	
		CS	4.9	4.5	116	107	120	111	32	-2	5	-7		
	Road	B7	PHEV	CD	2.9	2.9	76	76		62	10	15	-5	
CS	5.4		5.4	141	141		31	-1	5	-6				
C300 e	Chassis dyno	E10	PHEV	CD	2.3	2.3	52	52	52	52	73	11	16	-5
			CS	6.3	6.2	143	141	144	142	40	-1	6	-7	
		HEV	CS	6.3	6.1	143	139	144	140	38	-1	5	-6	
		E20	PHEV	CD	2.5	2.5	54	54	55	55	72	11	16	-5
	CS		6.5	6.5	144	143	145	144	38	-1	5	-6		
	Road	E10	PHEV	CD	3.1	3.1	71	71		69	11	15	-4	
			CS	7.1	7.0	162	160		43	-1	5	-6		

Table 10 Regulated pollutant emissions mean values

	NOx			CO			HC			SPN23			SPN10			PM
	EO	TP	AFTS Eff	EO	TP	AFTS Eff	EO	TP	AFTS Eff	EO	TP	AFTS Eff	EO	TP	AFTS Eff	TP
	mg/km	mg/km	%	mg/km	mg/km	%	mg/km	mg/km	%	nb/km	nb/km	%	nb/km	nb/km	%	mg/km
	raw gases	raw gases		raw gases	raw gases		raw gases	raw gases		raw gases	raw gases		raw gases	raw gases		soot filter weight

C300 de	Chassis dyno	B7	PHEV	CD	139.1	10.5	92.4	117.9	4.6	96.1	14.7	0.5	96.8	9.7E+12	8.3E+09	99.9	1.5E+13	1.4E+10	99.9	0.1	
			CS	373.3	4.8	98.7	324.9	7.7	97.7	47.5	0.9	97.9	2.2E+13	8.2E+09	100.0	3.6E+13	1.4E+10	100.0	0.1		
		HVO	PHEV	CD	367.1	4.7	98.7	310.7	6.6	98.0	37.5	0.9	97.6	2.2E+13	5.5E+09	100.0	3.6E+13	9.5E+09	100.0	0.0	
			CS	140.0	10.6	92.4	102.7	2.9	97.2	11.1	0.3	96.9	1.0E+13	1.5E+10	99.8	1.6E+13	2.4E+10	99.8	0.2		
		Road	B7	PHEV	CD		17.0			50.6					1.2E+10						
				CS		7.0			157.0						1.2E+10						
C300 e	Chassis dyno	E10	PHEV	CD	819.9	32.4	96.1	1871.3	61.1	96.7	178.7	6.6	96.3	3.4E+11	1.3E+11	64.1	7.8E+11	2.0E+11	72.7	0.2	
			CS	2403.2	5.7	99.8	4372.6	30.5	99.3	413.9	4.2	99.0	1.1E+11	4.8E+10	55.0	7.2E+11	7.7E+10	89.2	0.2		
		E20	PHEV	CD	2372.3	8.2	99.7	4349.2	29.9	99.3	419.2	3.5	99.2	1.1E+11	4.5E+10	59.7	6.1E+11	7.2E+10	88.2	0.1	
			CS	865.7	19.0	97.8	1801.4	39.7	97.8	250.9	9.4	96.3	4.6E+11	1.6E+11	73.6	2.2E+12	2.3E+11	92.0	0.2		
		Road	E10	PHEV	CD	2522.7	1.6	99.9	4410.7	65.1	98.5	601.8	4.8	99.2	4.9E+11	6.3E+10	83.8	2.6E+12	9.8E+10	95.7	0.1
				CS		25.2			58.0						5.4E+11						

Table 11 GHG and unregulated pollutant emissions mean values

	CH ₄				NH ₃		N ₂ O			Adblue
	EO	TP	AFTS Eff	TP	EO	TP	EO	TP	TP	
	<i>mg/km</i>	<i>mg/km</i>	%	<i>g CO₂eq /km</i>	<i>mg/km</i>	<i>mg/km</i>	<i>mg/km</i>	<i>mg/km</i>	<i>g CO₂eq /km</i>	<i>L/1000km</i>
	raw gases	raw gases		raw gases	raw gases	raw gases	raw gases	raw gases	raw gases	calculation from command signal

C300 de	Chassis dyno	B7	PHEV	CD	0.3	0.1	55.5	0.0	0.0	0.9	0.6	4.7	1.2	0.3
				CS	0.8	0.2	65.6	0.0	0.0	7.8	0.9	12.8	3.4	0.9
			HEV	CS	0.7	0.5	25.5	0.0	0.0	7.3	0.9	12.7	3.4	0.9
		HVO	PHEV	CD	0.2	0.1	56.2	0.0	0.0	1.4	0.5	5.4	1.4	0.3
				CS	0.6	0.3	49.4	0.0	0.0	8.5	0.9	12.9	3.4	0.8
		Road	B7	PHEV	CD									
CS	1.0													
C300 e	Chassis dyno	E10	PHEV	CD	6.7	0.7	89.7	0.0	0.0	0.2	1.0	1.7	0.5	
				CS	14.0	0.3	97.9	0.0	0.1	0.3	2.7	4.0	1.0	
			HEV	CS	13.9	0.3	98.1	0.0	0.0	0.3	2.7	3.9	1.0	
		E20	PHEV	CD	9.1	0.9	90.6	0.0	0.0	0.1	1.0	1.9	0.5	
				CS	18.4	0.6	96.8	0.0	0.1	0.2	2.8	3.1	0.8	
		Road	E10	PHEV	CD									
CS														

3. SIMULATION WORK

This chapter describes how to forecast real-life fuel and electrical consumptions of the Mercedes C300e and C300de vehicles for a wide range of uses and conditions. The methodology relies on a vehicle non-dimensional simulator which is calibrated to fit experiments previously detailed. After discussing its validation, projections over Design of experiment will be presented. Finally, mathematical methods are implemented to extract patterns from simulation results database, and to produce macroscopic trends under some assumptions.

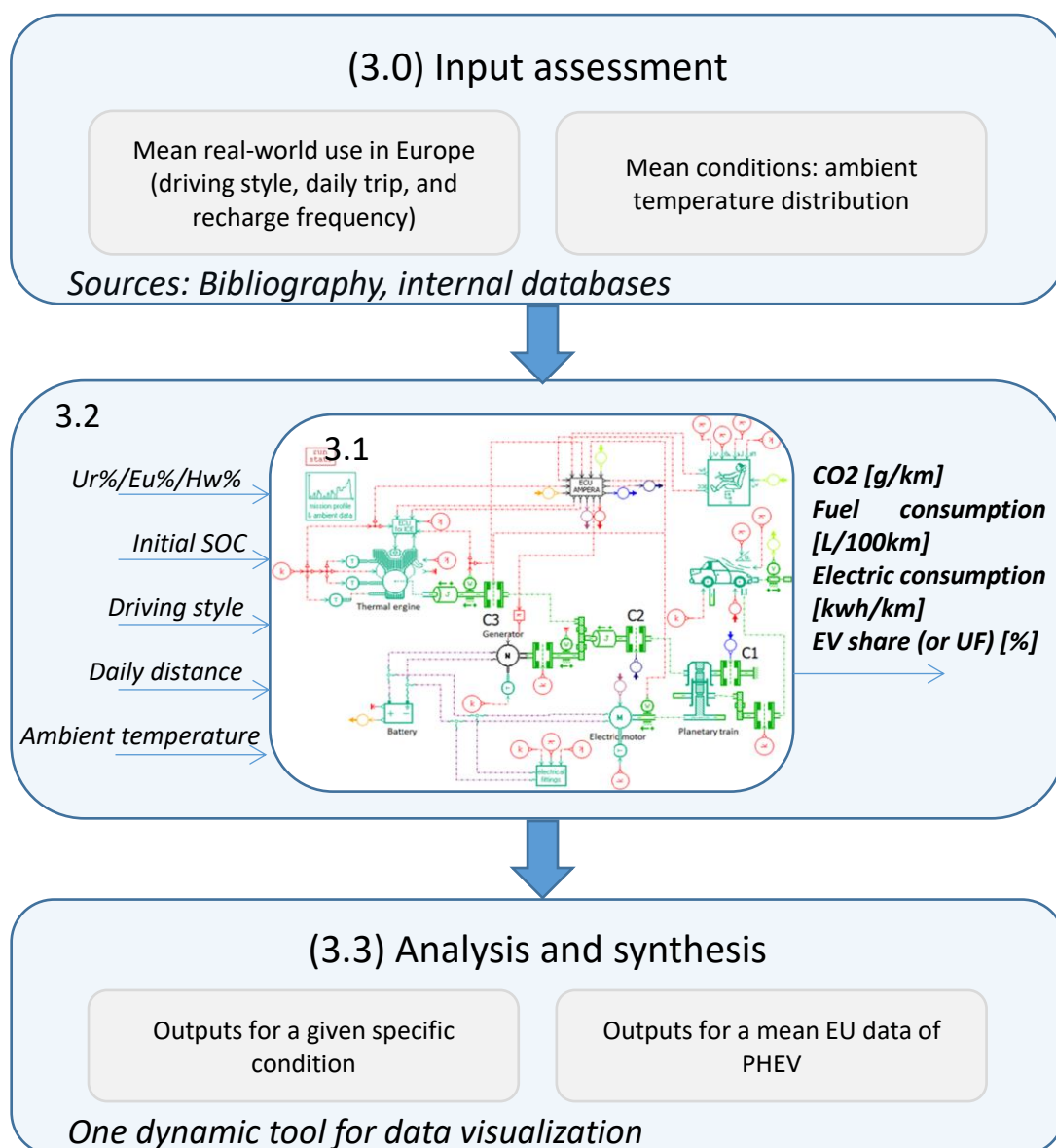


Figure 51 Simulation workflow for PHEV consumptions real use assessment

3.1. SIMULATION PLATFORM SET UP

3.1.1. Simulation platform description

The simulations were carried out using Simcenter Amesim™ software. The simulation platforms were based on "IFP-Drive" library components jointly developed by IFPEN and Siemens PLM Software. These models transcribe the physics of all devices present in conventional vehicles (combustion engine, transmission, etc.) and electric vehicles (battery, traction engine, power electronics etc.). The component performance maps are generated with automatic generation tools for the thermal engine, electric machine and battery, considering the detailed characteristics of these components.

A component dedicated to hybrid architectures (ECMS: Equivalent Consumption Minimization Strategy) was used to determine the optimal management strategy for internal combustion and electrical energy to minimize fuel consumption. This was calibrated to fit the experimental behavior characterized in the previous chapter. Further details on these tools can be obtained by consulting the SAE publication (Dabadie et al. 2017). As IFPEN was responsible for the development of these tools, a critical look can be made on the relevance of the results obtained.

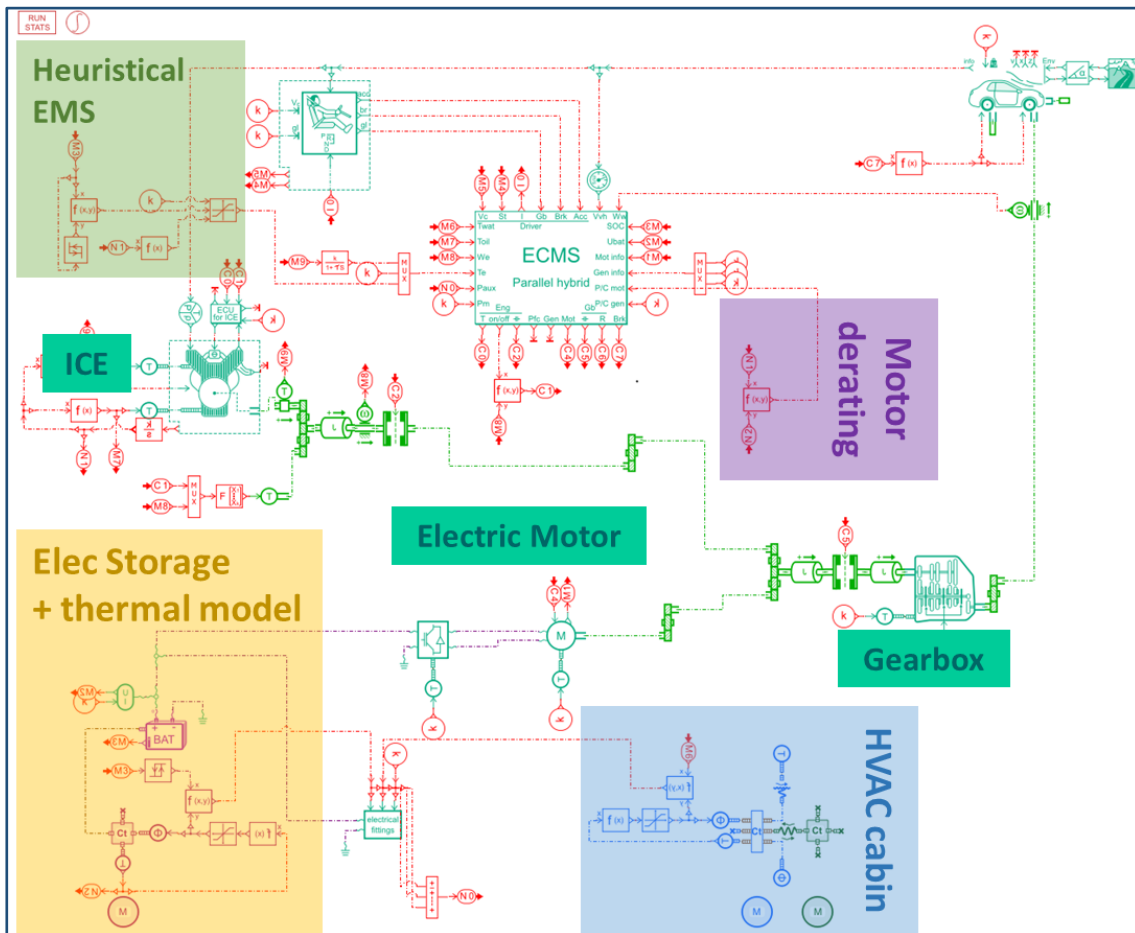


Figure 52 Detailed Amesim sketch of P2 hybrid powertrain

The Amesim powertrain simulator runs under direct method. This means that powertrain manager (i.e. ECMS) commands are based on the driver's comparison between imposed speed profile and feedback on vehicle's current attitude. At each

time steps, ECMS issues a set of optimized orders towards every component which effects are then assessed in the vehicle’s propelling model to update its attitude (speed).

One can recognize on the simulator sketch a P2 parallel hybrid architecture. The C-Class PHEV uses only one electric motor that is mounted on gearbox input, between the engine and the transmission.

3.1.2. Components calibration

3.1.2.1. Road laws

Road laws are needed to assess the energy required to propel the vehicle. The driving resistance force is given through a speed polynomial based on masses and dimensionless coefficients registered in the next table for all vehicle configurations.

$$F_{\text{wheel}} = mg(C_{rr,0} + C_{rr,1}v) + SC_x v^2$$

$C_{rr,0}$ and $C_{rr,1}$ stand respectively for constant and speed related rolling resistance coefficients of deformed tyres on road surface. SC_x represents car’s equivalent frontal area responsible for aerodynamic drag.

Table 12 Vehicle road laws according to configuration

Vehicle	Mass (kg)	$C_{rr,0}$ (N/kgF)	$C_{rr,1}$ (N/(m/s)/kgF)	SC_x (m ²)
C300e HEV	1765	0.0073	0.00011	0.58
C300de HEV	1850	0.0070	0.00010	0.58
C300e Low	1885	0.0073	0.00011	0.58
C300de Low	1970	0.0070	0.00010	0.58
C300e Heavy	2131	0.0073	0.00011	0.58
C300de Heavy	2211	0.0070	0.00010	0.58
C300e High	2131	0.010	0.0001	0.7
C300de High	2211	0.010	0.0001	0.7

For both the gasoline and Diesel versions, we established several road laws by interpreting homologation coefficients and by weighing real-life vehicles in running order. Chassis dyno measurements and corresponding validation simulations are mainly carried out thanks to the “Low” version. This is an optimistic set of parameters mentioned as such in the certification. “HEV” laws are only mass altered projections of “Low” to forecast a 120kg lighter non-plug-in hybrid vehicle equipped with a much smaller battery of presumably 1kWh instead of 13.5kWh. The two remaining versions deal with real-world road tests: “Heavy” is simply the actual weighed mass version of “Low”, whereas all “High” coefficients were worsened in addition. These latter “High” coefficients also come from vehicle’s certification where they are once again mentioned as such. They are the relevant and therefore chosen ones for real-world usage consumptions assessment in the last part projections (see further).

3.1.2.2. Transmission

Mercedes installed the same 9G-tronic gearbox in both gasoline and Diesel vehicles, and only the axle ratio drops from respectively 2.82 to 2.64, resulting in the overall ratios detailed on table below. Detailed transmission ratios are given *Table 13*.

The transmission efficiency is indiscriminately set to 97 %. Wheels radius comes from rear tyres size 245/40R18.

Table 13 Transmission parametrized ratios

	Gearbox (GB) ratio [-]	Gasoline vehicle axle ratio [-]	Gasoline vehicle V1000 [km/h/1000rpm]	Diesel vehicle axle ratio [-]	Diesel vehicle V1000 [km/h/1000rpm]
1 st	5.354	2.82	7.91	2.64	8.56
2 nd	3.243	2.82	13.06	2.64	14.13
3 rd	2.252	2.82	18.8	2.64	20.35
4 th	1.636	2.82	25.88	2.64	28.1
5 th	1.211	2.82	34.96	2.64	37.83
6 th	1	2.82	42.34	2.64	45.82
7 th	0.865	2.82	48.95	2.64	52.97
8 th	0.717	2.82	59.05	2.64	63.90
9 th	0.601	2.82	70.45	2.64	76.24

3.1.2.3. Engines

The quasi-static approach of Amesim vehicle simulator requires at least engine's operating range and efficiency map. For each subsequent time step, instantaneous power demand is met while reading corresponding consumption. Unfortunately, all we have is general knowledge of both engines summarized in next table.

Table 14 Engines general characteristics

Engine	Fuel	Low Heating Value (LHV) [kJ/kg]	Displacement [cm ³]	Bore [mm]	Stroke [mm]	Compression ratio (CR) [-]	Power [kW]	Torque [Nm]
M274	E10	41400	1991	83	92	9.8	155 @5500rpm	350 @1200-4000rpm
M274	E20	39780	1991	83	92	9.8	155 @5500rpm	350 @1200-4000rpm
OM654	B7	42130	1950	82	92.3	15.5	143 @3800rpm	400 @1600-2800rpm
OM654	HVO	44160	1950	82	92.3	15.5	143 @3800rpm	400 @1600-2800rpm

To make up for missing data, we relied on Amesim embedded generation tool that provides such maps based on accumulated expertise and feedback about ICE. It feeds on sizing data from the previous table to generate step by step virtual engine tables. In the step illustrated below for the E10 version, additional estimated points were included on maximum available torque to achieve a plausible curve. Dedicated algorithm relies on this maximum torque curve among other engine's general parameter to generate realistic efficiency shape. Regarding bio-fuels, we did not check maximum performance and kept an identical curve since its main purpose is to help assessing energy conversion efficiency sensitivity to fuel (which was already approximated). The assumption that the same maximum power can be achieved with E20 fuel as with E10 fuel despite a lower LHV is strong, but has very little bearing on the issues addressed in this study - fuel efficiency and emissions.

In the previous step, default peak efficiency is replaced. It is adjusted (e.g. 36% here) in order to get close to experimental fuel consumption from test bench in charge sustaining mode, since the effectiveness with which the internal combustion engine (ICE) provides energy remains the only lever left in CS once regenerative break has been settled.

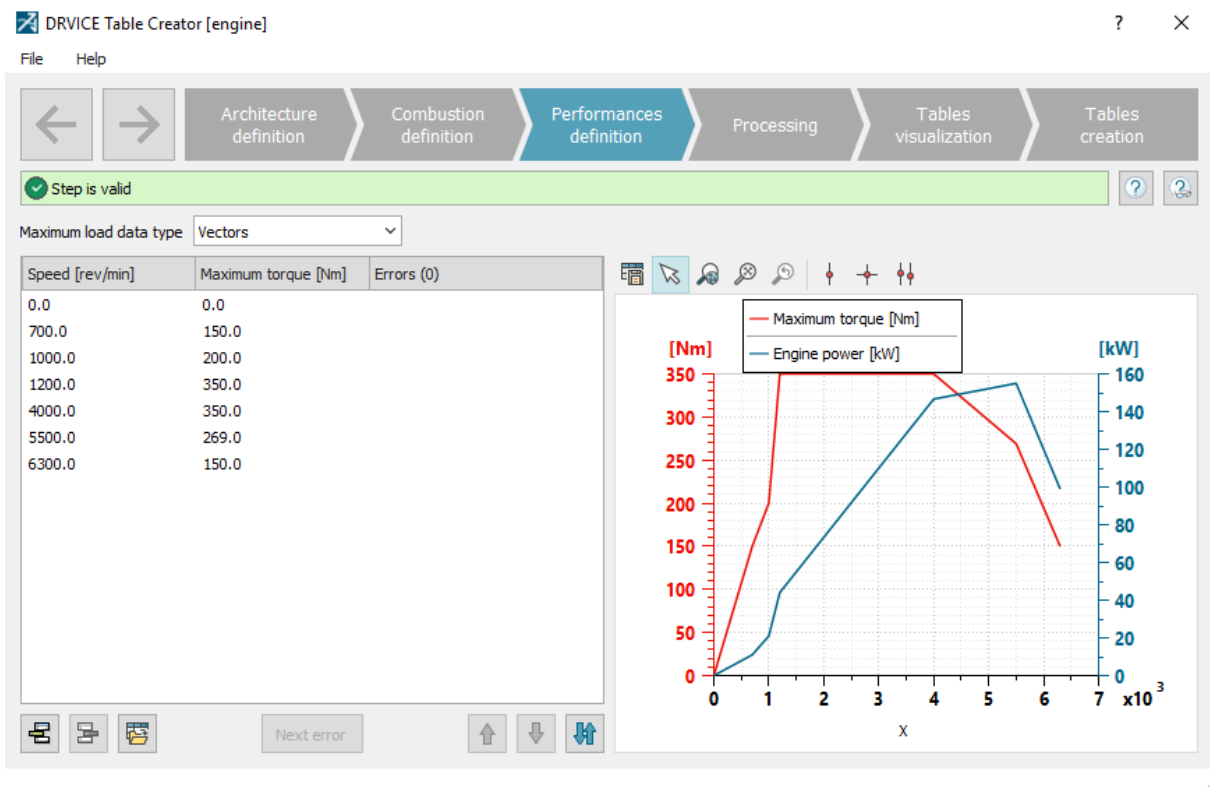


Figure 53 Amesim ICE performance maps generator (range operation tab)

For both gasoline and Diesel engine, fuel mass flow rate tables were regenerated through this process for biofuels, so that consumption rates remain consistent with altered fuel's energy density (Lower Heating Value).

Engine warm up is simulated regarding cumulative fuel consumption: coolant and oil virtual current temperatures are linearly correlated to the total amount of fuel burnt to this point. We calibrate the critical masses at which final -and optimal- engine temperature is reached by considering OBD surveys.

3.1.2.4. Electric Motor

We encountered the same lack on efficiency indication as we did with combustion engine during electric motor parametrization. Only the macroscopic design characteristics are known:

- 90 kW peak power, 60kW continuous power,
- 440 Nm peak torque,
- 365 V nominal voltage,
- Buried permanent magnet synchronous machine,
- Coaxial P2 mounted machine (upstream gearbox).

Amesim EM generation tool (example below) is provided with these inputs, and we assumed that the motor max speed must lay around 6000 rpm as for engine (P2 architecture). The bottom left map shows the generated efficiency map at nominal voltage 365V, and both envelopes for peak and continuous operation. The later will

be of some importance for derated control management implementation (see further). The other three maps show their sensitivity to available voltage from battery.

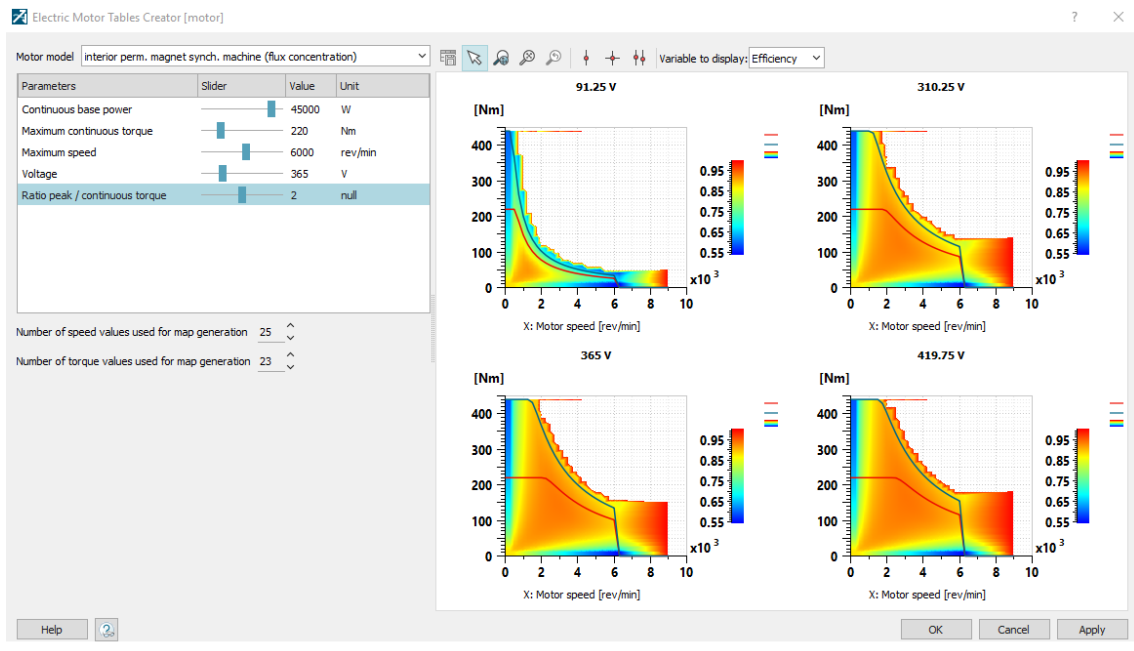


Figure 54 Amesim Electric Motor maps generation tool with gradient efficiency representation for four input voltages including nominal 365V, — max peak torque, - max continuous torque

3.1.2.5. Battery

Unlike engine and motor, the battery model benefits from some experimental data. Though simulated battery pack is pre-sized thanks to an embedded dedicated tool (next illustration), the cells used by Mercedes had previously been benchmarked by IFPEN. Consequently, we parametrized a 100 Nickel-Manganese-Cobalt (NMC) cells serially mounted Li-ion pack that provides 365 V under standard conditions and 13.5 kWh of rated capacity (37.0 Ah) weighting approximately 100kg. The *Deutsche ACCUmotive BT0023* Ni-rich cell itself was measured on IFPEN's facilities test bench, and we can therefore rely on pre-calibrated SOC dependant profiles for Open Circuit Voltage and internal resistance, with their respective sensitivity to temperature.

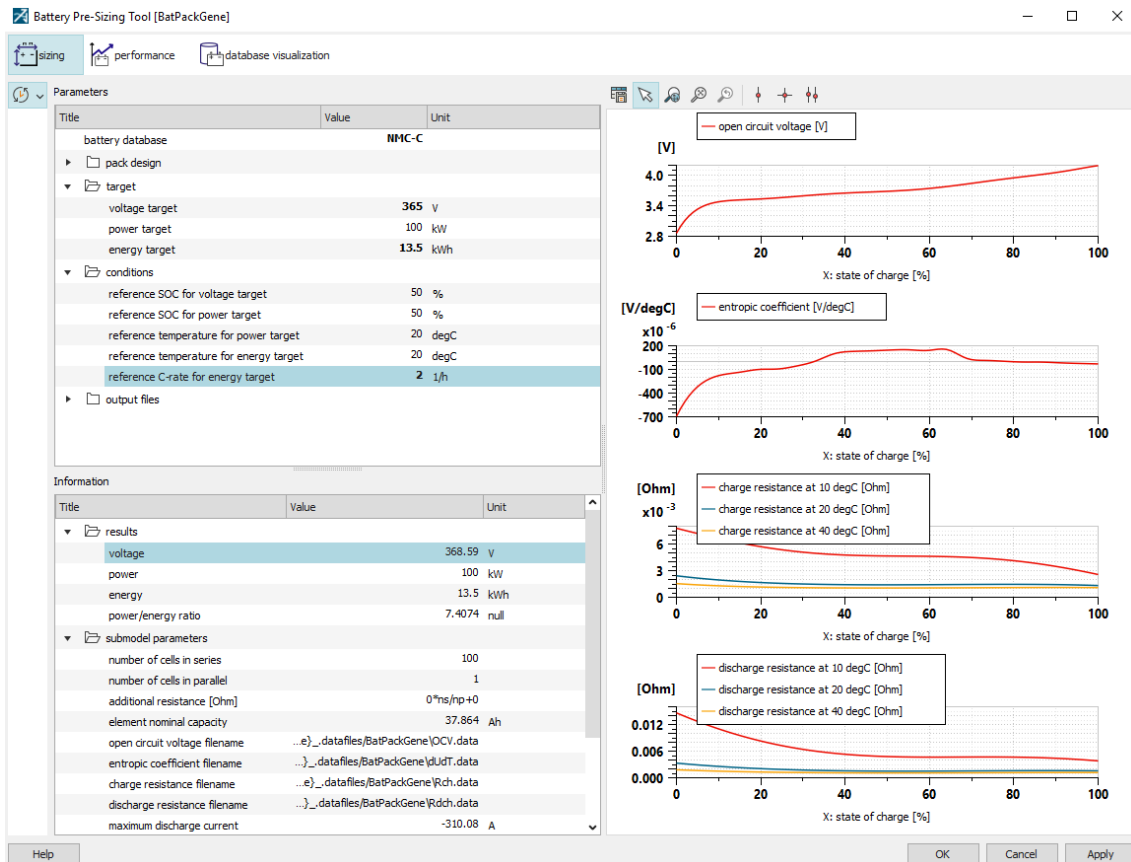


Figure 55 Amesim battery pre-dimensioning tool

One issue with battery calibration is to establish its effective operating SoC range. For that matter, we relied on electric consumption wall meter surveys when recharging the PHEVs. On average - end SoC dispersion depending on vehicle use - it indicates a 11.5 kWh wall plug consumption. We assumed that only ~11 kWh, thus approximately 80 % of the total 13.5 kWh, are stored effectively in the battery since we considered a 94% charging efficiency¹⁷. This remains quite high for this is slow charging through 2.2 kW charger on standard wall plug, and battery Joule effect we estimated thanks to internal resistance in such conditions (<1Ω with 6A) are negligible.

As illustrated in Figure 56, experimentally, the 80 % SoC rise of battery correspond to a 13 %→100 % charge from the OBD point of view. This means that OBD indicated SoC is relative but can be translated to absolute with simple affine relation. By stating a 5 % head margin convenient for our simulation tool, we deduce that a 3% foot margin plus a 12 % discharge reserve are left. Eventually, our PHEV will target SoC 15 % (13 % OBD) as depleting threshold, with still possible incursions in the depth below depending on real-world driving profile (cf. online hybrid powertrain management).

¹⁷ This assumption is rather in the high range of the charging efficiencies measured at 2.2kW (see <https://avt.inl.gov/content/charging-system-testing/vehicle-charging-system-testing.html>), but still realistic and characterized on some vehicles (BMW i3). It also allows, from the energies measured on the network during the charges, to obtain an effective range of the capacity of the battery consistent, around 80%.

Such no-go zones and 80 % effective SoC range illustrated with next stacked bars seem consistent with protection margins and effective capacity benchmarked for latest Li-ion PHEVs.

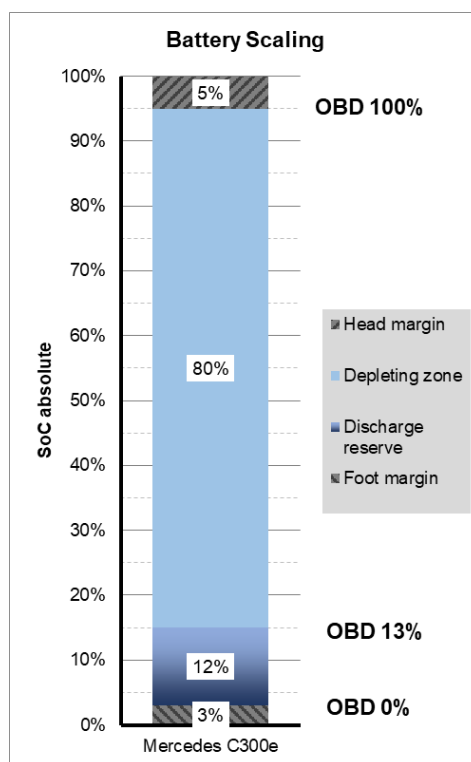


Figure 56 Battery assumed effective operation range

For initial conditions (at ambient) representativeness purpose, an elementary thermal model was added to the battery simulation next to its electrical storage model. It consists of a single homogeneous thermal capacity (1 node model) calibrated with 100 kg of material at 1200 J/kg/K specific heat capacity as an initial estimation. Temperature coming out from this modelling worsens internal resistance in electrical model, which in return indicates power losses for heating. Battery thermal conditioning implemented around 1 node model is dealt with in next paragraph.

3.1.2.6. Outside temperature effect auxiliaries

Powertrain components calibration described so far determines a general trend in energy consumption solely for vehicle propulsion. Our main guideline from now is to tune the power profile of additional auxiliaries to fit the vehicle global electricity consumption, especially in depleting phase. We focused on explaining SoC decreasing profile and observed electrical range, and their dependency to outside temperature. We also had some insights about power coming out of the battery itself thanks to current clamps that provides glimpses of pure auxiliaries output during the few moments the vehicle is stationary. For that part, the study benefits from climatic roller bench campaign that Mercedes C300e underwent at -2 °C, 23 °C and 35 °C.

At first, cycle simulations are implemented with analytical power consumers profile to draw dropping ramps that best suit experimental battery depletion. Resulting curves start with quite high figures, some kilowatts, even close to 10 kW depending on temperature, then decrease to a steady state value (1-2kW) after some

thousands of seconds of transient. Beyond that, consumptions seem to drop to a very low value once Charge Sustaining mode is reached.

As a second step, we translated our rebuild auxiliaries profiles into thermal conditioning models. This is merely an interpretation of what appears to be the most sensible thing to do about probable vehicle's behaviour.

Aside from the battery 1 node thermal model previously described, we added to the Amesim sketch a 2 nodes thermal model as cabin representation: 1 node for inside air, and 1 node for inside solid furnishing. The first model accounts for battery conditioning (protection, optimisation) while the second represents HVAC. They are both controlled with proportional laws from which additional power to the auxiliaries is extracted, as simulator aims to maintain battery between 35°C/40°C and 19°C/23°C for occupants' comfort.

The cabin thermal model is calibrated after some empirical iterations. The final steady state power level depends on cabin outside exchange surface and convective coefficient which are respectively set to 5 m² and 20 W/m²/K. An additional 2000W heat flux is given to the cabin at 35 °C to cope with solar radiation on vehicle. As air sole thermal capacity remains negligible (~5kg of cabin air under 1033/kg/K specific capacity), cabin solid furnishing and its exchange coefficient with confined air are mainly responsible for transient duration, and thus for energy over-consumption during warm up or cool down. Acceptable transient profile is reached with 150 kJ/K capacity and 200W/K exchange coefficient (10m² x 20W/K/m² specific convection).

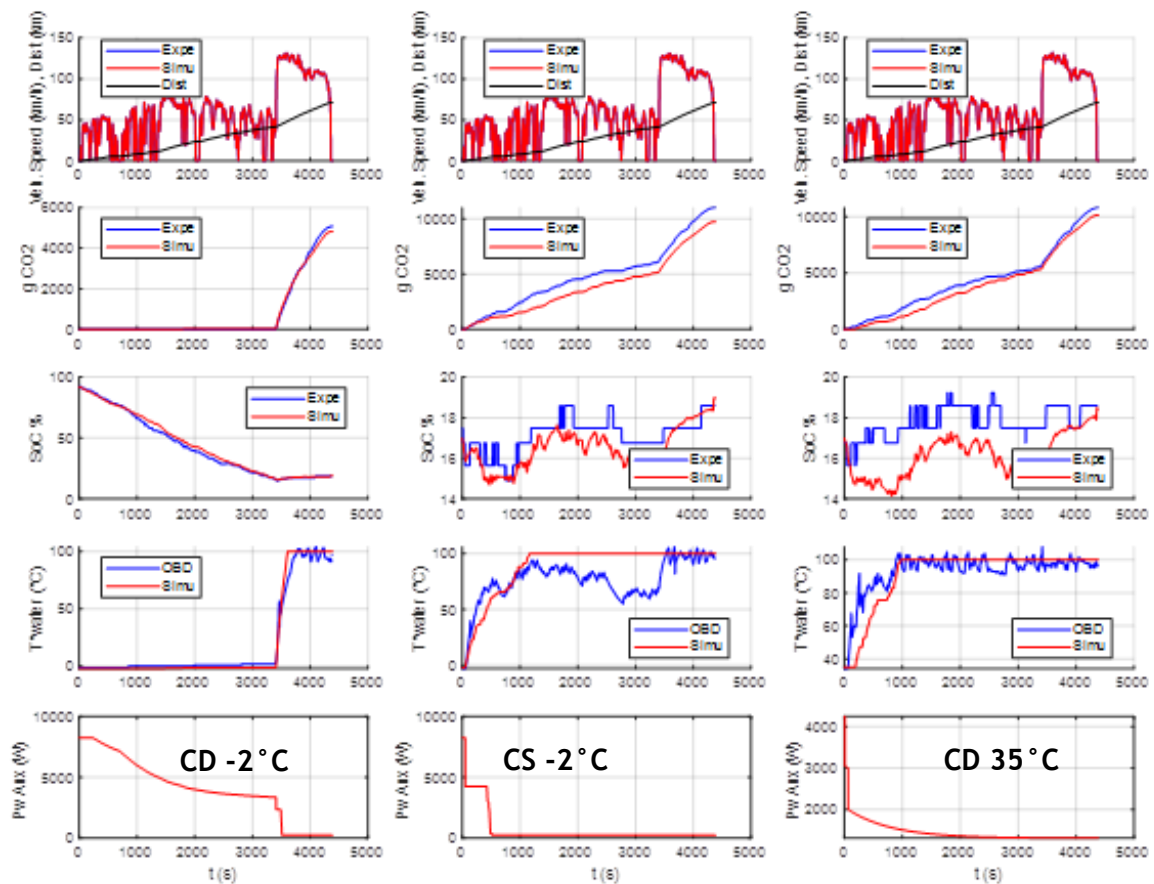


Figure 57 CD and CS vehicle climatic tests simulation features - 1st row: speed cycle and cumulated distance - 2nd row: measured vs. simulated cumulated CO₂ emission (~fuel consumption) - 3rd row: measured vs. simulated battery SoC profile - 4th row: OBD vs. simulation engine water coolant temperatures - 5th row: modeled auxiliaries power demand profile

Heating power was added to total auxiliary power consumptions since it is supposed to be operated by mere resistors, whereas only one third of cooling power is taken into account as we imagine compressors coefficient of performance around 3. Last row graphs of *Figure 57* illustrate resulting physical auxiliaries' power consumption (Pw Aux) for different temperatures and charging patterns.

In addition of this, some laws were added based on experimental current clamp observations but adjusted to match vehicle electric consumptions:

- Battery conditioning deactivates while running in charge sustaining mode,
- The electric cabin heater deactivates gradually when the engine coolant exceeds 50 °C and the heat exchanger takes over,
- 250W power general equipment always remains.

Finally, we had to arbitrarily add 1 kW of unexplained electrical consumption exclusively under CD phase, that might be linked to all electric operation of vehicle (electricity to power the auxiliaries such as coolant pumps, electronics control units, etc.), to precisely fit SoC profiles from 2nd row charts and respect CD to CS transition point.

The 4th row graphs show engine coolant & oil temperature curves according to which engine warm up coefficients were set up calibration in a previous paragraph.

3.1.3. Powertrain energy management laws

3.1.3.1. Online hybrid strategy

A key issue in hybrid vehicle simulation is the powertrain optimal control of all components. More precisely, it is to rule whether to run on electric or on liquid fuel depending on the instantaneous propulsion conditions. For that, IFPEN developed in-house ECMS algorithms¹⁸ based on Pontryagin's Minimum Principle and implemented it in Amesim's so-called component through its partnership with Siemens PLM Software.

Simply put, ECMS weights and compares at each time step the energy cost between ICE and battery usage thanks to an equivalence factor S to minimize overall consumption. The equivalence S provides bias to assess cost of electricity vs. fuel energy content and must be set under constraint of global SoC sustaining. This creates an electrical energy equivalent cost threshold above which motor is preferable and under which ICE is favoured, therefore high S tends to recharge vehicle, whereas low S tends to empty battery.

As one wishes to implement real-world-like on-line control strategy, without iterating on simulations to adapt to a given solicitation, we implemented heuristic laws in our sketch that overwrites S factor in real time. Therefore, it follows the following rules:

- Low S value while battery SoC allows CD operation, that massively favours massive electrical propulsion (detailed in next paragraph),
- Hysteresis detection of SoC depletion threshold to switch to CS mode,
- Variable S to targeted SoC (15 %) under CS sustaining operation.

Eventually, the control is calibrated with a single S factor for both gasoline and Diesel PHEVs, shared by all the considered driving cycles. A Proportional-Integral-Derivative (PID) corrected equivalence factor allows reliable and flexible vehicle control as illustrated by the simulation charts below, albeit final/starting SoC dispersion - battery does not always settle for the same final SoC depending on conditions¹⁹. The SoC profile in the 3rd row graphs shows remarkable correlations between experimental OBD survey and simulation, especially for the CS test in 2nd column yet starting notably undercharged. Heuristic control tightens electricity "cost" when SoC falls too low compared to the target, which urges ICE to compensate for, whereas it loosens this "cost" otherwise which favours electrical operation.

Thanks to this methodology, we managed to reach acceptable experimental vs. simulation agreement for both CO₂ emissions (i.e. fuel consumption) and battery electricity supply, as visible in 2nd and 3rd rows. As can be observed in the CO₂ emissions of the CD mode, the simulation reproduces well the moment when the engine starts, i.e. the switch between the charge depleting mode and the charge sustaining mode. It is of primary importance that the two power sources are

¹⁸ Dabadie J-C., Sciarreta A., Font G., Le Berr F.: *Automatic Generation of Online Optimal Energy Management Strategies for Hybrid Powertrain Simulation*, SAE Technical Paper 2017-24-0173

¹⁹ The vehicle on-line hybrid control cannot technically anticipate energy fluxes to reach a particular final SoC level at the end of any real use cycle. The current SoC at which vehicle stops depends on previous battery states and on power demand background history (no feed forward strategy).

considered alongside when calibrating global energy consumptions. Of course, the sharpness of these results comes from successive iterations on powertrain components calibrations, on control parametrisation, and on auxiliaries' power consumption illustrated in the last row.

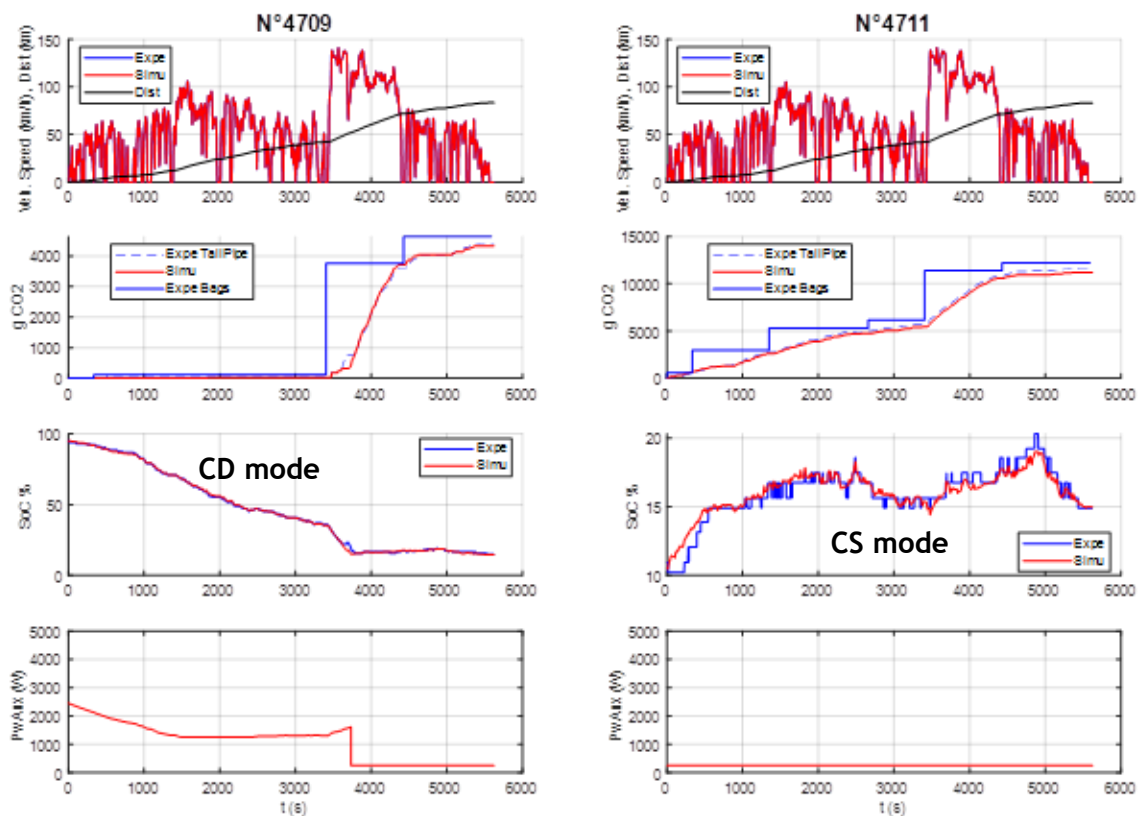


Figure 58 RDE test cycle simulation for CD and CS - 1st row: speed cycle and cumulated distance - 2nd row: measured vs. simulated cumulated CO₂ emission (-fuel consumption), blue steps show sub-cycle segments bag measurements - 3rd row: measured vs. simulated battery SoC profile - 4th row: modeled auxiliaries power demand profile

3.1.3.2. Driving conditions adaptation

One of the main issues about online control design was to fit with both the reference RDE cycle and the out-of-the-scope driving patterns. One shall not forget that a chosen compromise on powertrain management must not deteriorate outside temperature sensitivity validation. Specifically, we have to ensure that engine will be as engaged during harsh driving CD operation as it is with the real-world Mercedes C300e, even though in the simulator it could have theoretically achieved aforementioned driving by staying exclusively electric.

To do so, we implemented different levels of *S* control under CD, alongside motor capacity deratings. All the combined management modes are described in the following conditional table.

Table 15 ECMS heuristic hybrid control modes

Hybrid mode	Detection Conditions	ECMS Equivalence Factor S	Electrical Motor derating
Standard Depleting	Total cumulated consumption < m_{Fuel_crit}	$S=1$	Full peak potential
Harsh Depleting	Total cumulated consumption > m_{Fuel_crit}	$S=2$	Continuous envelope
Sustaining	Until SoC encounters 15%	On-line S with PID	Continuous envelope
Battery Protection	$T_{bat} < 20^{\circ}C$	See above S conditionality	70% of continuous → Full peak linearly for $0^{\circ}C \rightarrow 20^{\circ}C$

The first mode corresponds to standard charge depleting operation, in which propulsion power is provided quasi exclusively by motor at full potential thanks to sufficiently low S . In *Figure 60*, this is with such equivalence factor drawn in last row that nearly flat fuel consumption (i.e. no -or almost no- CO_2 emissions) is obtained at first in second row. Still, some punctual engine starts can occur, and if total cumulated (from the start) fuel consumption crosses a significant amount, heuristic control detects harsh driving style and switches to second mode. Then S is increased to 2 while motor operation potential is limited to its continuous envelope, as black operating dots cloud outlines in motor efficiency map below (*Figure 59*). This results into extensive use of ICE that supports electrical propulsion on peak power demands. The consequence on fuel consumption is visible in 2nd row time charts below, especially when higher speeds phase occurs.

Eventually, when depleting SoC is crossed, S follows PID driven law to sustain charge as described in previous paragraph. Moreover, the electric motor remains always derated to its continuous limit when in Charge Sustaining. In next charts' last row, last phase in S profiles illustrates such real-time control strategy adaptation.

Another heuristic layer was added on top of all these laws for battery protection purpose. This 4th mode derates motor operation range to only 70 % of its continuous envelope when battery cells stand below $0^{\circ}C$. With first projections of aggressive cycles starting immediately at really low temperatures, we identified and modelled huge internal resistance due to cold generates infinite current discontinuities. Consequently, the ICE must take over partly power supply in CD simulation that would crash otherwise. As the battery warms up (Joule losses + battery conditioning), the battery protection derating is gradually released until the cells reach $20^{\circ}C$.

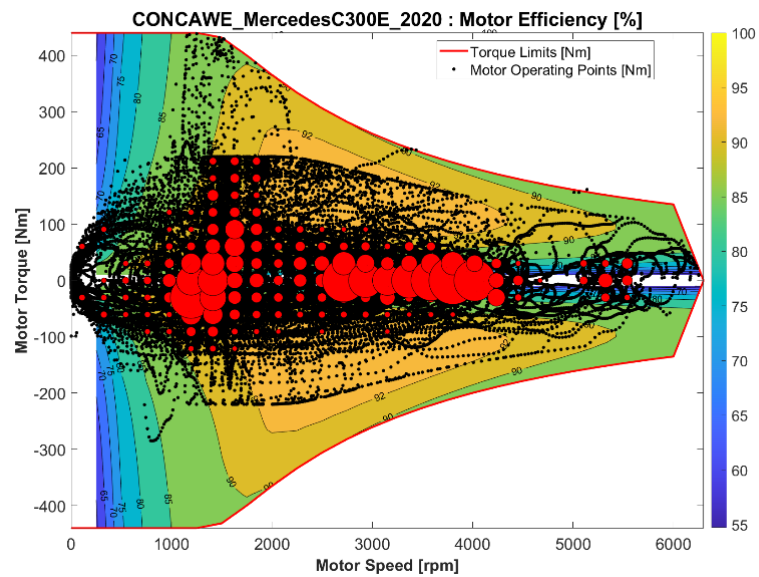


Figure 59 Motor efficiency map with time resolved operation points (black dots) under derated mode. Red circles stand for operation points density (i.e. weight during driving).

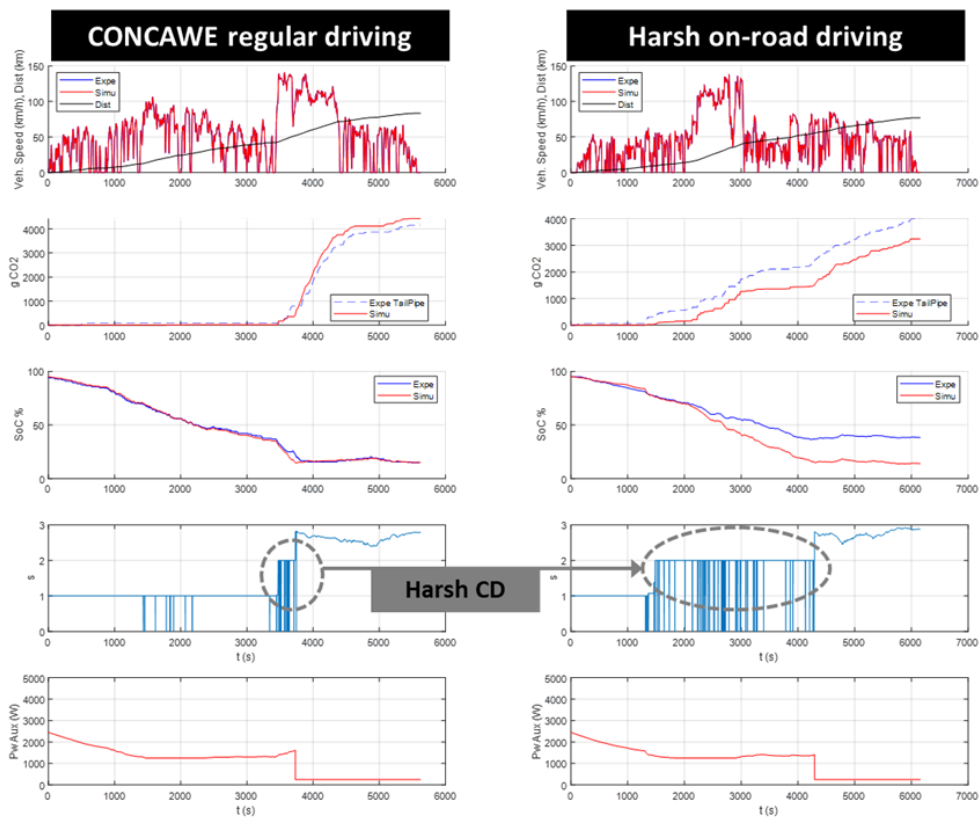


Figure 60 Simulated CD comparison of standard CONCAWE cycle vs. harsh road driving - 1st row: speed cycle and cumulated distance - 2nd row: measured vs. simulated cumulated CO₂ emission (~fuel consumption) - 3rd row: measured vs. simulated battery SoC profile - 4th row: S equivalence factor profile for hybrid management - 5th row: modeled auxiliaries power demand profile

3.1.4. Simulator validation

3.1.4.1. Detailed energy consumptions balances

This paragraph focuses on matching assessment between experimental and simulation energy consumption at both full cycle and subphases scales. With this mind, all the following box plots compare results level and dispersion for roller test bench and calibrated simulator. They represent the comparison between the experimental and simulation results, compared phase to phase and to the global cycle. Each green dot represents a given RDE test. The white dot represents the average value obtained. The box-and-whisker plot (or simply box-plot) represents graphically the statistical distribution of the results on the different RDE trials, as detailed in *Figure 61*.

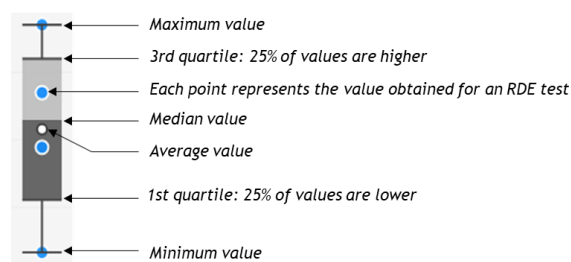


Figure 61 Explanation of the data representation mode

Examples shown below correspond to RDE study cycle for the gasoline PHEV. One will note that with very few exceptions, simulation results are much less dispersed, thanks to mathematical model determinism.

As much as possible, physical features are tackled along with corresponding isolated component calibration matter. Hence, negative electrical consumption, whose validation results are presented *Figure 62*, quasi-exclusively relates to regenerative braking. Results for CS quite remarkably overlap with the notable exception of first phase. This confirms the assumption of derating the continuous motor envelope in this mode. Letting motor access full peak power would have led to regenerative break overestimations. For the CD test, we estimated from OBD a wide variability of initial SoCs that were compensated for by engine recharging. Strategy responsible for this during the first of the 6 subphases must be more elaborated than what was implemented in simulator, and may for instance take into account exhaust treatment activation. Concerning Charge Depleting, simulation slightly underestimates (negative values) energy recovered. We linked that discrepancy to the SoC calculation method.

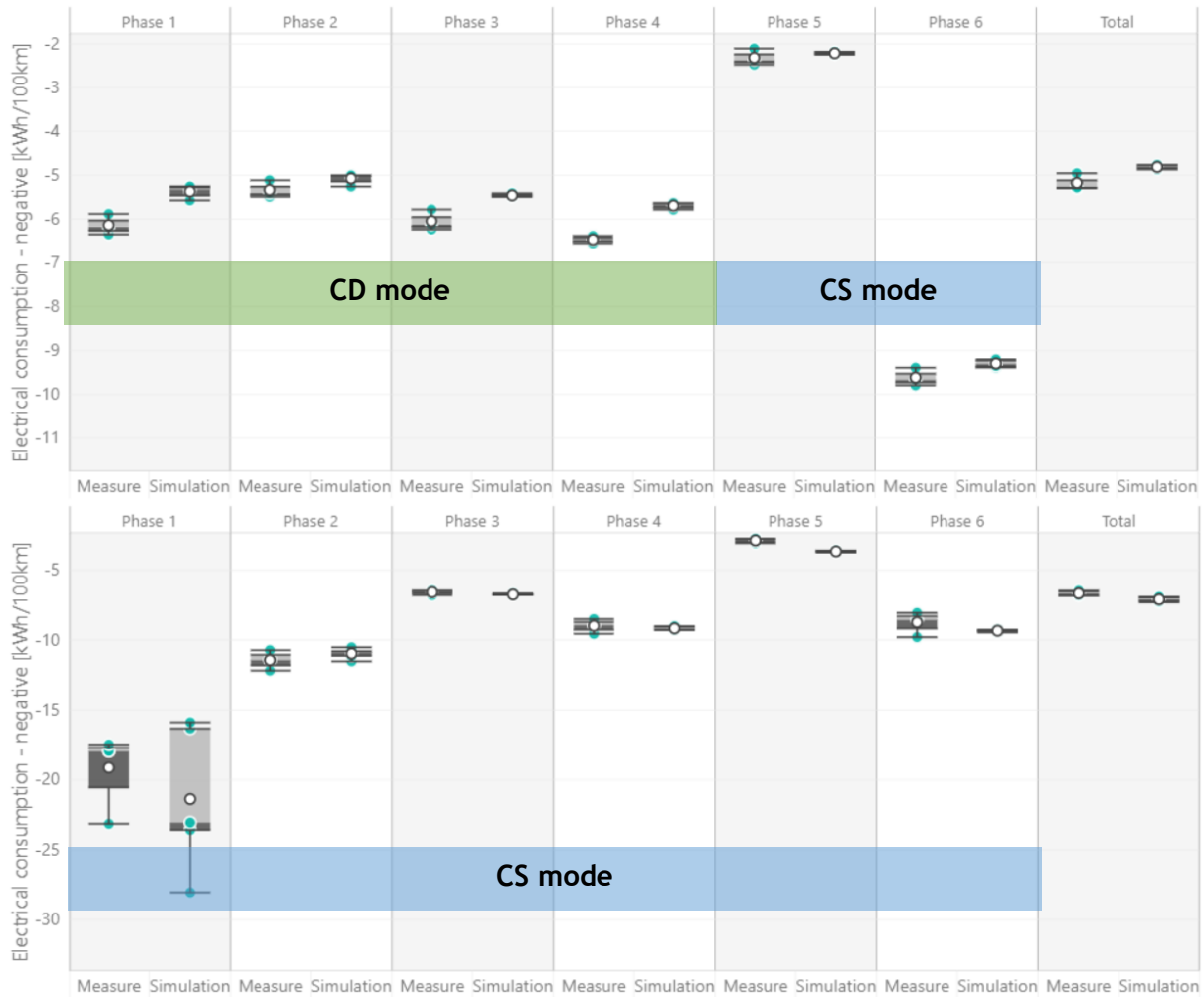


Figure 62 Phase to phase and cumulative battery regeneration power (negative power) for full (top) and empty battery (bottom)

Once regenerative braking calibration is validated, electricity consumption is isolated by taking a look at CD phase. *Figure 63* shows an overestimation of simulated net kilowatt-hours per 100 km, that can still be attributed partially to the methodology of SoC assessment. However, with this calibration, electricity consumption match is reached from another criterion: electrical range. If simulator tends to overestimate electricity consumption and yet drains out battery in the same fashion that the experiment does without starting ICE, that could imply that estimated effective battery range could be lowered.

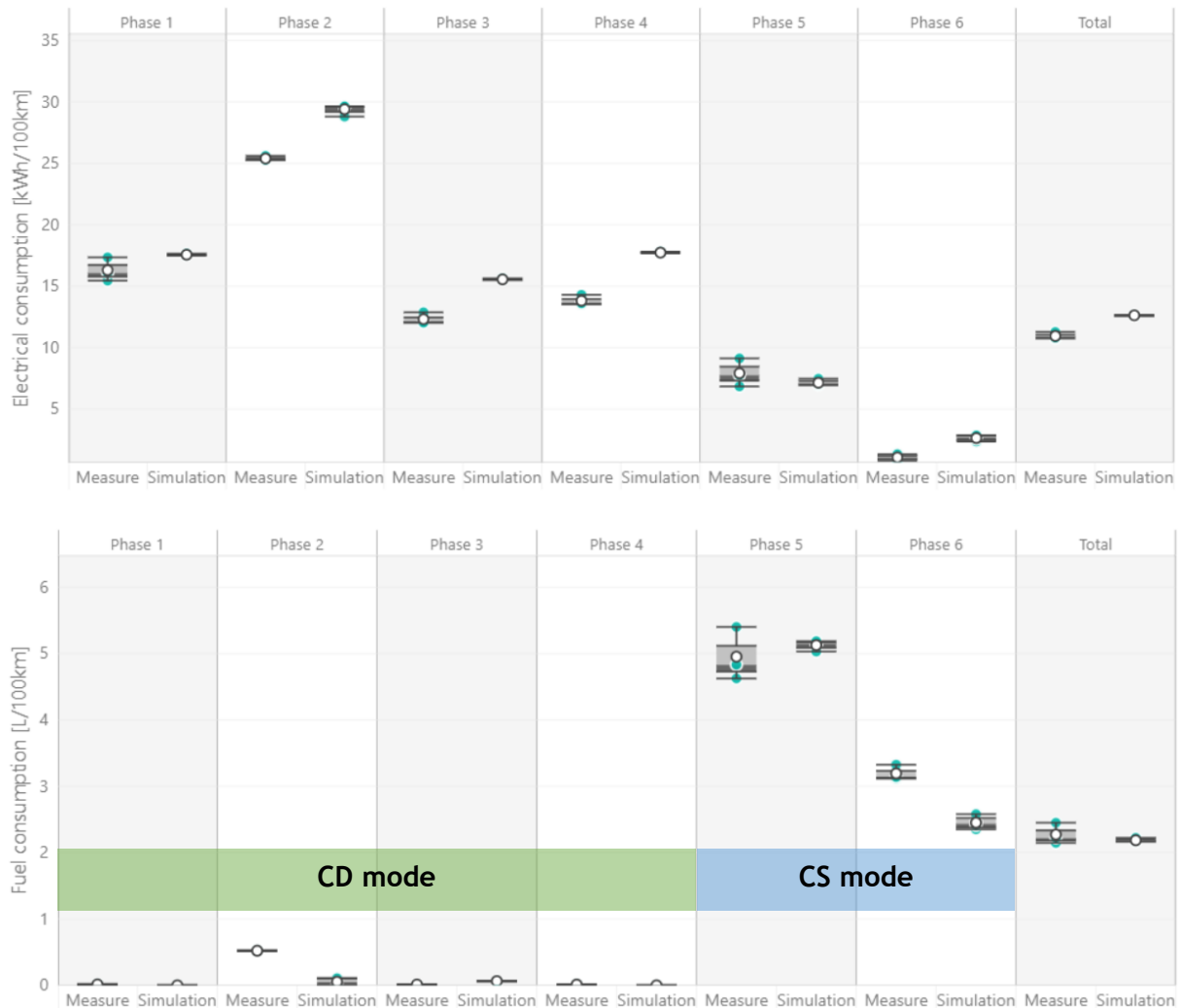


Figure 63 Electricity (top) and gasoline (bottom) consumptions starting full battery

One must pay attention to overall energetic accuracy by observing both electrical and fuel consumption with consideration over neighboring phases. Some overconsumption on one power source can be explained by a lower consumption on the other, or can be moved to the next phase without invalidating energy consumption: it has then more to do with command strategy.

This conjugated effect can be observed in the last example below showing CS test under the scope of again electricity and fuel. The acceptable overlap of results now comes from ICE fuel conversion efficiency since electrical part has already been dealt with. Of course, all these results come after iterations on components calibration since consumptions have mutual interactions and assumptions, even if the methodology explained here aims to dissociate effects.

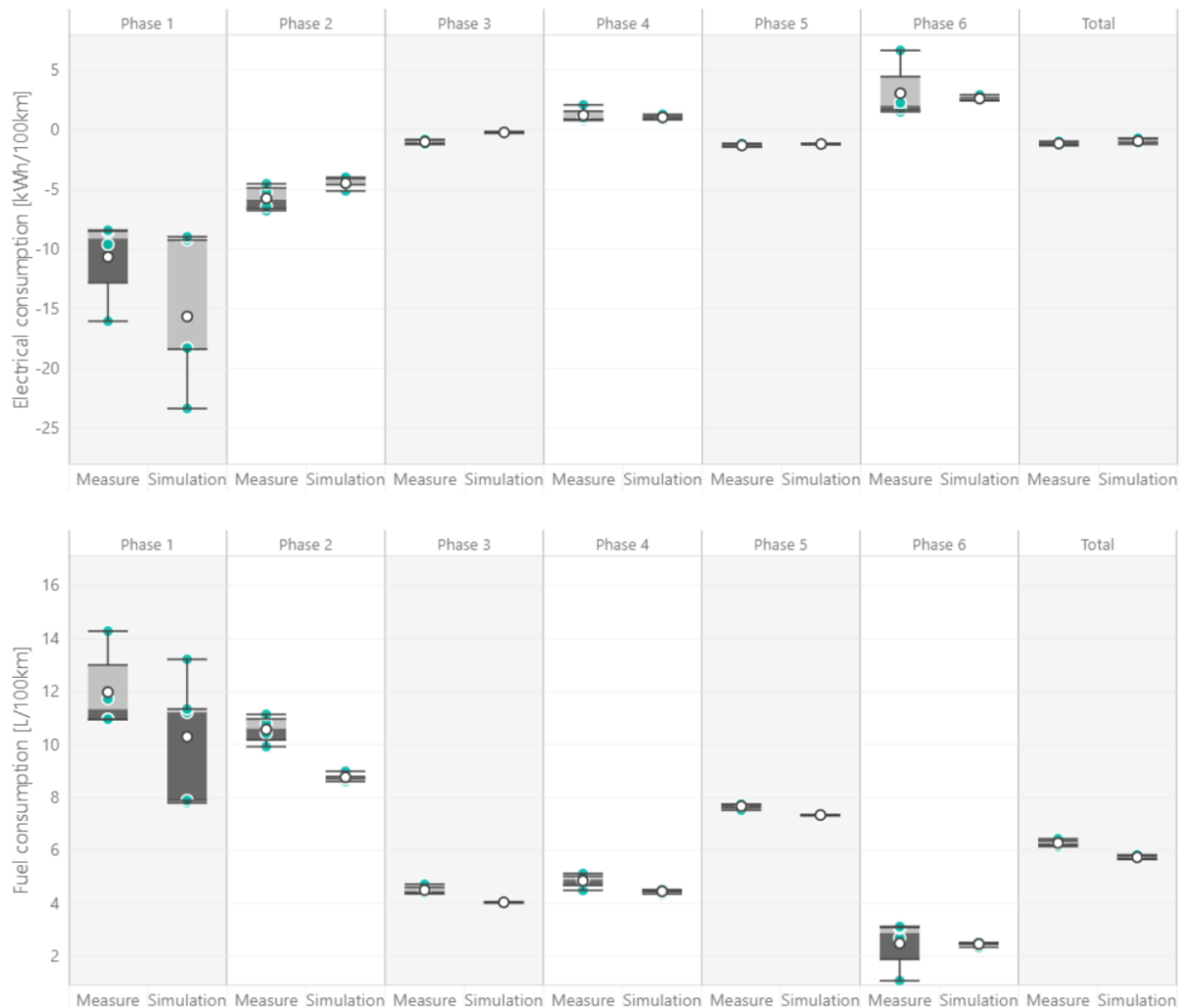


Figure 64 Electricity (top) and gasoline (bottom) consumptions starting empty battery

3.1.4.2. Road law selection

The simulation tool is now used to explain the difference in fuel consumptions between dyno test bench and on-road measurements. The next bar graph confirms that vehicle simulations under “Low” version of road law crosscheck experiments on which they were fitted in the first place: the blue bars match for both vehicles and both modes. However, simulations with this same road law get far from on-road figures which are significantly higher (shades of orange). Because on-road (RDE) cycles are less demanding (less aggressive driving), the simulated fuel consumptions are even lower than when chassis dyno driving profile was considered.

To bridge the gap, more charged road laws were tested. Increasing laden mass (to be representative of the additional mass incurred by the PEMS equipment) is clearly not enough (“Heavy”), although it already has moderate effect on road law coefficients since they are dimensionless. Using tougher coefficients (“High” law) enables to match road results, and therefore provides suitable explanations for experimental discrepancies. “High” road law, closer to real road requirements, is therefore chosen for further real-world projections in the next paragraphs. Better fit with real-world results could come from too optimistic “Low” law, or real road surface roughness.

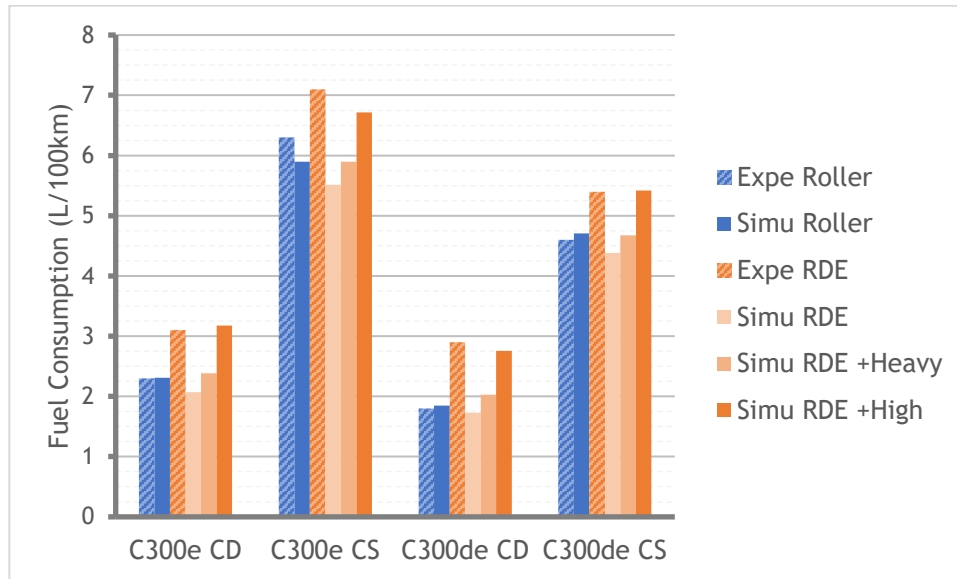


Figure 65 Road law sensitivity - Experimental vs. simulated fuel consumptions results

3.2. PROJECTION OVER COMPREHENSIVE RANGE OF CASES

In this part, we aimed to generate a whole set of simulation results, ideally over all possible vehicle conditions of use. The above calibrated simulator is thus used as projections for a wide range of driving conditions and styles, weather temperatures, battery sizing and conditioning, etc.

Then, to easily forecast real-world sequences of PHEV usage, we managed to develop a simplified linear model from the aforementioned database. Therefore, we ended up with a light mathematical method for prediction, without having to run again long simulations.

3.2.1. Simulations Design of Experiment

3.2.1.1. IFPEN's Clustered cycles projection base

As projection base, we take advantage of in-house IFPEN's clustered cycles [*article reference soon available*]. These cycles originate in GPS tracks reaped from Geco air database. To build them, trip samples underwent unsupervised classifications based on statistical features, such as average/max speed, stop time, acceleration sparsity, etc. and road qualifications, mainly based on speed limit. Then for each cluster, speed profile was generated using Markov chain process.

Eventually, this provides for the 4 types of road in France (< 30km/h, < 50km/h, < 90km/h, < 130km/h) a set of representative velocity profiles of characterized behaviour. Indicated as "road Conditions", and marked ascending from 1 to 7, they stand for jammed circulation, moderate driving, growingly dynamic patterns, even harsh ones, and finally speeding.

For comparison purpose, we added up the Artemis cycles typical for each of the 4 road types and WLTP homologation cycle. They are plotted in *Figure 66* among IFPEN's clusters against average speeds and 95th percentile of positive propulsion power. The latter stands as a statistically relevant upper limit in power demands distribution encountered along the driving cycle.

Table 16 DoE cycles categorization including IFPEN’s cluster-based generated cycles

Inner City	Outer City	Extra Urban	Highway
roadType1- roadConditions1	roadType2- roadConditions1	roadType3- roadConditions1	roadType4- roadConditions1
		roadType3- roadConditions2	roadType4- roadConditions2
		roadType3- roadConditions3	roadType4- roadConditions3
roadType1- roadConditions5	roadType2- roadConditions5	roadType3- roadConditions4	roadType4- roadConditions4
	roadType2- roadConditions6	roadType3- roadConditions6	roadType4- roadConditions5
roadType1- roadConditions7	roadType2- roadConditions7	roadType3- roadConditions7	roadType4- roadConditions7
Artemis TJam	Artemis Urb	Artemis Road	Artemis Mot

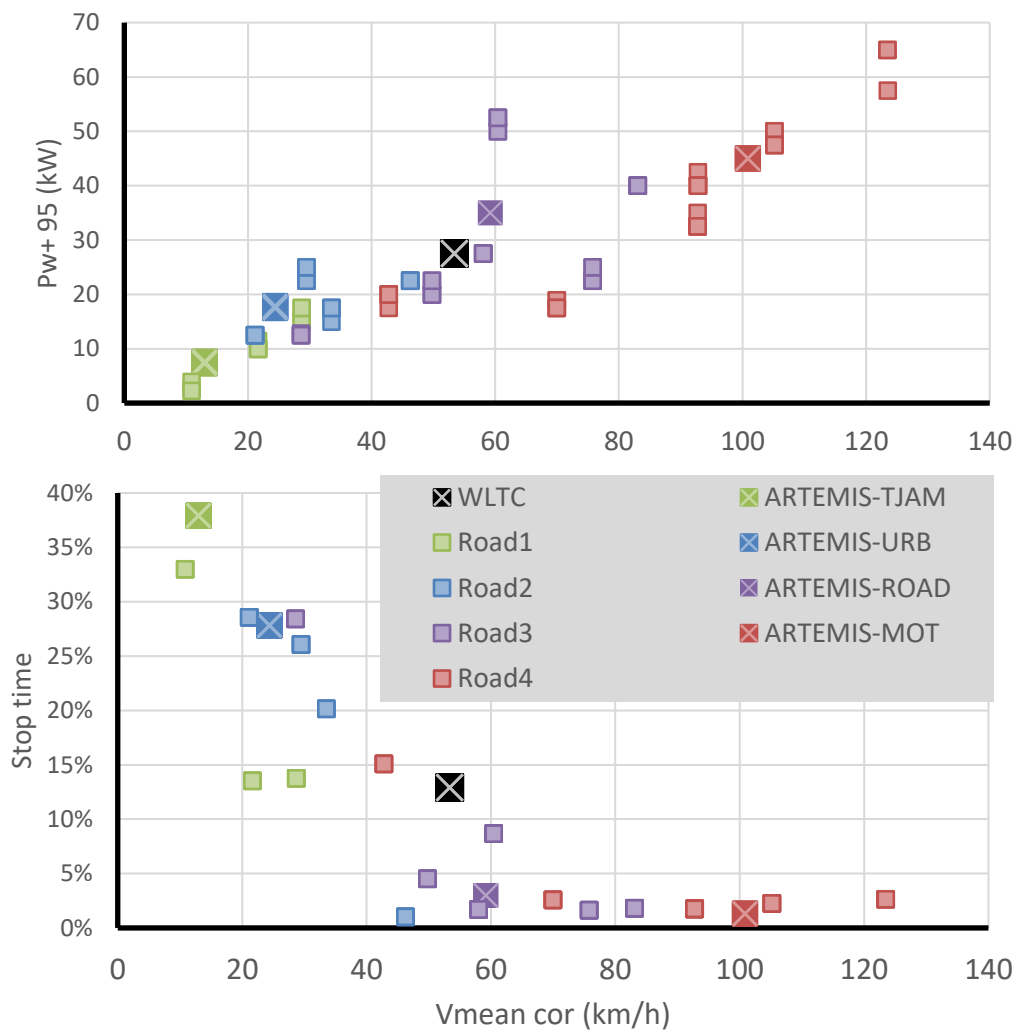


Figure 66 Clustered cycles positioning compared to common benchmarks in the view of some of the most consistent features (“Pw+ 95” means 95th percentile of positive propulsion power)

3.2.1.2. PHEV depletion modes

This paragraph describes the protocol with which CD and CS are simulated for each clustered cycle.

Components' heating behaviors were implemented, and induce transient auxiliaries consumptions. Therefore, one could not settle solely for one vehicle CD and one CS achieved under standard conditions to recombine all possible results. Therefore, we performed:

- a complete succession of depleting cycles until PHEV has reached SoC targeted threshold,
- then, a “hot CS” relevant for vehicle asymptotic consumptions once every component has been heated up,
- finally, a “cold CS” starting with all components at outside temperature, as if battery had not been charged (-HEV vehicle).

All the possible shades of sustaining modes reached with some heating left to realize (because depleting phase was not enough to reach vehicle's thermal steady state) are supposed to lay between these last 2 extreme CSs. For instance, a small or partially charged battery might empty before cabin and battery are totally conditioned: vehicle will then switch to charge sustaining with starting conditions somewhere between “Cold CS” and “Hot CS”.

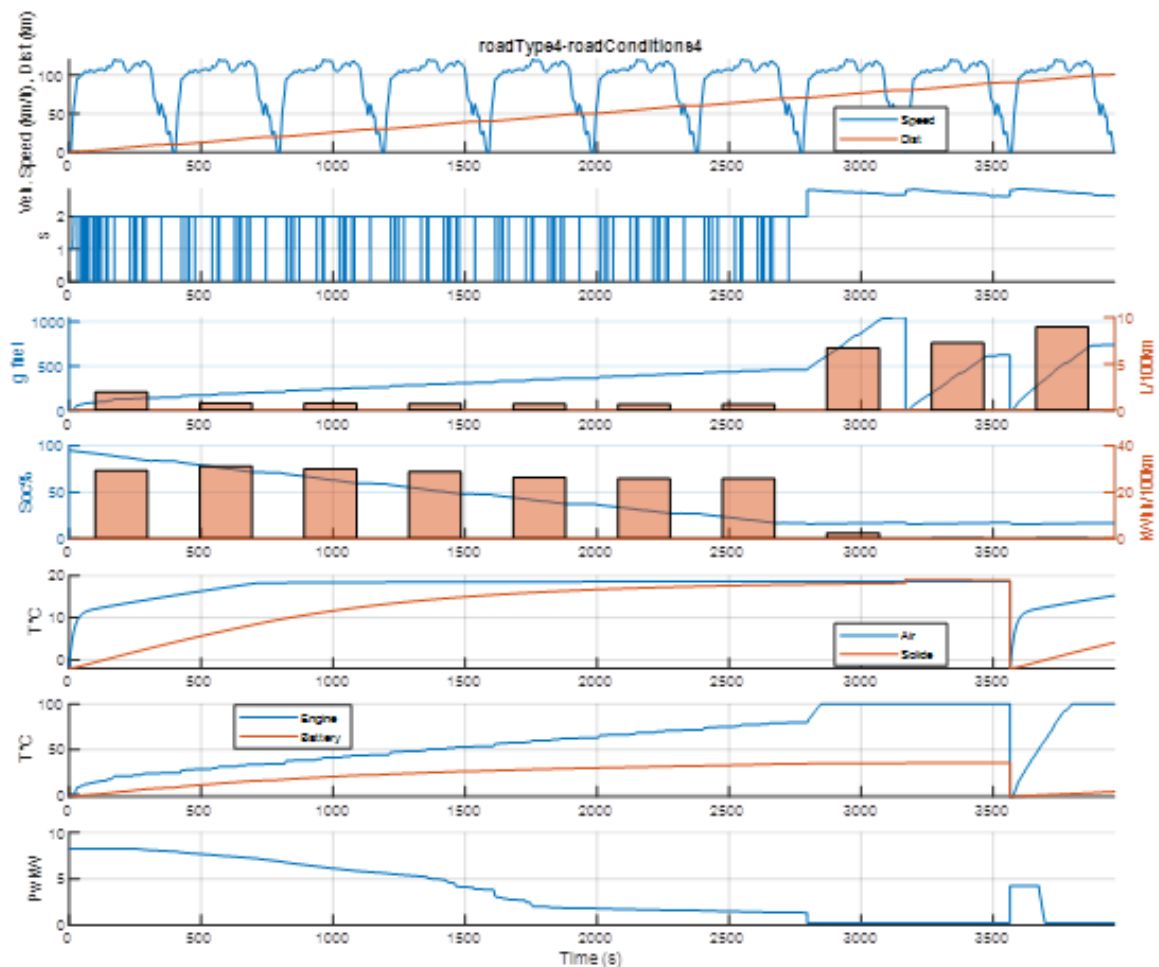


Figure 67 Concatenated simulation results for repeated sequence of moderate driving highway cycle

The example here of highway moderate driving shows that PHEV switches from depleting to sustaining mode at the very beginning of the 8th cycle repetition. As a consequence, 8th cycle fuel consumption becomes very close to “Hot CS” simulated right after it. Such depleting sequence puts forward the effect of transient thermal behavior and of engine coming up to temperature²⁰ allowing to switch off cabin heater. It thus shows progressive drop in auxiliaries power that result in CD electrical consumption to fall from ~30 kWh/100km to ~25 kWh/100km towards the end battery use. With the same pattern, sustaining fuel consumption is significantly higher over the last cycle than during its predecessor, because of heater requirement and cold engine overconsumption under low initial temperatures operation.

Transition cycle results are deliberately obliterated since it would be complicated to sort out which consumptions share to attribute respectively to CD and CS. It is noticeable that luckily cabin solid temperature and battery temperature endure approximately same dynamic, as we calibrated them both.

²⁰ During this highway cycle example engine starts though battery SoC is sufficient, especially on kick off acceleration over the first seconds.

3.2.1.3. Vehicles configurations

Each depleting and sustaining sequence described above for each clustered cycle is simulated for cold (-2°C), temperate (+23°C), and warm (+35°C) outside/initial temperature. Moreover, all situations are performed with both the gasoline and Diesel versions of the PHEV.

Finally, our test cases matrix is multiplied by the 3 different sized battery options:

- 13.5 kWh, nowadays Mercedes C300e/de capacity, allowing around 50 km of All Electrical Range (AER) under homologation cycle (WLTC) and conditions,
- 25 kWh, next generation benchmark, already starting production, aiming to reach 100 km AER in standard conditions,
- 7 kWh, previous generation observed capacity.

It is to be noted that the battery calibrated thermal capacity is supposed to change proportionally to its actual capacity, compared to the reference set up at 13.5 kWh. Virtually, the bigger the battery, the greater amount of electricity required to bring it to optimal temperature. Since we are trying to address the optimal capacity of batteries, we suppose that energy density remain the same, hence the proportionality between thermal and electrical capacities.

3.2.1.4. DoE overview

In summary, our test cases matrix holds multiple dimensions that are reminded in the table below.

Obviously, the whole DoE does not only hold for 1296 cases, but stands for more than 3000 simulations and detailed results, because of the variable number of successive depleting cycles necessary to drain battery. As a consequence, complete results generation takes a few days of continuous simulation performed by one scientific-aimed laptop.

Table 17 Simulation DoE dimensions and features

Dimensions explored	Number of variations	Values
ICE Energy	2 fuels	Gasoline, Diesel
PHEV mode	≥3 initial SoC	CD 95 % until 15 % depletion + CS hot + CS cold
Driving cycle	5+19 speed profiles	WLTC, ARTEMIS x4 [Road Type 1->4] x [Road Conditions 1->7]
Battery size	3 capacities	7 kWh, 13.5 kWh, 25 kWh
Outside Temperature	3 initial T°	-2°C, 23°C, 35°C

3.2.2. Analytical model rendering

Though simulation can provide any result from any situation, it remains a heavy process that cannot be generalized for each practical application. As we intend to aggregate day-to-day PHEV users' pattern over a whole population, we need to

make the best out of the previously generated database through an analytical method. Instead of rerunning simulations, we sought and found a mathematical post-processing way to bring the results altogether.

3.2.2.1. Results linearization principle

As a reminder, simulated energy consumptions seem to converge towards asymptotic levels after transient warm up. Therefore, the general idea of the mathematical process that we are seeking relies on identifying base figure for each speed profile, to which overconsumptions are then added. Since, the latter correlates yet achieved thermal conditioning, we need to quantify progression unified scales relevant to vehicle's components. For that purpose, we define the following deviation variables:

$$\begin{cases} \Delta T_{bat_i} = \text{Max}(0, 35^\circ\text{C} - T_{bat_i}) \\ \Delta T_{cab_i} = \text{Max}(0, 19^\circ\text{C} - T_{cab_i}, T_{cab_i} - 23^\circ\text{C}) \\ \Delta T_{eng_i} = 100^\circ\text{C} - T_{eng_i} \end{cases}$$

$$\Delta T_{env} = \text{abs}(\Delta T_{env} - 23^\circ\text{C})$$

These formulas bring forward the gap between actual and final (i.e. asymptotic) temperatures for the battery (optimal range 35°C-40°C), the cabin (passenger comfort 19°C-23°C), and engine (hot operation 100°C). The last formula states how far from standard temperature (23°C) the vehicle's environment is. This allow us to quantify steady state contribution: this stands as a permanent term to which transient consumption to reach target temperatures is added.

To draw simple dependencies (linear if possible), we had to select among such deviations the most suitable features consistent with the response that we were trying to model. After a few tests, we found the best response surfaces fittings (least squares method) with the 2D combinations illustrated in next graphs showing RoadType4-RoadConditions5 example.

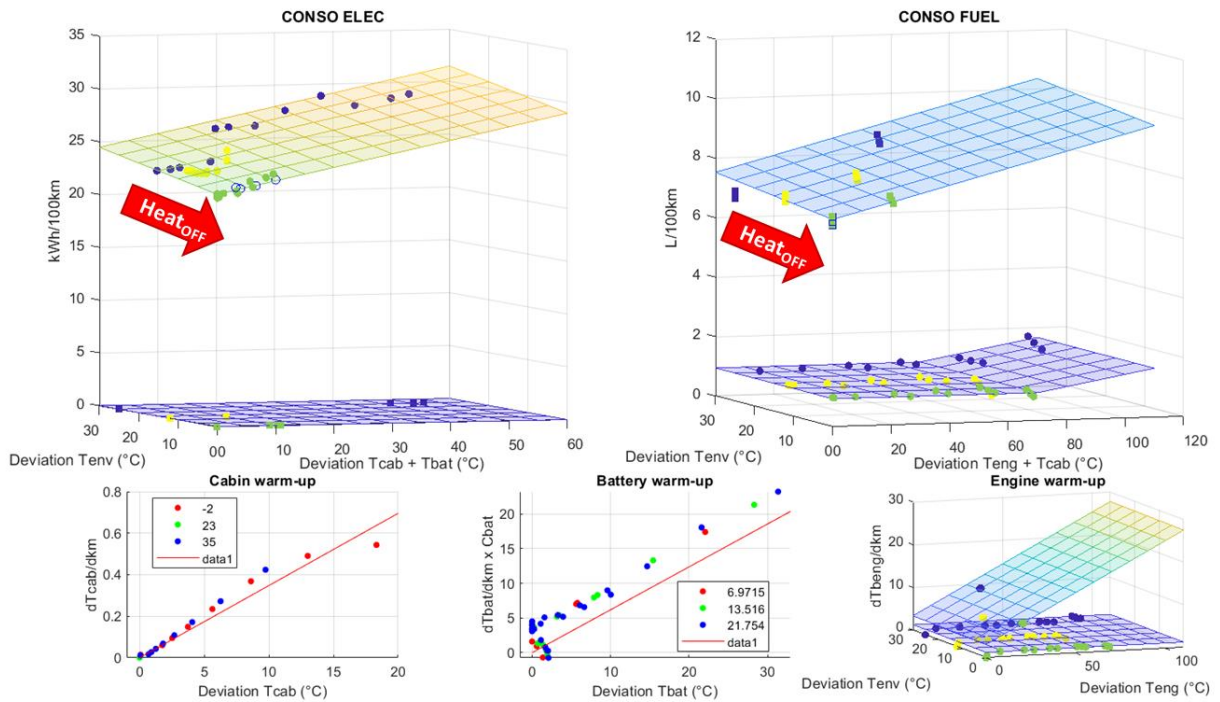


Figure 68 Fast highway driving example of linear learning method

Starting with battery’s electricity consumption in upper left graph, minimum energy rate in CD (dotted, squares are for CS and are considered zero) appears in green as the surface closest corner:

- Any displacement along X-axis induces overconsumption because battery and cabin still need to be heated up or cooled down. As they both have approximately the same dynamic, their respective deviation effects can be tangled.
- Any displacement along Y-axis means steady state overconsumption due to power required to maintain cabin temperature in warm or cold outside conditions.

As for electricity consumption, any combination of the 2 dissociated dimensions can be forecasted using simple linear coefficients, as next expression sums-up.

$$\begin{cases} \text{Cons}_i^{\text{Batt}} = \text{Cons}_i^{\text{Batt}} + \alpha_i \Delta T_{\text{bat}_i} + (\alpha_i \Delta T_{\text{cab}_i} + \beta_i \Delta T_{\text{env}}) \cdot \text{Heat}_{\text{OFF}} & \text{under CD} \\ \text{Cons}_i^{\text{Batt}} = 0 & \text{under CS} \end{cases}$$

$$\text{Heat}_{\text{OFF}} = (\Delta T_{\text{env}_i} > 50^\circ\text{C} \cup T_{\text{env}} > 23^\circ\text{C})$$

To get clean surfaces, some -2°C points had to be graphically rebased because of the cabin heater being turned off. Indeed, thanks to engine reaching 50°C at least, the cabin is provided with free heat from the engine coolant, and such -2°C points can virtually be considered as standard 23°C , hence the deviations terms cancel out in formulas. For the sake of simplification and because it appeared to be of 2nd order influence, SOC levels are not discriminated and points relative to different battery capacities are mixed up. This might explain some of small discrepancies visible around response surfaces.

For fuel consumption (upper right graph in *Figure 68*), the same 2D linear learning method can be implemented. In the following equations, the affine formulation of the fuel consumption on CS remains quite similar to the one just described for the electrical energy, including the rebasing of the points related to the heating shutdown. CD fuel consumption is simplified solely to X-axis dependency, with 70 °C offset on engine temperature. The deviation of the engine temperature from its set point is the descriptor that replaces that on the battery temperature.

$$\begin{cases} \text{Cons}_i^{\text{Fuel}} = \text{Cons}_i^{\text{CD}} + C_i (\text{Max}(0, \Delta T_{\text{eng}_i} - 70^\circ\text{C}) + \Delta T_{\text{cab}_i} \cdot \text{Heat}_{\text{OFF}}) & \text{under CD} \\ \text{Cons}_i^{\text{Fuel}} = \text{Cons}_i^{\text{CS}} + A_i \Delta T_{\text{eng}_i} + (A_i \Delta T_{\text{cab}_i} + B_i \Delta T_{\text{env}}) \cdot \text{Heat}_{\text{OFF}} & \text{under CS} \end{cases}$$

Thankfully, 2 uncorrelated dimensions linearization pattern also works to predict Utility Factors, still with outside temperature deviation for steady state and deviations term disabling for hot engine, as shown in next 3D graphs. However, engine/cabin/battery cumulated deviations are here considered for X-axis transient effect. Under CD mode, both upper response surfaces (dots) show 100 % electric drive or close. On the contrary, CS mode surfaces (squares) implies degradation of electric share much more responsive to temperature deviations for Road1 profile than for Road4.

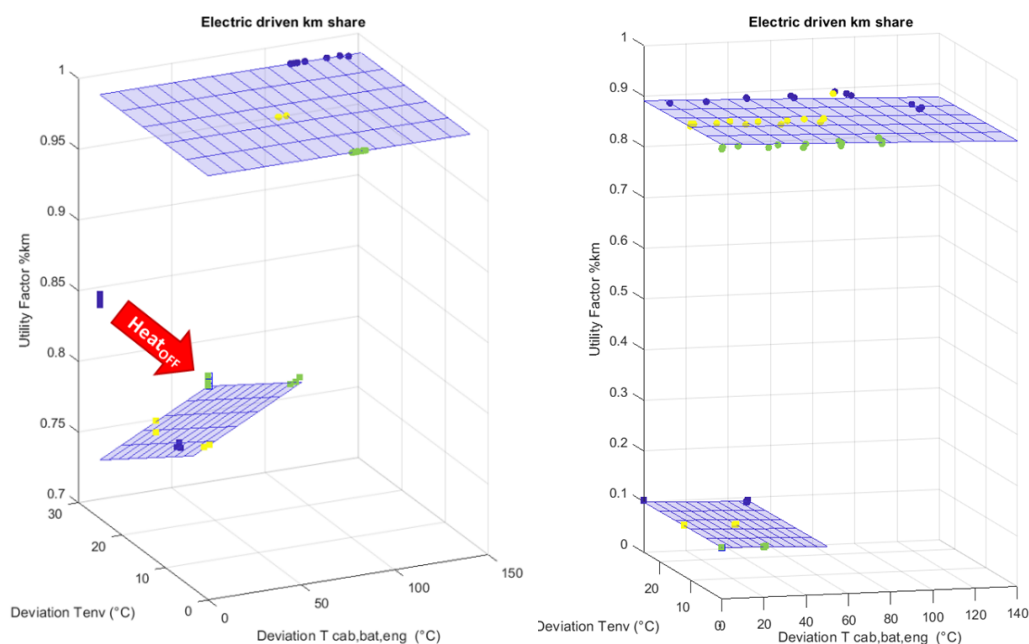


Figure 69 Fast driving highway cycle example of linear response surfaces to predict UFs

3.2.2.2. Temperature deviations assessment

Electrical and fuel consumption can quite confidently be calculated with linear combinations of vehicle temperature deviations. Yet, these thermal progression indicators still need to be assessed in the first place. For that purpose, temperatures evolution rates over driven kilometres were estimated during database post-processing.

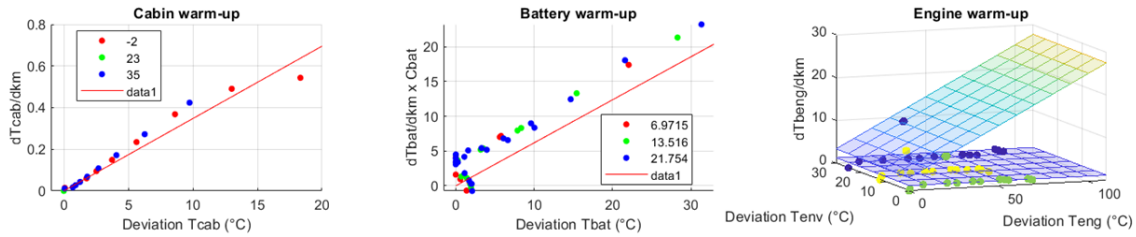


Figure 70 Fast driving highway cycle example of temperature deviations results linearization - Graph 1 (cabin T°): each point represents a simulation classified by ambient temperature - Graph 2 (battery T°): each point represents a simulation classified by battery capacity - Graph 3 (engine T°): each point represents a simulation classified by ambient temperature

Concerning cabin and battery, their derivatives appear quite remarkably proportional to their own value, which remains reassuringly consistent with proportional command implemented in the simulator. This means that a first order solution using slope coefficient interpolated from considered driving cycle can easily be implemented over driven kilometres in transient exponential profile below. For simplification’s sake, battery temperature derivative is specified in comparison to its capacity.

$$\Delta T_{bat_i}(Km) = \Delta T_{bat_i}^0 e^{-\lambda_{bat}^i \cdot Km}$$

$$\Delta T_{cab_i}(Km) = \Delta T_{cab_i}^0 e^{-\frac{\lambda_{cab}^i}{C_{Batt}} \cdot Km}$$

Engine temperature derivative over distance is a bit more elaborated. Its 3D shape stays logically close to the corresponding fuel consumption response surfaces, since engine warm-up was calibrated in the simulator proportionally to the amount of burnt fuel. A first order solution still exists for engine temperature progression profile.

3.2.2.3. Coefficients results

Thanks to a very reasonable number of coefficients recorded in next tables, we are now able to forecast simply fuel and electricity consumptions of each vehicle for wide range of typical driving cycles. Colormap scale was added to base specific consumptions to stress their correlation to speed profile. Neighbor slope coefficients quickly give overconsumption contribution of components transient warming up and of steadying vehicle temperature. CS Electricity are not mentioned as they are considered zero.

Similar coefficient tables are edited in annex for deviation evolution profile assessment and for utility factors generation.

Table 18 Linear coefficients for base and marginal energy consumptions

Cycles	C300e Consumptions regressions							
	Electricity CD			Fuel CD		Fuel CS		
	kWh/100km	kWh/100km /°C ΔBat+Cab	kWh/100km /°C ΔEnv	L/100km	L/100km /°C ΔEng	L/100km	L/100km /°C ΔCab+Eng	L/100km /°C ΔEnv
'roadType1-roadConditions1'	29.9	1.51	1.138	0.0	0.000	7.0	-0.010	0.257
'roadType1-roadConditions5'	22.4	0.61	0.451	0.0	0.000	5.8	0.013	0.140
'roadType1-roadConditions7'	22.3	0.45	0.282	0.0	0.017	5.8	0.015	0.108
'roadType2-roadConditions1'	24.9	0.76	0.553	0.0	0.000	6.1	0.012	0.161
'roadType2-roadConditions5'	23.3	0.40	0.221	0.0	0.018	5.8	0.018	0.108
'roadType2-roadConditions6'	24.0	0.53	0.278	1.8	0.064	7.6	0.016	0.099
'roadType2-roadConditions7'	19.6	0.22	0.126	0.4	0.013	5.7	0.020	0.054
'roadType3-roadConditions1'	24.2	0.48	0.416	0.0	0.008	6.0	0.006	0.097
'roadType3-roadConditions2'	20.8	0.23	0.107	0.5	0.008	5.8	0.021	0.061
'roadType3-roadConditions3'	23.1	0.18	0.105	0.1	0.011	5.7	0.020	0.045
'roadType3-roadConditions4'	20.8	0.15	0.073	0.5	0.011	6.0	0.022	0.029
'roadType3-roadConditions6'	21.9	0.09	0.191	2.0	0.098	7.3	0.030	0.037
'roadType3-roadConditions7'	22.6	0.12	0.101	1.5	0.029	7.4	0.029	0.026
'roadType4-roadConditions1'	23.7	0.30	0.153	0.0	0.013	5.9	0.016	0.059
'roadType4-roadConditions2'	21.8	0.16	0.136	0.0	0.003	5.7	0.021	0.037
'roadType4-roadConditions3'	22.6	0.13	0.064	1.0	0.021	6.9	0.025	0.023
'roadType4-roadConditions4'	26.2	0.11	0.065	0.2	0.027	7.2	0.026	0.020
'roadType4-roadConditions5'	26.6	0.12	0.069	1.4	0.026	8.4	0.028	0.016
'roadType4-roadConditions7'	32.5	0.12	0.026	2.2	0.035	10.5	0.042	0.013

Cycles	C300de Consumptions regressions							
	Electricity CD			Fuel CD		Fuel CS		
	kWh/100km	kWh/100km /°C ΔBat+Cab	kWh/100km /°C ΔEnv	L/100km	L/100km /°C ΔEng	L/100km	L/100km /°C ΔCab+Eng	L/100km /°C ΔEnv
'roadType1-roadConditions1'	29.8	1.51	1.137	0.0	0.000	5.6	0.004	0.293
'roadType1-roadConditions5'	22.1	0.61	0.449	0.0	0.001	4.6	0.024	0.162
'roadType1-roadConditions7'	21.8	0.45	0.288	0.0	0.023	4.4	0.027	0.134
'roadType2-roadConditions1'	24.6	0.76	0.553	0.0	0.000	4.8	0.024	0.190
'roadType2-roadConditions5'	22.7	0.40	0.226	0.1	0.029	4.5	0.027	0.122
'roadType2-roadConditions6'	23.2	0.54	0.304	1.6	0.047	5.8	0.030	0.117
'roadType2-roadConditions7'	19.2	0.23	0.130	0.3	0.017	4.3	0.029	0.069
'roadType3-roadConditions1'	23.7	0.51	0.404	0.0	0.011	4.4	0.028	0.132
'roadType3-roadConditions2'	20.3	0.24	0.114	0.5	0.012	4.4	0.028	0.070
'roadType3-roadConditions3'	22.9	0.21	0.069	0.1	0.009	4.5	0.027	0.056
'roadType3-roadConditions4'	20.5	0.15	0.090	0.4	0.011	4.7	0.027	0.039
'roadType3-roadConditions6'	20.9	0.37	0.113	1.8	0.058	5.7	0.030	0.041
'roadType3-roadConditions7'	21.6	0.45	-0.019	1.3	0.026	5.9	0.033	0.021
'roadType4-roadConditions1'	23.2	0.29	0.172	0.0	0.019	4.5	0.030	0.085
'roadType4-roadConditions2'	22.0	0.18	0.093	0.0	0.005	4.6	0.025	0.043
'roadType4-roadConditions3'	22.2	0.12	0.078	1.0	0.025	5.5	0.028	0.026
'roadType4-roadConditions4'	26.8	0.07	0.073	0.0	0.043	5.8	0.030	0.021
'roadType4-roadConditions5'	25.6	0.12	0.085	1.4	0.026	6.9	0.033	0.016
'roadType4-roadConditions7'								

3.2.2.4. Mathematical Implementation

Thanks to an adapted regression routine, energy consumption rates restitution has been mathematically narrowed to a linear combination of constants and exponential functions witnessing components transient behaviour. This results into analytical solutions for cumulative scores, easily integrated over driven kilometres, as formalized with next practical example.

$$kWh_i(Km) = Cons0_i^{kWh} Km + \beta_i \Delta T_{env} Km^{**} + \alpha_i \Delta T_{bat}^0 \frac{1 - e^{-\lambda_{bat}^i Km}}{\lambda_{bat}^i} + \alpha_i \Delta T_{cab}^0 \frac{1 - e^{-\lambda_{cab}^i Km^{**}}}{\lambda_{cab}^i}$$

For each driving cycle *i*, each contribution - constant, temperature maintenance, warm up - can obviously be identified. One should be careful to consider the

corrected integration distance Km^{**} , above which heater is turned off thanks to engine exceeding $50^{\circ}C$ and thus integrating overconsumption can be stopped.

$$Km^{**} = \begin{cases} \min \left[Km, \frac{\text{Max}(0, \Delta T_{eng_i^0} - 50^{\circ}C)}{K_{eng}^i} \right] & \text{if } T_{env} \leq 23^{\circ}C \\ Km & \text{if } T_{env} > 23^{\circ}C \end{cases}$$

Once we are able to integrate consumptions over any clustered cycle, we can sum them into the process pictured by the flow chart below, in order to forecast real-world vehicle solicitation.

The latter, which is divided into a sequence of identified speed profiles, is provided as cycles list and respective mileages, along with vehicle's characteristics and weather conditions. Thereby in a loop pattern, temperatures deviation profile and then consumptions are successively estimated for each segment. Eventually, the addition of all segments indicates the total amounts of electricity and fuel required to follow this specific use.

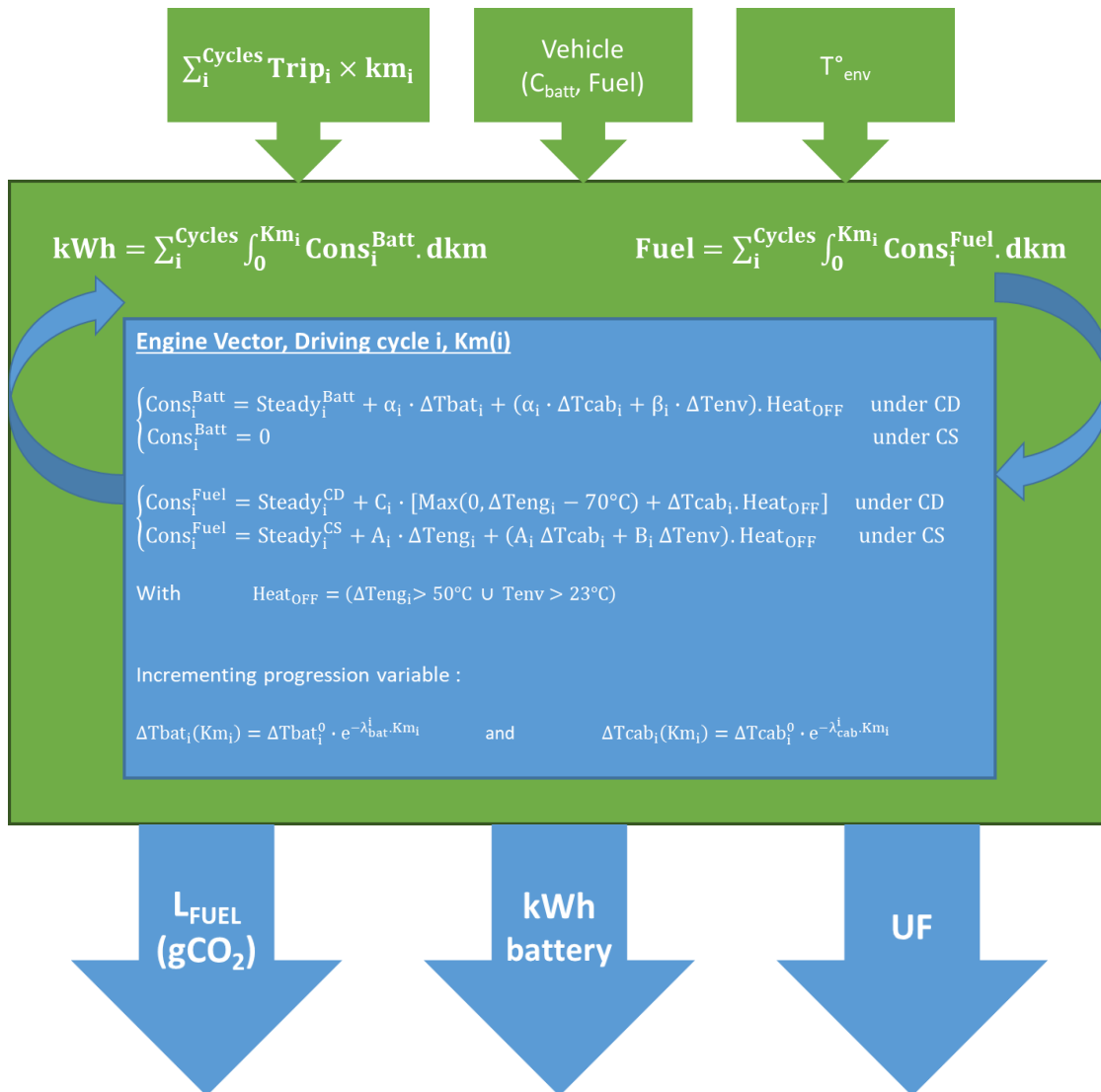


Figure 71 General processing sketch of PHEV behavior analytical assessment

The next multi-diagrams illustrate such a practical example through a countryside to inner city trip. For that we considered the C300e equipped with a full 25 kWh battery driven by a cold -2°C day 10km on road, then 60 km on highway, entering 10 km of city, and finishing with 3 km of city centre.

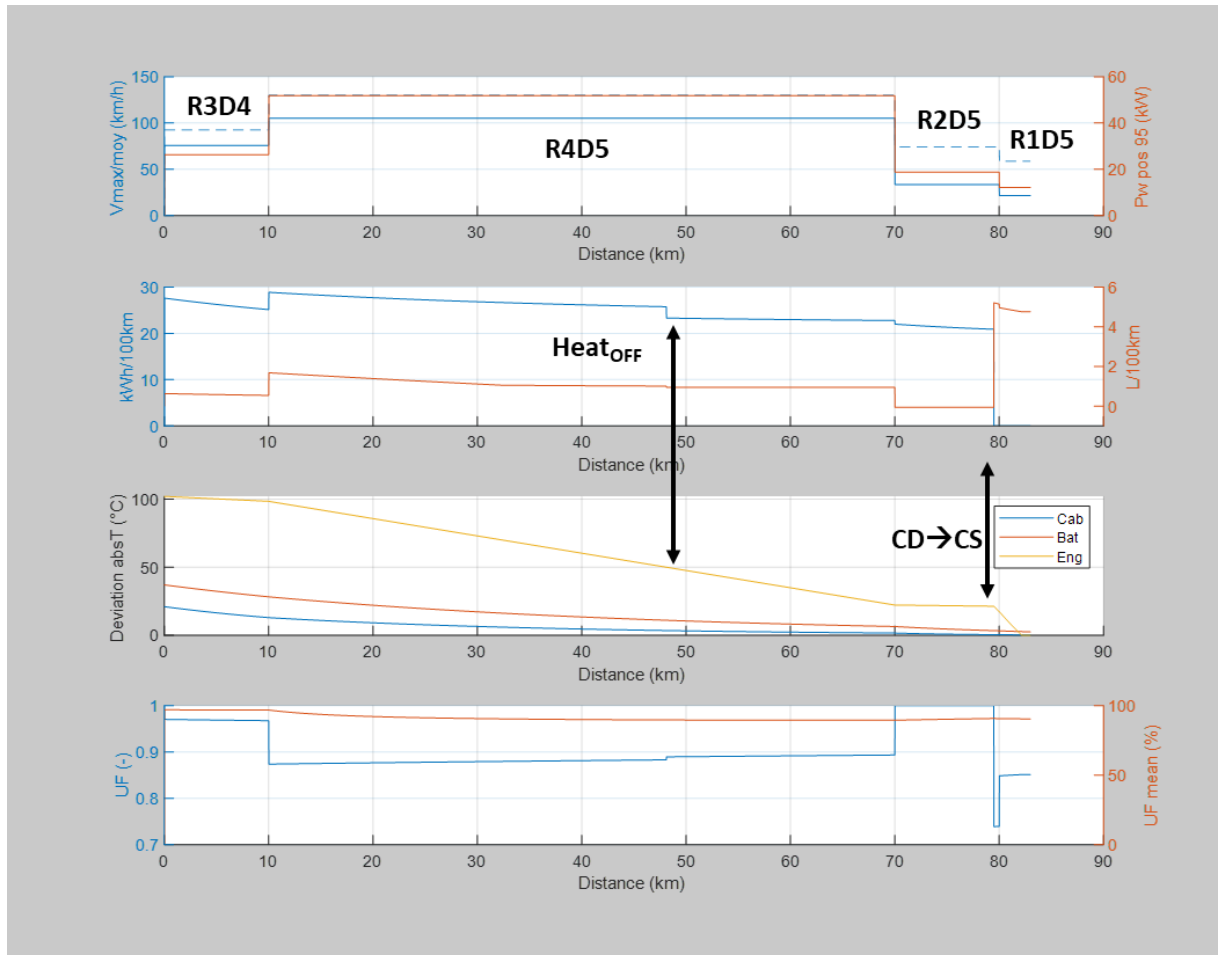


Figure 72 Time resolved example of analytical model practical exercise other country to city sequence

Obviously, one cannot expect to get time resolved detailed curves from our analytical approach: vehicle physical behaviour is considered homogeneous along each distinctive segment characterized in top chart indicators (speeds & power 95th percentile). Yet, 1st order transient warm up can be acknowledged from the 3rd chart concerning engine/cabin/battery temperature deviations progression. Its direct impact on consumptions can also be observed in the 2nd chart, as they progressively drop to their asymptotic values.

Aside from switches from a driving pattern to the next that induce expected steps, singularities are recorded when:

- engine reaches 50°C , inducing a sudden drop in consumptions thanks to coolant heat availability,
- electrical and fuel consumptions overturn because of CD to CS transition.

3.2.2.5. Mathematical model validation with physical simulation

In accordance with the previous example, the same sequence is parametrized as a whole and re-run as a single cycle in the vehicle physical simulator to check for discrepancies between the 2 methods. The fact that next bar graph shows only a few percent gaps for the 3 features legitimizes the learning and restitution process that we implemented to analytically model the database. Moreover, we tested an intermediate case at 10°C for further verification. As we noticed no wider discrepancy with bars, it can be concluded that the mathematical model is predictive in the range of learned ambient temperatures [-2°C, 35°C].

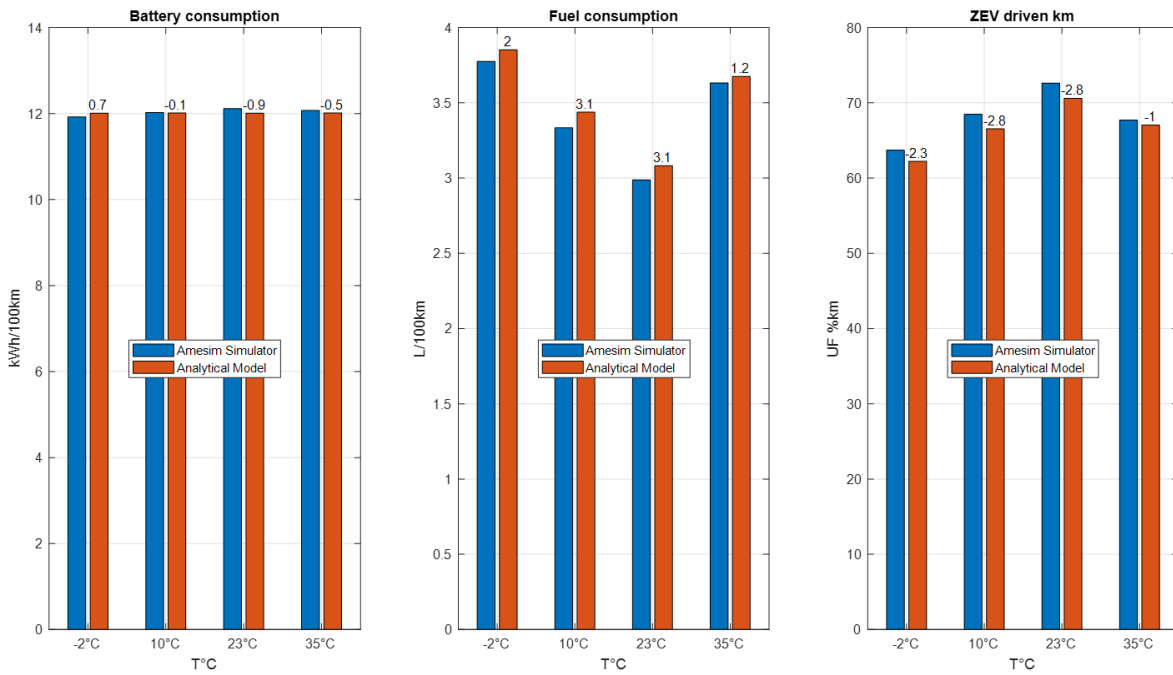


Figure 73 Simulation vs. mathematically assessed driving sequence for the complete range of ambient temperatures

3.3. SUMMARY OVER GENERALIZED USAGE

Due to the degrees of freedom induced by the architecture of PHEVs, they are extremely versatile: equally capable of operating almost exclusively on electrical or chemical energy depending on the conditions of use. However, not all the conditions are encountered as frequently as the others in the actual uses carried out. It is therefore necessary to assess the actual behaviour of PHEVs:

- By capturing the sensitivity of technologies to the conditions.
- By assigning a weighting to each condition according to its representativeness.

The WLTP certification procedure, including a full battery test, an empty battery test, and a weighting between the two resulting from a strong hypothesis of daily charging and daily distance distribution, applies these two necessary steps.

We therefore propose here, thanks to this simulation work, to go further by:

- considering more sensitivities of technologies (particularly to ambient temperature).
- considering more usage statistics.
- not necessarily considering daily recharging but a whole range of recharging frequencies.
- varying the size of the battery.

3.3.1. Capturing the sensitivity of technologies: Assessment of results on a large matrix

Based on the analytical model detailed in paragraph 3.2.2, each individual use case is simulated as a combination of:

- **v** conditions of daily vehicle kilometers travelled (VKT) and associated driving patterns, 24 cases [4:400km]
- **t** conditions of ambient temperature, 20 cases [-2:36 °C]
- **r** conditions of recharge period, 11 cases [0.5:10days]
- **b** conditions of battery sizing, 10 cases [2:35kWh]

Figure 74 presents the results of simulations made for one given value of battery size and recharge frequency for the gasoline PHEV. A total of 480 cases of temperature/daily mileage are considered.

The simplified mathematical model reproduces the behavior of the physical model, and therefore also of the vehicles evaluated experimentally. A sharp increase in power consumption in cold ambient conditions is observed. Consequently, the fuel consumption increases faster with VKT at low temperature, due to the decrease of the electric range.

The same simulations were made for every battery size [2 to 35kWh] and recharge period [0.5 to 10 days], for both Diesel and gasoline vehicles, leading to around 53000 use cases simulated including variation of technology sizing, environmental and driving conditions.

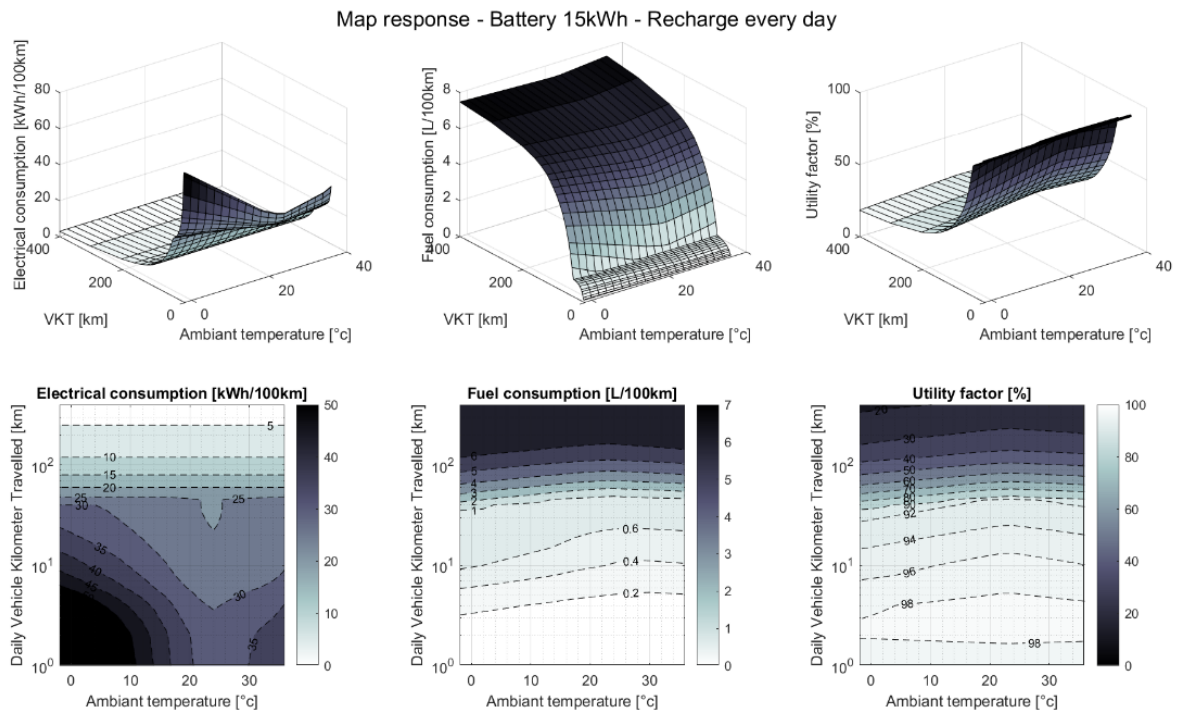


Figure 74 Example of results, for one given battery capacity and recharge frequency (Gasoline PHEV 15 kWh recharged every driving day)

3.3.2. Statistics of use: Representativeness of each use case

The most influential parameter on the behavior of a PHEV for a given charging period is the daily distance travelled. Also, as is the case for highly electrified vehicles in general, the electrical consumption of PHEVs is particularly sensitive to ambient temperature conditions.

We present in this paragraph the statistical distributions of use observed for these two influencing parameters, taken both from the literature data and from the internal database. These statistical distributions will then be used to weigh the different use cases according to their representativeness.

Ambient temperature

Through the Geco air eco-mobility application, IFPEN has collected daily mobility data from thousands of non-professional drivers. Although the application is available across Europe, most users are located in France. The frequency of temperature recorded during each trip (weighted by distance) is represented in *Figure 75*. The average temperature of 12.8°C is slightly below the average annual temperature in mainland France (around 13.8°C).

This distribution is approximated for a gamma distribution law whose equation and parameters are given below.

$$P(t; k, \theta) = \frac{(t - t_0)^{k-1} e^{-\frac{t-t_0}{\theta}}}{\Gamma(k)\theta^k} \quad (3.3-1)$$

$$k = 15.74; \theta = 2.017; t_0 = -18.99$$

To study the climatic sensitivity, this same distribution is shifted by an offset of +10°C and -10°C to arbitrarily represent warmer and colder climate conditions. For

information, the average temperatures thus reproduced are respectively close to the average Australian (22 °c) and Swedish (2 °c) temperatures.

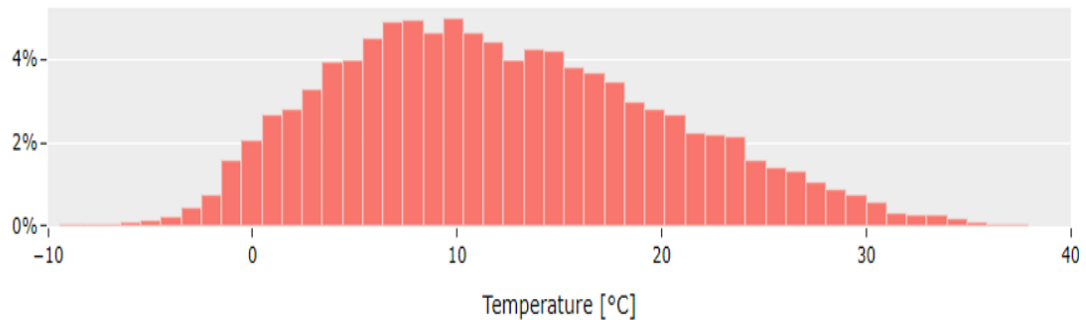


Figure 75 Distribution of the ambient temperature while driving (weighted by travelled distance) - IFPEN data (Geco air)

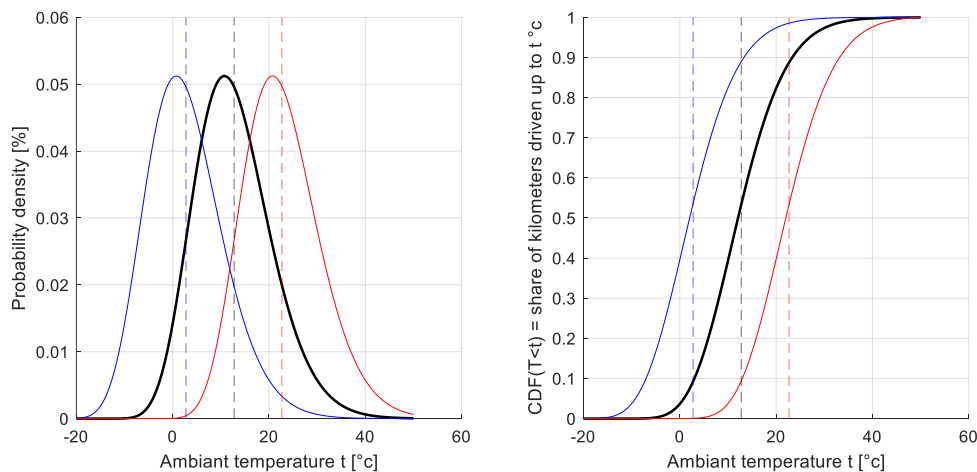


Figure 76 Ambient temperature distributions retained for the current work. Black curves: central case (France); blue curves: colder case; red curves: warmer case.

Daily vehicle mileage travelled

The utility factors defined by the WLTP protocol for the approval of PHEVs come from mobility studies aimed at determining the daily distances operated. Assuming daily charging, they represent the possible electrification percentage of the distance covered by a fleet according to the vehicle's electric range.

Other data are available in the literature, in particular from mobility surveys in Germany²¹ and across Europe²². These data are used for the rest of the study thanks to the availability of the coefficients of the laws which fit the data sets. Data from the JEMA database are approximated by a polynomial distribution in *Paffumi and al.*, while data from the German mobility survey are in *Plotz and al.* approximated by a log-normal law. They are represented in *Figure 77*.

²¹ Plötz, Patrick & Gnann, Till & Wietschel, Martin. (2012). *Total Ownership Cost Projection for the German Electric Vehicle Market with Implications for its Future Power and Electricity Demand*. 7th Conference on Energy Economics and Technology Infrastructure for the Energy Transformation.

²² Elena Paffumi, Michele De Gennaro, Giorgio Martini, *Alternative utility factor versus the SAE J2841 standard method for PHEV and BEV applications*, Transport Policy, Volume 68, 2018, Pages 80-97, ISSN 0967-070X, <https://doi.org/10.1016/j.tranpol.2018.02.014>. (<https://www.sciencedirect.com/science/article/pii/S0967070X17305310>)

Figure 78 represents more specifically the log-normal distribution (3.3-2) from the German mobility survey by Plotz and al for the “medium” vehicle class.

$$Prob(d; \mu, \sigma) = \frac{1}{d\sigma\sqrt{2\pi}} \exp\left(-\frac{\ln(d) - \mu}{2\sigma^2}\right) \quad (3.3-3)$$

$$\sigma = 0.81; \mu = 3.3;$$

It is important to specify that these probabilities are **distance-weighted** and not vehicle-weighted: the cumulative distribution function CDF(X) represents the share of the total distance travelled by the fleet that is operated with vehicles traveling less than X kilometres per day. This is different from the share of vehicles traveling less than X kilometres per day.

Other studies are available^{23,24,25,26} but without access to the raw data or to the coefficient of the distribution laws obtained, which does not make them usable in the context of this study.

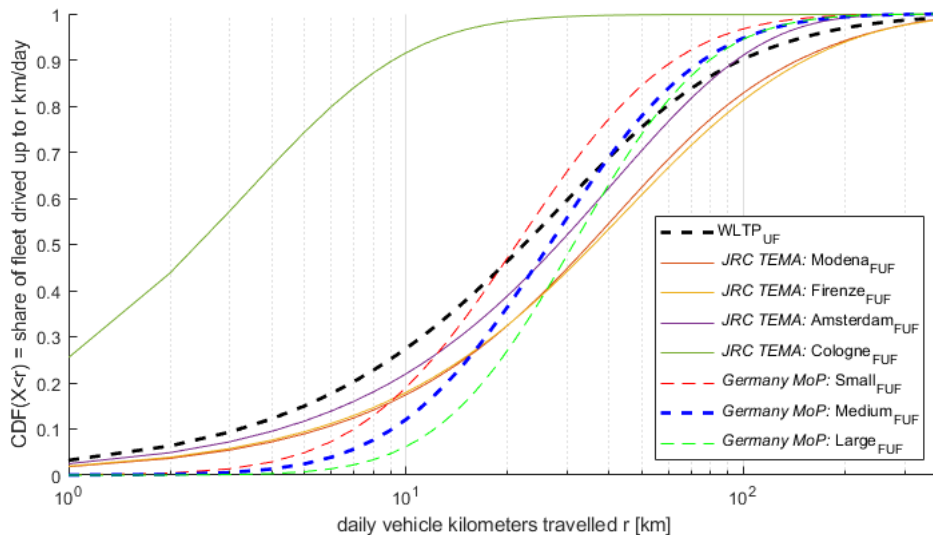


Figure 77 Cumulative frequency distribution of daily vehicle kilometres travelled, issued from literature

²³ Xing, Yan & Jenn, Alan & Wang, Yunshi & Li, Chunyan & Sun, Shengyang & Ding, Xiaohua & Deng, Siwen. (2020). *Optimal range of plug-in electric vehicles in Beijing and Shanghai*. Mitigation and Adaptation Strategies for Global Change. 25. 10.1007/s11027-020-09912-7.

²⁴ Plötz, Patrick & Funke, Simon & Jochem, Patrick & Wietschel, Martin. (2017). CO2 Mitigation Potential of Plug-in Hybrid Electric Vehicles larger than expected. Scientific Reports. 7. 10.1038/s41598-017-16684-9.

²⁵ H. Wang, L. Wu, C. Hou and M. Ouyang, *A GPS-based research on driving range and patterns of private passenger vehicle in Beijing*, 2013 World Electric Vehicle Symposium and Exhibition (EVS27), 2013, pp. 1-7, doi: 10.1109/EVS.2013.6914985.

²⁶ Boston, Daniel & Werthman, Alyssa. (2016). Plug-in Vehicle Behaviors: An analysis of charging and driving behavior of Ford plug-in electric vehicles in the real world. World Electric Vehicle Journal. 8. 916-925. 10.3390/wevj8040926.

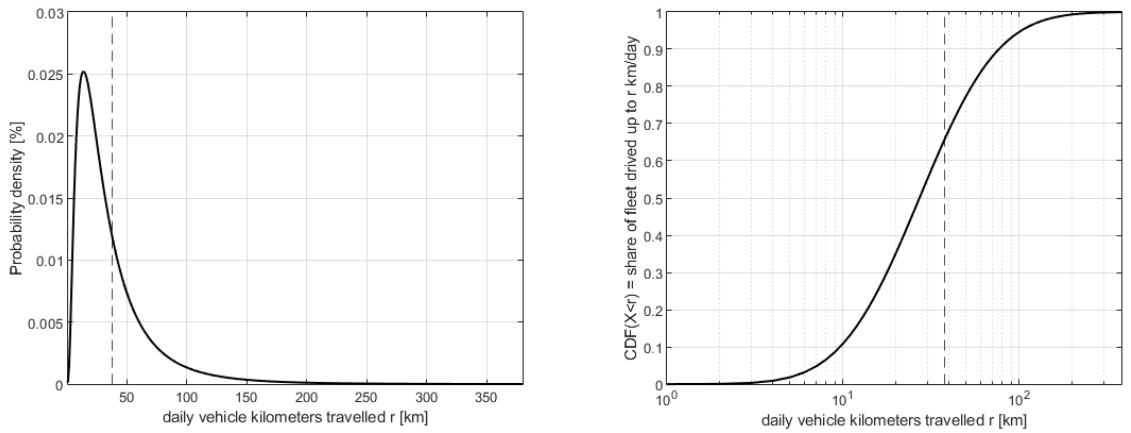


Figure 78 VKT distribution retained for the current work

Driving pattern (function of VKT)

The type of route also has an impact on vehicle consumption levels and electrical thermal distribution. On the IFPEN real driving database, the distribution between the kilometres travelled on roads of the slow urban, urban, rural and motorway type is determined for each VKT considered. The mathematical laws 3.3-4, 3.3-5, 3.3-6 and 3.3-7 are then fitted to this data, as shown in *Figure 79*. For the sake of simplification, the adopted order of the driving order was always from the slowest (slow urban) to the fastest (motorway).

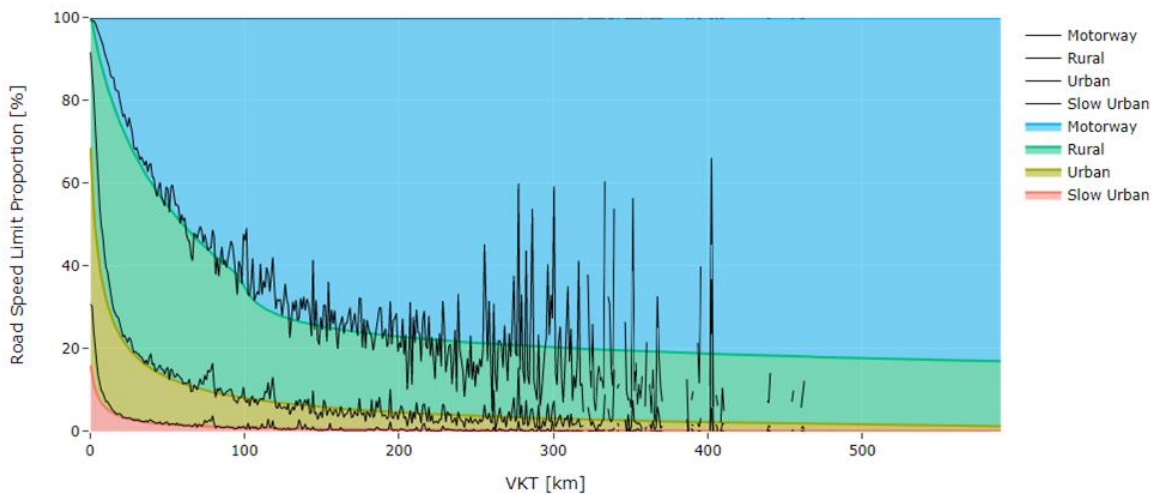


Figure 79 Typology of road function of daily mileage

$$r_{slow}(vkt) = \left(\frac{vkt}{a_{slow}} \right)^{-b_{slow}} + c_{slow} \quad (3.3-4)$$

$$r_{urban}(vkt) = \left(\frac{vkt}{a_{urban}} \right)^{-b_{urban}} + c_{urban} \quad (3.3-5)$$

$$r_{mty}(vkt) = a_{mty} + b_{mty} \log(vkt + c_{mty}) \quad (3.3-6)$$

$$r_{rural}(vkt) = 100 - r_{slow}(vkt) - r_{urban}(vkt) - r_{mty}(vkt) \quad (3.3-7)$$

Table 19 Sets of coefficients of mathematical laws for the repartition by road types as a function of VKT

Road type		a	b	c
Slow		105.3	0.8802	0.04477
Urban		6258	0.5542	2.534
Motorway	d ≤ 100 km	-83.76	31.03	10.03
	d > 100 km	59.23	3.833	-103.6

Resulting probability matrix

Making the hypothesis that these two factors are independant (the distribution of VKT remains the same whatever the ambient temperature), the probability of a couple VKT-ambient temperature is directly obtained by the multiplication of the laws previously established for the VKT and the ambient temperature.

Thereby, considering the driving temperature distribution in France issued from IFPEN database and the daily vehicle mileage issued from literature (Germany mobility survey), a probability matrix is determined and makes it possible to determine the representativeness of each situation with regard to the real use.

The sensitivity of results to these two distributions is presented later in this work.

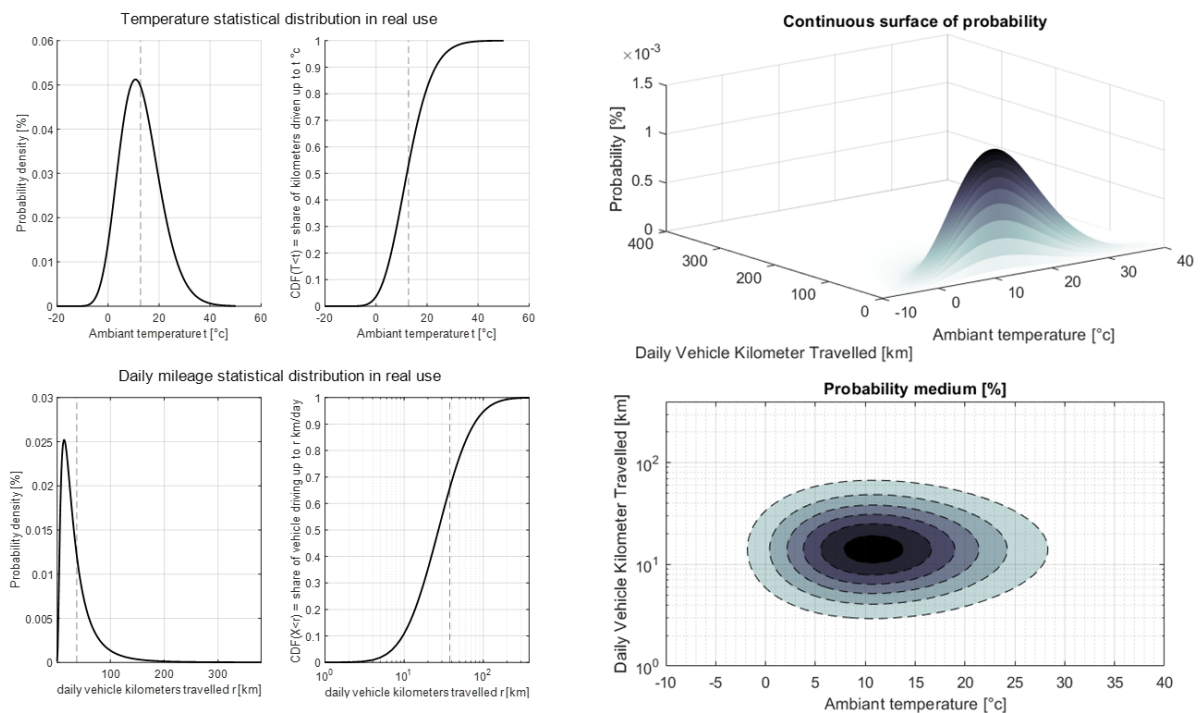


Figure 80 Representativeness of use cases function of ambient temperature and daily mileage

3.3.3. Weighted average outputs

For each couple of battery capacity and recharge frequency, weighted average values are calculated taking into account each individual use case on the whole range of VKT and ambient temperature and its representativity :

$$EC_{r,b} = \sum_v \sum_t probP_{v,t} \times ec_{v,t,r,b} \quad (3.3-8)$$

$$FC_{r,b} = \sum_v \sum_t probP_{v,t} \times fc_{v,t,r,b} \quad (3.3-9)$$

$$UF_{r,b} = \sum_v \sum_t probP_{v,t} \times uf_{v,t,r,b} \quad (3.3-10)$$

Where,

- v : the daily vehicle kilometers travelled (VKT) and associated driving patterns, 24 cases [4:400km];
- t : the ambient temperature, 20 cases [-2:36 °C];
- r : the recharge period, 11 cases [0.5:10days];
- b : the battery capacity, 10 cases [2:35kWh];
- $prob_{v,t}$: the representativity of the use case (v,t);
- $ec_{v,t,r,b}$, $fc_{v,t,r,b}$ and $uf_{v,t,r,b}$ respectively the electrical consumption, the fuel consumption and the utility factor for a given VKT, temperature, recharge frequency and battery capacity;
- $EC_{r,b}$, $FC_{r,b}$ and $UF_{r,b}$ respectively the weighted average electrical consumption, fuel consumption and utility factor for a given recharge frequency and battery capacity.

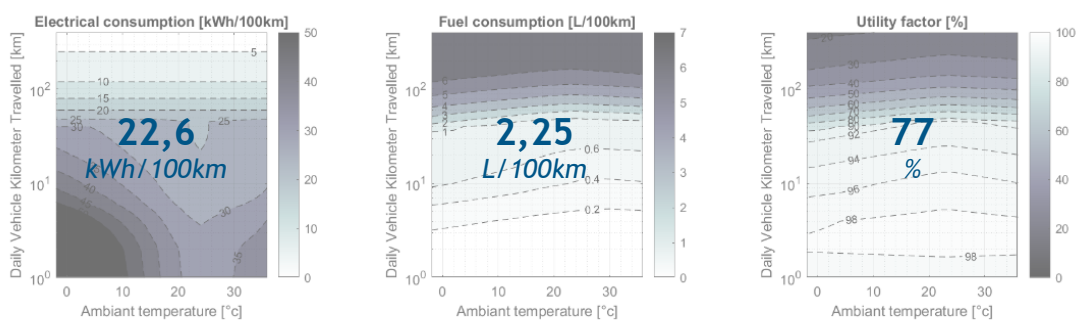


Figure 81 Example of weighted average outputs for one given couple of recharge frequency and battery capacity (Gasoline PHEV 15 kWh recharged every driving day)

We thus obtain, for a given battery capacity and charging frequency couple, mean scores representative of the actual use, resulting from the weighting of the scores in each use-case weighted by its representativeness.

This being done for each pair battery-recharge frequency, we obtain the variation in average consumption in real use as a function of these key parameters. The *Figure 82* represents the visualization of the weighted average outputs on the full range of variation for recharge frequency and battery capacity. This figure is key to represent the sensitivity of real-life average consumptions of PHEVs to both the technological sizing and the final user behaviour.

The next paragraph studies the sensitivity of these average consumptions to the assumptions made regarding the statistical distributions of use. These results are then further discussed in the paragraph 3.3.5.

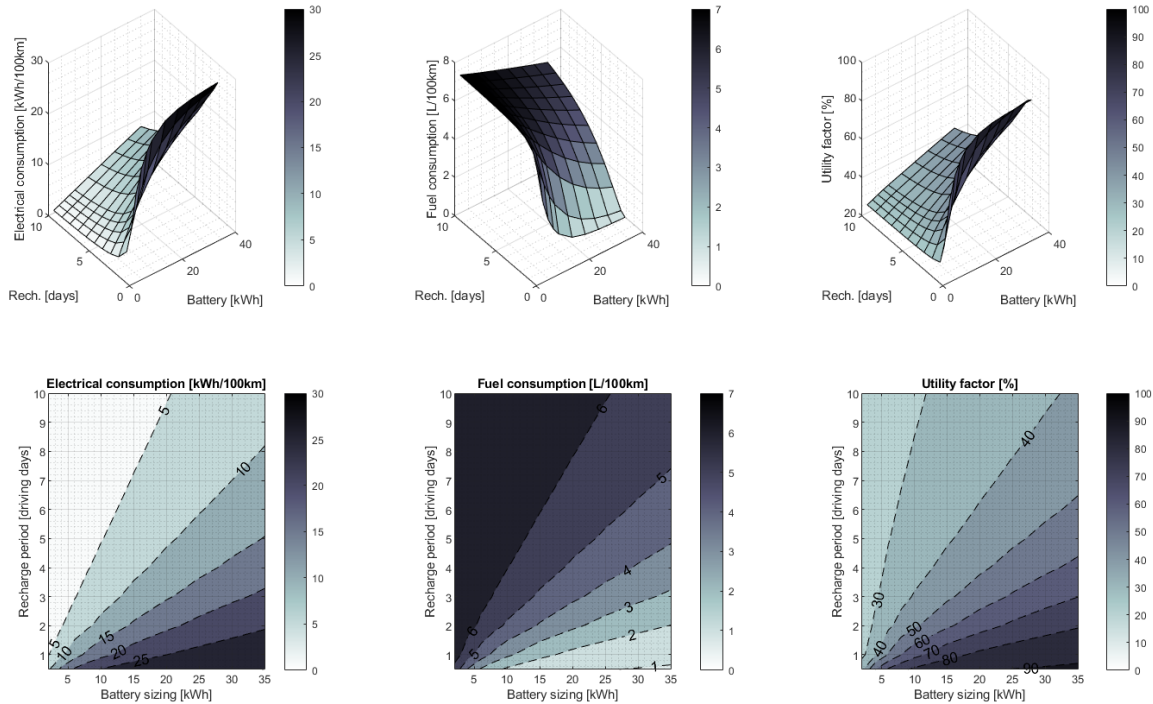


Figure 82 Weighted average outputs on the full range of variation for recharge frequency and battery capacity

3.3.4. Sensitivity to ambient temperature and daily mileage distributions

The results presented above are based on the statistical distributions of ambient temperature and VKT presented in paragraph 3.3.3. We propose here to establish the sensitivity to these input data.

Figure 83 represents a comparison between the weighted average results obtained for a gasoline PHEV of 15 kWh recharged every two driving days with different usage distributions:

- three ambient temperature distributions, called “temperate”, “hot” and “cold” which correspond respectively to the distribution extracted from the IFPEN database in France, and two theoretical laws shifted by +10°c and -10°c.
- two distributions of daily distance: the first one resulting from the German mobility survey for medium class vehicles, and the second one resulting from the WLTP protocol.

Whatever the VKT distribution law considered, the cold law is the most critical one with increased electrical and thermal consumption compared to the temperate and hot laws.

The hot law is itself less critical than the temperate law, which was perhaps less intuitive. This is explained by the greater overconsumption induced by cold

temperatures than by hot ones (see *Figure 74*). Despite the higher induced air conditioning needs, the hot law is more centred on temperatures close to the living comfort temperature, and above all minimizes the call for the most penalizing heating needs.

This sensitivity is not the same depending on the size of the battery and the frequency of recharging. The details of these effects are provided in *Figure 84*, *Figure 85* and *Figure 86*.

The extreme variations in:

- weighted average fuel consumption are in relative terms from -10 % (hot climate) to +18 % (cold climate), and in absolute terms from -0.2 L/100km to +0.4 L/100km.
- weighted average electrical consumption are in relative terms from -10 % (hot climate) to +14 % (cold climate), and in absolute terms from -2.5 kWh/100km to +3.5 kWh/100km.
- weighted average utility factor are in relative terms +/- 6 % and in absolute terms +/- 3 points.

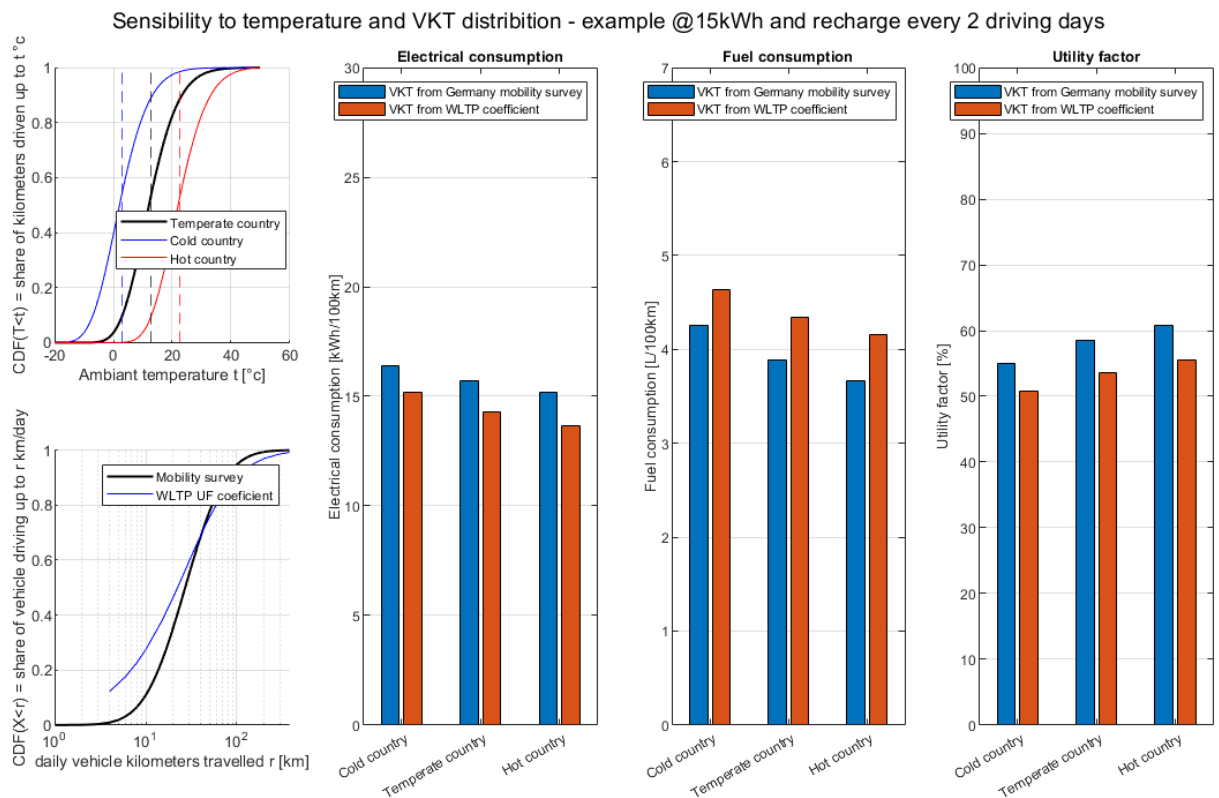


Figure 83 Sensitivity to ambient temperature and daily mileage distributions - example @15kWh battery and recharge frequency every 2 driving days

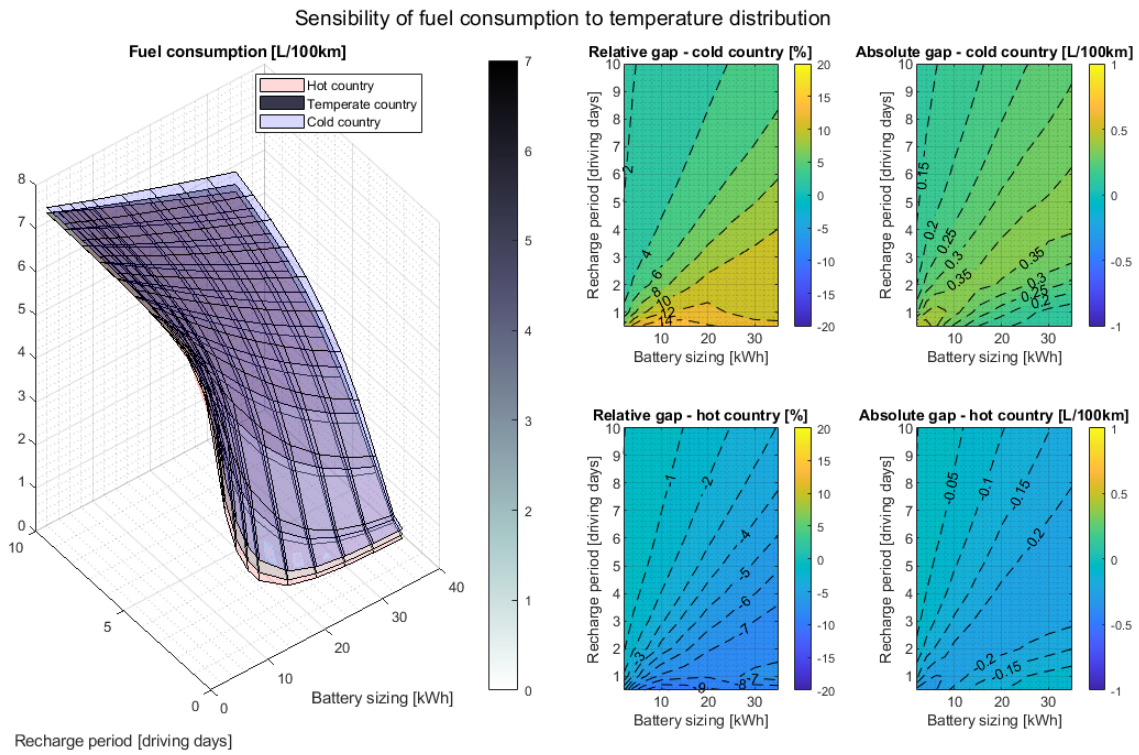


Figure 84 Sensitivity of fuel consumption to the hypothesis of temperature and daily mileage distributions

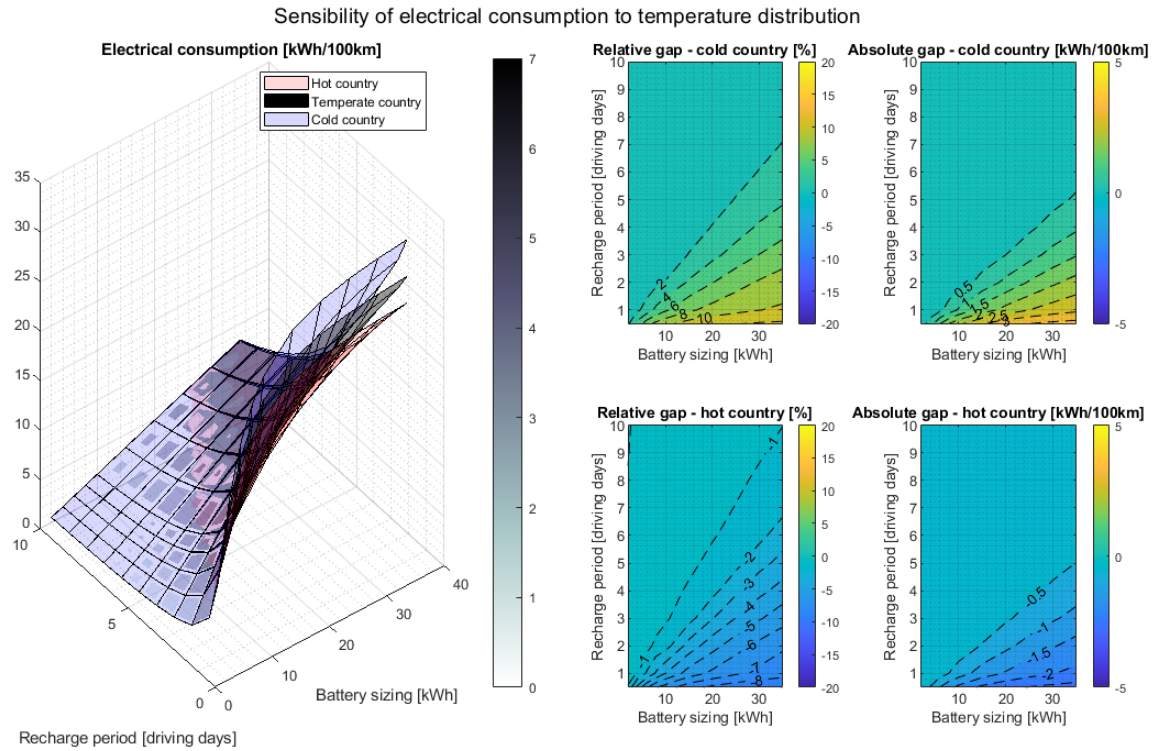


Figure 85 Sensitivity of electrical consumption to the hypothesis of temperature and daily mileage distributions

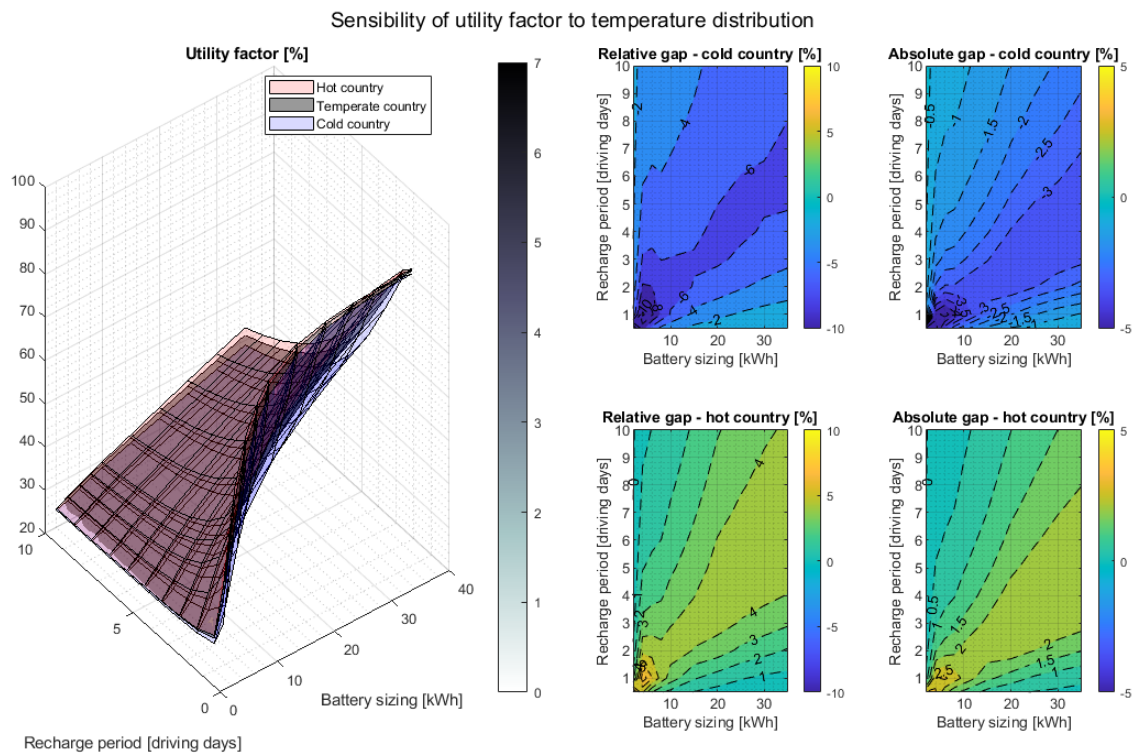


Figure 86 Sensibility of utility factor to the hypothesis of temperature and daily mileage distributions

3.3.5. Discussion of results

Figure 87 represents the same set of results as presented previously in Figure 82: the weighted average scores for fuel consumption, electricity consumption and UF for the gasoline PHEV. This visualization makes it possible to emphasize the influence of the dimensioning of the battery according to the frequency of recharging.

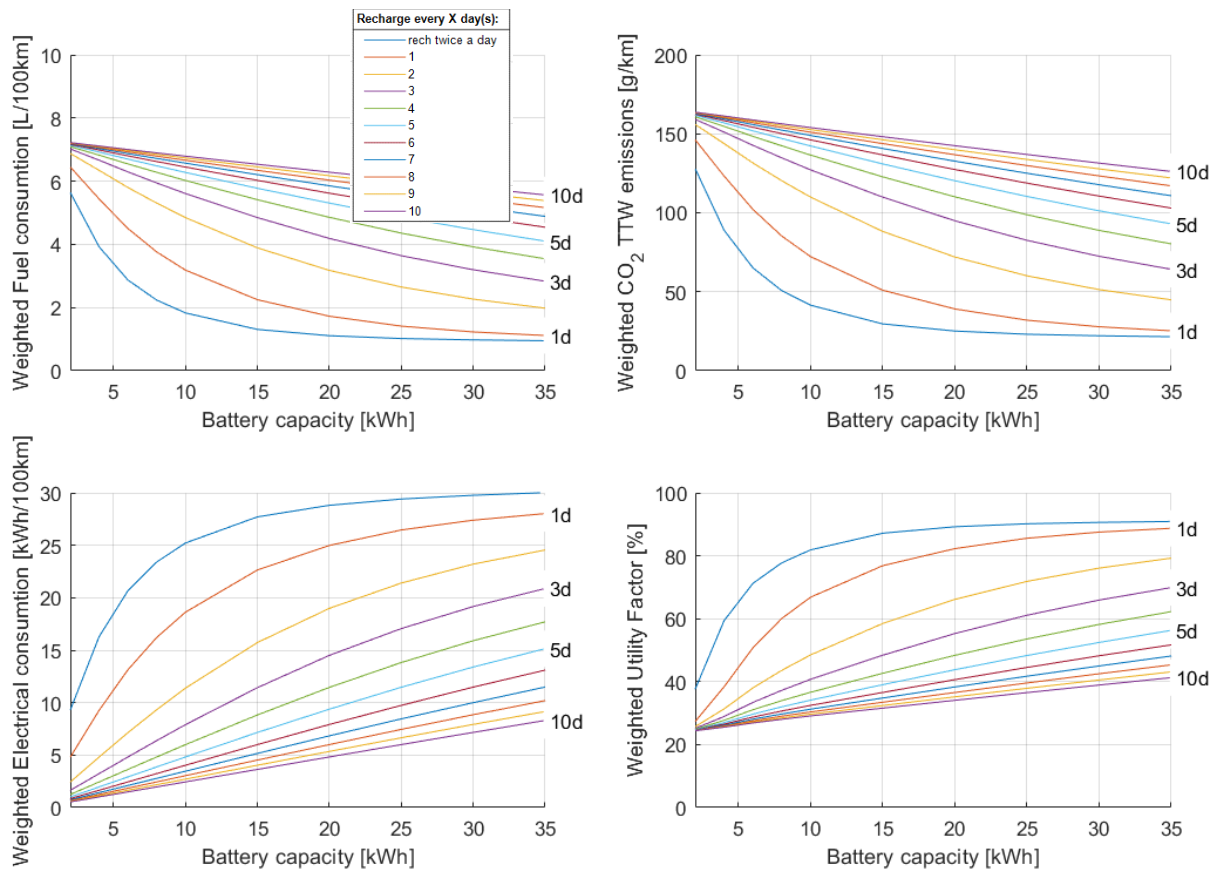


Figure 87 Sensitivity of weighted average fuel consumption, CO₂ emissions, electrical consumption, and utility factor to the battery sizing (from 2 kWh to 35 kWh) and recharge frequency (from twice a day to every 10 days) - gasoline PHEV

Considering the **technology sensitivity to real use conditions** (caught on experimental campaign, and reproduced in simplified model), considering the **statistical conditions of use around Europe** (temperature and daily mileage), this approach allows to quantify the weighted average scores of PHEV depending on battery sizing and recharge frequency:

- Quite intuitively, **frequent recharging of PHEVs is a necessary condition for a high electrification rate**: recharging everyday allows to reach an average weighted fuel consumption of 2.25 L/100km and utility factor around 77 % with a 15 kWh gasoline PHEV. Recharging every 3 days instead induces a fuel consumption of 4.85 L/100km (+116 %) and a UF around 48 % (-29 points).
- A weighted average utility factor of 50% is reached at around 6 kWh of battery, and 80 % is reached at around 18 kWh of battery for an every-driving-day recharge.
- **The first few kWh of battery are the most effective in reducing the weighted average fuel consumption**: considering 1 recharge/day, the gain in increasing the battery above 20 kWh is low. For instance, adding another 15 kWh of battery to the vehicle, leading to a 30 kWh PHEV, would increase by only 10 points the utility factor, from 77 % to 87 %, if recharged every day; instead, the same 15 kWh battery could electrify 77% of the mileage

of another PHEV, which is more efficient if the total amount of available batteries is constrained²⁷.

As shown in *Figure 88*, the same trends are observed for the Diesel PHEV results. A daily charge achieves a weighted average consumption of 1.94 L/100km and a utility factor of around 77% with a 15 kWh Diesel PHEV. A charge every 3 days, on the contrary, induces a consumption of 4.10 L/100km (+111%) and a UF around 48% (-29 points). A weighted average utility factor of 50% is reached at about 6 kWh of battery, and 80% is reached at about 18 kWh of battery for a recharge every driving day. Finally, increasing the battery capacity of a Diesel PHEV recharged every day from 15 to 30 kWh increases the UF from 77 to 87%.

Regarding the difference between the two types of fuel, it depends on the size of the battery and the recharging frequency. The larger the battery or the higher the recharging frequency, the more the gap between the performance of petrol and Diesel engines tends to narrow (*Figure 89*). Indeed, this tends to use more and more vehicles in electric traction, and therefore to minimize the impacts of the performances of the internal combustion engines.

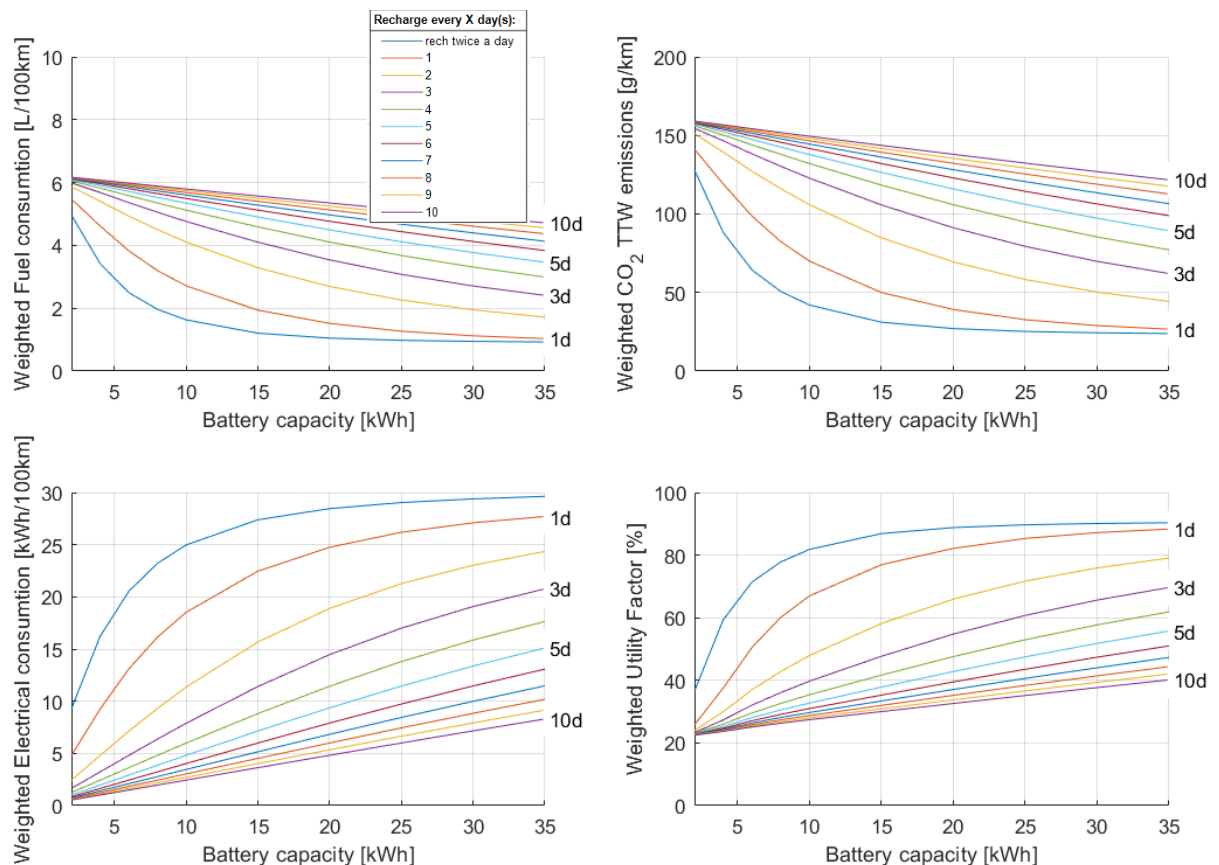


Figure 88 Sensitivity of weighted average fuel consumption, CO₂ emissions, electrical consumption, and utility factor to the battery sizing and recharge period - Diesel vehicle

²⁷ Ehsan Shafiei, Roland Dauphin, Marta Yugo, Optimal electrification level of passenger cars in Europe in a battery-constrained future, *Transportation Research Part D: Transport and Environment*, Volume 102, 2022, 103132, ISSN 1361-9209, <https://doi.org/10.1016/j.trd.2021.103132>

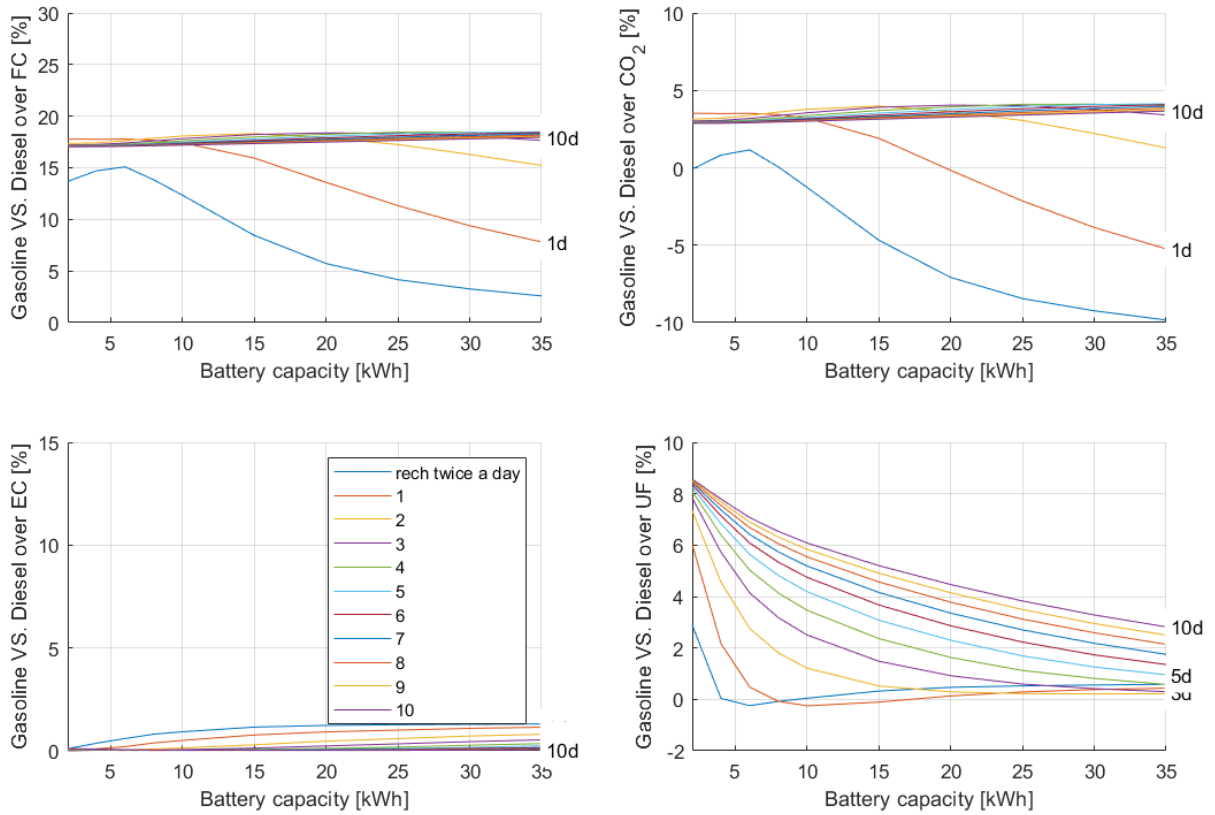


Figure 89 Comparison between gasoline and Diesel PHEV as a function of battery sizing and recharge period

4. CONCLUSION AND OUTLOOK

Two Euro 6d PHEVs were selected to allow a relevant comparison between gasoline and Diesel internal combustion engines. These vehicles were tested on a chassis dynamometer and on-road, both with standard and renewable fuels, in charge depleting and charge sustaining mode.

Concerning pollutants, the two PHEVs show low regulated (well below Euro 6d limits) and non-regulated (in the range of Euro 7 proposals) pollutant emissions. The Diesel PHEV allows, compared to the gasoline one, a reduction of TtW CO₂ emissions of up to 22.3% (and a reduction of 20.5% of TtW GHG emissions) in charge sustaining mode, and a reduction of pollutant emissions except for NH₃ and N₂O. The distance where the vehicle switched to CS mode on the RDE driven (i.e. the all-electric range) was around 54 km, close to the 57 km homologated on WLTP. Regarding the gasoline PHEV, switching from a standard E10 fuel to a 100% renewable E20 fuel does not have a significant impact on the pollutant tailpipe emissions under the tested conditions, neither on TtW CO₂ emissions. However, it implies a higher volumetric fuel consumption (+4.5% on CS). With the Diesel PHEV, switching from a standard B7 fuel to a 100% renewable HVO fuel does not have any significant effect on the pollutant tailpipe emissions under the tested conditions. It decreases by 2.0% the TtW CO₂ emissions and increases the volumetric fuel consumption by 8.4% on CS.

Two simulators for the gasoline and diesel PHEV were configured and validated. A Design of Experiments (DoE) was performed under various conditions (temperature, cycles, battery capacity) to extend the energy performance findings of these two vehicles. Finally, a simplified mathematical model was established and validated. It allows to estimate these same energy performances quickly for all combinations of uses. This work established that the behavior of PHEVs is extremely variable depending on the conditions of use (temperature, daily distance, recharging frequency, and battery sizing): the rate of use of each of the two energy sources available on board is extremely variable. A weighting methodology based on available real use statistics was implemented on the parameters of ambient temperatures and daily distance. Furthermore, the recharging frequency and battery capacity factors, which depend on end-users and manufacturers respectively, were also varied (but not weighted as too few statistics are available), so as to provide insights via a sensitivity analysis. It shows that frequent recharging of PHEVs is a necessary condition for a high electric drive rate: **recharging every day a gasoline PHEV having a battery of 15 kWh leads to an average fuel consumption of 2.25 L/100km and a share of electric drive (utility factor, UF) of 77%, whilst recharging it every 3 days leads to a fuel consumption of 4.85 L/100km (+116 %) and a UF of 48 % (-29 points).** By comparison, the non-rechargeable gasoline HEV with a 2kWh battery evaluated under the same conditions shows an average fuel consumption of 7.3 L/100km and a UF of 24%. **Compared to this reference HEV, the gasoline 15kWh PHEV vehicle allows a consumption reduction of 69% if it is recharged every day and a reduction of 34% if it is recharged every three days.** Furthermore, it is observed that **the first kilowatt-hours of battery capacity are the most effective in electrifying the PHEVs:** for instance, adding another 15 kWh of battery capacity to the vehicle, leading to a 30 kWh PHEV, would increase by only 10 points the utility factor, from 77 % to 87 %, if recharged every day; instead, the same 15 kWh battery capacity could have electrified 77% of the mileage of another PHEV, which is more efficient if the total amount of available batteries is constrained.

Due to the nature of PHEVs, the quantities of interest to be evaluated are multiple: fuel and electricity consumption. It is therefore necessary to establish a single

reference system to judge the best compromise for technology sizing. Given the very different issues at stake in the various energy sectors, this reference system cannot be limited to the analysis of consumption and emissions at the vehicle level during its use: it must consider the entire life cycle of the vehicle. The total equivalent CO₂ emissions related to the analysis of the vehicle's life cycle must be determined by taking into account the TtW consumption of the vehicle during its use, but also the WtT emissions related to the energy sources and finally to the production and end of life of the vehicle itself, including the battery. This calculation is also based on many parameters: the CO₂ intensity of the electricity production, the CO₂ WtT emissions according to the different types of fuels considered and their potential advantages in terms of renewability (energy sector), the CO₂ emissions related to the production of the vehicles, in particular of the battery (industrial sector), the lifetime of the vehicles, etc. These LCA and WtT aspects are outside the scope of this study, but will be the subject of future work. Also, given the high number of assumptions and their variability, it is planned to develop a dynamic LCA GHG footprint assessment tool. It will be configured by default on the assumptions relevant to the available data, but can also be configured on any possible combinations of them. The evaluation of PHEV behavior in real use presented in this study will feed the TtW component of this tool under development. To this end, the approach will also be generalized to other levels of electrification: HEV and BEV.

5. GLOSSARY

AER:	All Electrical Range
AFTS:	After Treatment System
B7:	Diesel fuel with up to 7% by volume of EMAG biodiesel
BEVs:	Battery Electric Vehicles
CD:	Charge Depleting
CDF:	Cumulative Distribution Function
CH ₄ :	Methane
CI:	Compression Ignition
CO:	Carbon Oxide
CO ₂ :	Carbon Dioxide
CR:	Compression Ratio
CS:	Charge Sustaining
CVS:	Constant Volume Sampling
DC:	Direct Current
DOC:	Diesel Oxidation Catalyst
DoE:	Design of Experiments
DPF:	Diesel Particulate Filter
E10:	Petrol fuel with up to 10% by volume of ethanol
E20:	Petrol fuel with up to 20% by volume of ethanol
ECMS:	Equivalent Consumption Minimization Strategy
EFM:	Exhaust Flow Meter
FC:	Fuel Consumption
GB:	Gearbox
GHG:	Green House Gases
GPF:	Gasoline Particulate Filter
GPS:	Global Positioning System
GWP:	Global Warming Potential
HEVs:	non-plug-in Hybrid Electric Vehicles
HV:	High-Voltage
HVAC:	Heating, Ventilation and Air Conditioning
HVO:	Hydrotreated vegetable oil
ICE:	Internal Combustion Engine
LCA:	Life Cycle Analysis
LHV:	Low Heating Value
LV:	Low-Voltage
N ₂ O:	Nitrous Oxide
NH ₃ :	Ammonia
NMC:	Nickel, Manganese and Cobalt
NOVC HEVs:	Not Off-Vehicle Charging Hybrid Electric Vehicles, simply called HEVs
NOx:	Nitrogen Oxide
OBD:	On-Board Diagnostic
OEMs:	Original Equipment Manufacturer
OVC HEVs:	Off-Vehicle Charging Hybrid Electric Vehicles, simply called PHEVs
P2:	Hybrid configuration where the electric machine is integrated between the internal combustion engine and the transmission.
PEMS:	Portable Emissions Measurement System
PHEVs:	Plug-in Hybrid Vehicles
PID:	Proportional-Integral-Derivative (controller)
PM:	Particulate Matter
PN:	Particulate Number
PN10:	Particulate Number with a diameter greater than 10 nm
PN23:	Particulate Number with a diameter greater than 23 nm
RDE:	Real Driving Emissions
RPA:	Relative Positive Acceleration

SCR:	Selective Catalytic Reduction
SCRf:	Selective Catalytic Reduction with a soot Filter
SI:	Spark Ignition
SoC:	State of Charge
THC:	Total Hydrocarbon
TtW:	Tank-To-Wheels
TWC:	Three Way Catalyst
UF:	Utility Factor
$v \cdot a_{pos}$:	Driving dynamic parameter, velocity x positive acceleration
VKT:	Vehicle Kilometres Travelled
WLTP:	Worldwide Harmonized Light Vehicles Test Procedure
WtT:	Well-To-Tank
WtW:	Well-To-Wheels

6. APPENDIX - DETAILED FUEL PROPERTIES

6.1. B7



9850

d_v = 833,1



TOTAL ADDITIFS ET CARBURANTS SPECIAUX
Place du Bassin - 69700 Givors - France
Tél +33 4 72 49 84 10 - Fax +33 4 72 49 84 20

CERTIFICAT D'ANALYSE

PRODUIT: DIESEL B7 EURO6 CERT

LOT: B61819061

ANALYSES	RÉSULTATS	MÉTHODES
Teneur en EMAG	6.2 % (w/v)	NF EN 14078
Indice de cétane calculé	51.3 Index	NF EN ISO 4264
HFRR	174 µm	NF EN ISO 12156-1
Indice d'acide	0.06 mg KOH/g	ASTM D 974
Point de trouble	-11 °C	NF EN 23015 / ISO 3015
Stabilité à l'oxydation- Rancimat	>40.0 heures	NF EN 15751
Teneur en Cuivre	<0,1 mg/kg	ASTM D 5185
Teneur en Zinc	<0,1 mg/kg	
Couleur ASTM	0.8	ASTM D 1500
Corrosion cuivre 3h, 50°C	1b	NF EN ISO 2160
Masse volumique à 15°C	834.3 kg/m³	NF EN ISO 12185
Viscosité à 40°C	2.412 mm²/s	NF EN ISO 3104
PI	161.2 °C	NF EN ISO 3405
5 % Vol	188.2 °C	
10 % Vol	197.8 °C	
20 % Vol	214.6 °C	
30 % Vol	233.1 °C	
40 % Vol	250.7 °C	
50 % Vol	264.9 °C	
60 % Vol	278.1 °C	
70 % Vol	294.0 °C	
80 % Vol	312.9 °C	
90 % Vol	333.4 °C	
95 % Vol	347.7 °C	
PF	354.1 °C	
E 250 °C	39.6 % (w/v)	
E 350 °C	95.8 % (w/v)	
E 370 °C	>97.0 % (w/v)	
Teneur en eau	60 mg/kg	NF EN ISO 12937
Température limite de filtrabilité	-29 °C	NF EN 116
Teneur en soufre	4.1 mg/kg	NF EN ISO 20846
Point éclair	63 °C	NF EN ISO 2719
Teneur en Aromatiques totaux	22.2 % (m/m)	NF EN 12916
Teneur en poly-aromatiques	2.5 % (m/m)	
Indice de cétane mesuré	52.5 Index	NF EN ISO 5165
Pouvoir Calorifique Inférieur Mesuré	42.13 MJ/kg	ASTM D 240

Document Confidentiel. L'interprétation des résultats répond à la norme NF EN ISO 4259 ;
TOTAL Additifs et Carburants Spéciaux est certifié ISO 9001 et ISO 14001.

1/2



TOTAL ADDITIFS ET CARBURANTS SPECIAUX
 Place du Bassin - 69700 Givors - France
 Tél +33 4 72 49 84 10 - Fax +33 4 72 49 84 20

PRODUIT: DIESEL B7 EURO6 CERT
 LOT: B61819061

ANALYSES	RÉSULTATS	MÉTHODES
Teneur en carbone	85.8 % (m/m)	ASTM D 5291
Teneur en hydrogène	13.6 % (m/m)	
Teneur en oxygène total	0.7 % (m/m)	MO238LA2008
Teneur en Cendres	0.001 % (m/m)	NF EN ISO 6245
Résidu Carbone (10%)	<0.1 % (m/m)	NF EN ISO 10370
Teneur en sédiments	<12.0 mg/kg	NF EN 12662

: hors spécifications; (...): en cours d'analyse; en italique : analyse sous-traitée

OBSERVATIONS:

DATE
 Givors, le 24/06/2019

Technicien méthode
 Tommy VERNAY
 J0384373

SIGNATURE



6.2. E10



TOTAL ADDITIFS ET CARBURANTS SPECIAUX
 Place du Bassin - 69700 Givors - France
 Tél +33 4 72 49 84 10 - Fax +33 4 72 49 84 20

CERTIFICAT D'ANALYSE

PRODUIT: ULG E10 EURO6 CERT
LOT: PCV100242

ANALYSES	RÉSULTATS	MÉTHODES
Corrosion cuivre 3h, 50°C	1b	NF EN ISO 2160
Teneur en C	83.1 % (m/m)	GC-Calculated
Teneur en H	13.4 % (m/m)	
Teneur en O	3.5 % (m/m)	
Rapport C/H	6.210	
Rapport H/C	0.161	
Rapport C/O	23.984	
Pouvoir Calorifique Inférieur Mesuré	41.40 MJ/kg	ASTM D 240
Teneur en Silicium	<0.1 mg/kg	ASTM D 5185
Teneur en Manganèse	<2.0 mg/L	ASTM D 3631
Teneur en gommes actuelles lavées	<1 mg/100mL	NF EN ISO 6246
Teneur en gommes actuelles non-lavées	<1 mg/100mL	
Teneur en Phosphore	<0.2 mg/L	ASTM D 3231
Période d'Induction	>480 minutes	NF EN ISO 7536
Driveability Index	509 Index	ASTM D 4814
Masse volumique à 15°C	748.0 kg/m³	NF EN ISO 12185
Pression de vapeur PVSE	58.3 kPa	NF EN 13016-1
PI	38.4 °C	NF EN ISO 3405
5 % Vol	51.4 °C	
10 % Vol	55.1 °C	
20 % Vol	58.7 °C	
30 % Vol	64.2 °C	
40 % Vol	69.2 °C	
50 % Vol	81.8 °C	
60 % Vol	101.7 °C	
70 % Vol	108.6 °C	
80 % Vol	113.1 °C	
90 % Vol	132.9 °C	
95 % Vol	165.0 °C	
PF	180.2 °C	
Résidu	0.5 % (w/v)	
Pertes	0.3 % (w/v)	
E 70 °C	41.4 % (w/v)	
E 100 °C	57.6 % (w/v)	
E 150 °C	82.9 % (w/v)	
E 180 °C	98.7 % (w/v)	
RON	97.0 Index	NF EN ISO 5164
MON	85.9 Index	NF EN ISO 5163

Document Confidentiel. L'interprétation des résultats répond à la norme NF EN ISO 4259 ;
 TOTAL Additifs et Carburants Spéciaux est certifié ISO 9001 et ISO 14001.



TOTAL ADDITIFS ET CARBURANTS SPECIAUX
 Place du Bassin - 69700 Givors - France
 Tél +33 4 72 49 84 10 - Fax +33 4 72 49 84 20

PRODUIT: ULG E10 EURO6 CERT

LOT: PCV100242

ANALYSES	RÉSULTATS	MÉTHODES
Anti Knock Index	91.5	CALCUL
Sensibilité	11.1	CALCUL
Teneur en soufre	<3.0 mg/kg	NF EN ISO 20846
Aspect visuel	Clair et limpide	VISUELLE
Aspect visuel -7°C	Clair et limpide	
Pression de vapeur absolue à 100°C	388.8 kPa	EN 13016-2
Teneur en Aromatiques	26.7 % (v/v)	NF EN ISO 22854
Teneur en Saturés	57.0 % (v/v)	
Teneur en Oléfines	6.9 % (v/v)	
Teneur en Benzène	0.2 % (v/v)	
Teneur en Ethanol	9.4 % (v/v)	
Teneur en autres composés oxygénés	<0.2 % (v/v)	
Teneur en Oxygène total	3.47 % (m/m)	
Teneur en eau	0.016 % (v/v)	NF EN ISO 12937
Teneur en Plomb	<5.0 mg/L	NF EN 237

: hors spécifications; (...): en cours d'analyse; en italique : analyse sous-traitée

OBSERVATIONS:

The ethanol has to respect the EN15376. No performance additive allowed. The fuel may contain oxidation inhibitors and metal deactivators normally used to stabilize refinery gas streams, but detergent/dispersant additives and solvents oils forbidden.

DATE

Givors, le 21/10/2020

Technicien méthode

Tommy VERNAY
 J0384373

SIGNATURE



6.3. 100% RENEWABLE PARAFFINIC DIESEL

Certificate of Analysis

Fuel Batch No:	CAF-G19/1919	Contact:	Hannu Kuutti
Fuel Description:	Concawe HH0319 Fuel 3 EN15940	Order No:	#28201900125
Part No:	10001275	Customer:	Concawe
		Date:	16/01/2020

Test	Method	Unit	Limit		Result
			Min	Max	
Appearance	Visual		Report		C&B
Derived Cetane Number *	ASTM D6890		70.0	-	78.2
Cetane Index	ASTM D4737		Report		81.5
Density @ 15°C *	EN ISO 12185	kg/L	0.7640	0.7660	0.7643
Cloud Point *	EN ISO 23015	°C	Report		-31
CFPP	EN 116	°C	Report		-34
Carbon Residue (10% Dis. Res)	EN ISO 10370	% m/m	-	0.30	<0.01
Flash Point (Procedure A) *	ASTM D93	°C	55.0	-	67.0
Lubricity, wear scar diameter @ 60°C *	EN ISO 12156-1	µm	-	460	413
Sulfur *	EN ISO 20846	mg/kg	-	5.0	2.3
Total Acid Number	ISO 6618	mgKOH/g	Report		0.03
Viscosity at 40°C *	EN ISO 3104	mm²/s	Report		1.909
Water Content	EN ISO 12937	mg/kg	-	200	60
FAME Content	EN 14078	% v/v	-	7.0	<0.1
Mono Aromatics Content	IP 391 mod	% m/m	Report		0.1
Di Aromatics Content	IP 391 mod	% m/m	Report		<0.1
Tri+ Aromatics Content	IP 391 mod	% m/m	Report		<0.1
Polycyclic Aromatics Content	IP 391 mod	% m/m	Report		<0.1
Total Aromatics	IP 391 mod	% m/m	-	1.0	0.1
Oxidation Stability	EN 15751	h	20.0	-	>20.0
Oxidation Stability (16h)	EN ISO 12205	g/m³	-	25	<1
Ash Content	EN ISO 6245	% m/m	-	0.010	<0.001
Copper Corrosion (3h at 50°C)	EN ISO 2160	Rating	Class 1	-	1A
Total Contamination	EN 12662	mg/kg	-	25	<6
Carbon	ASTM D3343 mod	% m/m	Report		84.62
Hydrogen	ASTM D3343	% m/m	Report		15.38
Oxygen	EN 14078	% m/m	Report		0.00
H/C Mole Ratio	Calculation		Report		2.17
Gross Calorific Value	ASTM D3338 mod	MJ/kg	Report		47.43
Net Calorific Value	ASTM D3338 mod	MJ/kg	Report		44.16

Certificate of Analysis

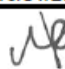
Fuel Batch No:	CAF-G19/1919	Contact:	Hannu Kuutti
Fuel Description:	Concawe HH0319	Order No:	#28201900125
Part No:	Fuel 3 EN15940	Customer:	Concawe
	10001275	Date:	16/01/2020

Test	Method	Unit	Limit		Result
			Min	Max	
Distillation (Evaporated) *					
E250	ASTM D86	% v/v	-	65.0	60.2
E350	ASTM D86	% v/v	85.0	-	98.6
IBP	ASTM D86	°C	Report		189.9
10% Volume Evaporated	ASTM D86	°C	Report		208.0
20% Volume Evaporated	ASTM D86	°C	Report		214.1
30% Volume Evaporated	ASTM D86	°C	Report		220.4
40% Volume Evaporated	ASTM D86	°C	Report		228.6
50% Volume Evaporated	ASTM D86	°C	Report		237.9
60% Volume Evaporated	ASTM D86	°C	Report		249.7
70% Volume Evaporated	ASTM D86	°C	Report		263.4
80% Volume Evaporated	ASTM D86	°C	Report		276.2
90% Volume Evaporated	ASTM D86	°C	Report		285.8
95% Volume Evaporated	ASTM D86	°C	-	360.0	290.8
FBP	ASTM D86	°C	Report		302.5
Residue	ASTM D86	% v/v	Report		1.4

* Test UKAS accredited * Test performed by sub-contracted laboratory

Sample Received Condition: Good (No Seal)
Date Sample Received: 24/12/2019

Notes:

Date:	16/01/2020
Authorised by: M Babiarz Fuels Formulation Scientist	

Coryton Advanced Fuels Ltd
 The Manorway
 Stanford-le-Hope
 Essex SS17 9LN, UK

Tel: +44 (0)1375 665930
 Email: lab@corytonfuels.co.uk
 Website: www.corytonfuels.co.uk



6.4. 100% RENEWABLE E20



TOTAL ADDITIFS ET CARBURANTS SPECIAUX
 Place du Bassin - 69700 Givors - France
 Tel +33 4 72 49 84 10 - Fax +33 4 72 49 84 20

CERTIFICATE OF ANALYSIS

PRODUCT: E20 RENEWABLE GASOLINE

BATCH: PCV120416P

ANALYSES	SPECIFICATIONS	RESULTS	METHODS
Induction period	≥360	>360 minutes	NF EN ISO 7536
Washed existent gums content	≤5	<1 mg/100mL	NF EN ISO 6246
Unwashed existent gums content	-	1 mg/100mL	
Water content	-	330.000 mg/kg	NF EN ISO 12937
Lead content	≤5.0	<5.0 mg/L	ASTM D 5059
Manganese content	-	<2.00 mg/kg	NF T 60-106
Copper corrosion 3h, 50°C	1a - 1b	1b	NF EN ISO 2160
Visual aspect	Clear and bright	Clear and bright	Visual method
Density at 15°C	720.0 - 775.0	761.8 kg/m³	NF EN ISO 12185
Vapour pressure	45.0 - 60.0	60.0 kPa	NF EN 13016-1
IP	-	37.0 °C	NF EN ISO 3405
5 % Vol	-	52.8 °C	
10 % Vol	-	57.3 °C	
20 % Vol	-	63.9 °C	
30 % Vol	-	68.8 °C	
40 % Vol	-	71.9 °C	
50 % Vol	-	74.2 °C	
60 % Vol	-	113.4 °C	
70 % Vol	-	136.3 °C	
80 % Vol	-	155.2 °C	
90 % Vol	-	170.7 °C	
95 % Vol	-	185.8 °C	
FP	≤210.0	201.7 °C	
Residue	≤2.0	0.8 % (wv)	
Losses	-	1.5 % (wv)	
E 70 °C	22.0 - 48.0	34.9 % (wv)	
E 100 °C	45.0 - 71.0	59.3 % (wv)	
E 150 °C	-	78.7 % (wv)	
E 180 °C	-	94.9 % (wv)	

*Confidential document. The interpretation of the result answers the NF standard IN ISO 4259;
 TOTAL Additives and Special Fuels is ISO-certified 9001 and ISO 14001.*

1/2



TOTAL ADDITIFS ET CARBURANTS SPECIAUX
 Place du Bassin - 69700 Givors - France
 Tel +33 4 72 49 84 10 - Fax +33 4 72 49 84 20

PRODUCT: E20 RENEWABLE GASOLINE
BATCH: PCV120416P

ANALYSES	SPECIFICATIONS	RESULTS	METHODS
Iso-paraffin content	-	35.5 % (v/v)	NF M 07-086
content of N + Isoparaffins	-	43.5 % (v/v)	
naphthene content	-	6.6 % (v/v)	
Olefin content	≤18.0	1.3 % (v/v)	
Aromatics content	≤35.0	28.7 % (v/v)	
Aromatic content C9, C9+	-	19.6 % (v/v)	
Benzene content	≤1.0	0.2 % (v/v)	
Oxygen content	-	7.21 % (m/m)	
Ethanol content	19.0 - 20.0	19.8 % (v/v)	
Methanol content	-	<0.2 % (v/v)	
ETBE content	-	<0.2 % (v/v)	
MTBE content	-	<0.2 % (v/v)	
Other oxygenates content	-	<0.2 % (v/v)	
Aromatic content C9	-	10.3 % (v/v)	
Low calorific value calculated	-	39.78 MJ/kg	GC-Calculated
C content	-	79.4 % (m/m)	
H content	-	13.4 % (m/m)	
O content	-	7.2 % (m/m)	
Research octane number	≥95.0	99.4 Index	NF EN ISO 5164
Motor octane number	≥85.0	88.0 Index	NF EN ISO 5163
Sulfur content	≤10.0	0.6 mg/kg	NF EN ISO 20884

: out of specification; (...): In progress; In Italics : outsourced analysis

OBSERVATIONS:

DATE
 Givors, 04/01/2021

Method Technician
 Tommy VERNAY
 J0384373

SIGNATURE





Centre de
Datation par le
Radiocarbone

<http://carbon14.univ-lyon1.fr>

46 boulevard Niels Bohr
69622 Villeurbanne Cedex

T. 04 72 44 82 57
F. 04 72 43 13 17
UMR 5138

TOTAL Additifs & Carburants Spéciaux
A l'attention de Madame Lisa SERVE
Place du Bassin
69702 Givors Cedex

Villeurbanne, 19th January 2021

RADIOCARBON ANALYSIS
PERFORMED ON A CHEMICAL PRODUCT

Sample : **Nature of the sample: gasoline**
Reference: PCV120416P

Result : Counting number in the CDRC : Ly-18236
Isotopic ratio $^{13}\text{C}/^{12}\text{C}$: - 18.71 ‰ PDB
Radiocarbon activity : **13.64 ± 0.09 dpm/g**
(dpm/g = disintegrations per minute per gram of carbon)
Whether: 227.3 ± 1.5 Bq/kg
(Bq/kg = disintegration per second per kilogram of carbon)

Comments: As a result of the thermonuclear bombs effect in the 1960s, all organic matters of natural origin present a radiocarbon activity around 13.70 ± 0.10 dpm/g (229 Bq/kg) in 2019, in France. Those prepared from petroleum products are radiocarbon free (0 dpm/g). Therefore, products with intermediate radiocarbon activity are obviously a mix of natural and synthetic products.

Conclusion:
The chemical product, here measured, can be regarded as natural considering the statistical margins.

For the Centre de Datation par le
Radiocarbone
Christine Oberlin



Sous la co-tutelle



Lyon 1

7. APPENDIX - RELATIVE GAPS BETWEEN TESTED CONFIGURATIONS

The tables below represent the relative differences between the different configurations tested. The cells are colored when the differences are greater than the sum of the standard deviations. For more readability, the cells in red correspond to a degradation and in green to an improvement.

7.1. CONFIGURATION RELATIVE DIFFERENCES IN % FOR CHARGE DEPLETING MODE ON TOTAL RDE CYCLE

Gaps**				
B7 to HVO (CD mode)	E10 to E20 (CD mode)	E10 to B7 (CD mode)	Lab to road (B7 CD)	Lab to road (E10 CD)
rel [%]	rel [%]	rel [%]	rel [%]	rel [%]

FC		9.87	8.06	-20.09	59.87	37.31
FC _{corr} *		9.87	8.06	-20.09	59.87	37.31
CO ₂	CVS	-0.73	5.29	-7.68	59.75	37.60
CO _{2,corr} *		-0.73	5.29	-7.68	59.75	37.60
GHG		-0.33	5.36	-6.15		
UF	share of distance engine off	-0.08	-1.40	-8.80	-7.27	-5.56
E Wheel net	Vreal	-0.01	-0.06	-0.35	-3.42	-7.79
E Wheel +	Vreal	-0.14	-0.09	1.80	-13.67	-19.11
E Wheel -	Vreal	-0.34	-0.13	5.26	-29.24	-37.26
EC		-3.24	-0.89	-9.37	1.94	4.72
EC+		-1.74	-1.82	-3.00	-5.98	-4.79
EC-		0.85	-3.78	10.46	-19.73	-24.92
NOx EO	raw gases	0.65	5.59	-83.03		
NOx TP	raw gases	0.50	-41.19	-67.52	61.48	-22.07

		Gaps**				
		B7 to HVO (CD mode)	E10 to E20 (CD mode)	E10 to B7 (CD mode)	Lab to road (B7 CD)	Lab to road (E10 CD)
		rel [%]	rel [%]	rel [%]	rel [%]	rel [%]
NOx Eff		-0.01	1.82	-3.77		
NOx TP	CVS	-2.91	-33.49	-72.29		
CO EO	raw gases	-12.90	-3.74	-93.70		
CO TP	raw gases	-36.67	-35.05	-92.50	1003.72	-5.13
CO Eff		1.09	1.11	-0.64		
CO TP	CVS	-33.13	-48.22	-92.89		
HC EO	raw gases	-24.40	40.38	-91.76		
HC TP	raw gases	-28.97	41.13	-92.80		
HC Eff		0.14	0.03	0.55		
HC TP	CVS	-17.95	43.95	-94.69		
SPN23 EO	raw gases	4.81	36.82	2751.99		
SPN23 TP	raw gases	83.30	18.36	-93.69	38.84	313.26
SPN23 Eff		-0.07	14.82	55.88		
SPN23 TP	CVS					
SPN10 EO	raw gases	3.95	187.41	1845.30		
SPN10 TP	raw gases	72.67	13.60	-92.90		
SPN10 Eff		-0.06	26.50	37.34		
SPN10 TP	CVS	71.05	12.78	-93.00		
PM	soot filter weight	94.04	2.42	-59.63		
CH ₄ EO	raw gases	-24.31	34.70	-96.25		
CH ₄ TP	raw gases	-33.44	24.85	-84.45		
CH ₄ Eff		1.33	0.97	-38.16		
CH ₄ TP	CVS	-35.39	26.75	-59.11		

		Gaps**				
		B7 to HVO (CD mode)	E10 to E20 (CD mode)	E10 to B7 (CD mode)	Lab to road (B7 CD)	Lab to road (E10 CD)
		rel [%]	rel [%]	rel [%]	rel [%]	rel [%]
CH ₄ TP (CO ₂ eq)	raw gases	-33.44	24.85	-84.45		
	CVS	-35.39	26.75	-59.11		
NH ₃ EO	raw gases	62.67	-55.54	-80.16		
NH ₃ TP	raw gases	55.26	-67.89	331.14		
NH ₃ Eff						
NH ₃ TP	CVS					
N ₂ O EO	raw gases	-18.12	2.25	-32.59		
N ₂ O TP	raw gases	15.01	11.79	169.41		
N ₂ O Eff						
N ₂ O TP	CVS					
N ₂ O TP (CO ₂ eq)	raw gases	15.01	11.79	169.41		
	CVS					
Urea	calculation for command signal	-2.22				

7.2. CONFIGURATION RELATIVE DIFFERENCES IN % FOR CHARGE SUSTAINING MODE ON TOTAL RDE CYCLE

Gaps**						
B7 to HVO (CS mode)	E10 to E20 (CS mode)	E10 to B7 (CS mode)	PHEV to HEV (B7)	PHEV to HEV (E10)	Lab to road (B7 CS)	Lab to road (E10 CS)
rel [%]	rel [%]	rel [%]	rel [%]	rel [%]	rel [%]	rel [%]

FC		6.64	3.55	-26.66	-0.03	-0.18	16.97	13.06
FC _{corr} *		8.43	4.50	-32.55	0.46	-1.38	29.10	13.56
CO ₂	CVS	-3.65	0.73	-15.51	-0.02	-0.18	16.79	13.00
CO _{2,corr} *		-2.03	1.64	-22.30	0.46	-1.39	28.90	13.50
GHG		-1.94	1.48	-20.48	0.43	-1.39		
UF	share of distance engine off	0.48	-2.98	-20.65	-2.94	-3.34	-0.55	9.25
E Wheel net	Vreal	-0.03	-0.08	-0.34	0.37	0.34	-3.82	-4.82
E Wheel +	Vreal	-0.44	-0.22	2.04	-3.08	-3.28	-13.89	-16.85
E Wheel -	Vreal	-1.05	-0.45	5.87	-8.31	-9.10	-29.12	-36.19
EC		-5.94	-12.14	80.15	9.84	23.06	-47.17	-7.10
EC+		-0.65	-4.21	-11.32	-6.41	-8.79	4.05	-6.76
EC-		-2.24	-5.59	4.59	-1.54	-3.25	-11.30	-6.82
NOx EO	raw gases	0.35	4.97	-84.47	-1.68	-1.29		
NOx TP	raw gases	16.49	-71.51	-16.50	-0.47	42.75	46.71	-50.36
NOx Eff		-0.20	0.17	-1.05	-0.01	-0.11		
NOx TP	CVS	1.91	-63.54	-31.70	-13.52	30.39		
CO EO	raw gases	-24.44	0.87	-92.57	-4.35	-0.54		
CO TP	raw gases	-59.06	113.29	-74.82	-14.34	-2.17	1941.20	261.65

		Gaps**						
		B7 to HVO (CS mode)	E10 to E20 (CS mode)	E10 to B7 (CS mode)	PHEV to HEV (B7)	PHEV to HEV (E10)	Lab to road (B7 CS)	Lab to road (E10 CS)
		rel [%]	rel [%]	rel [%]	rel [%]	rel [%]	rel [%]	rel [%]
CO Eff		1.08	-0.78	-1.65	0.30	0.02		
CO TP	CVS	-42.21	94.35	-65.29	-10.27	5.70		
HC EO	raw gases	-54.03	45.41	-88.52	-21.16	1.28		
HC TP	raw gases	-28.04	13.91	-79.73	5.29	-15.54		
HC Eff		-0.75	0.22	-1.05	-0.37	0.18		
HC TP	CVS	-32.14	9.25	-86.67	24.57	1.98		
SPN23 EO	raw gases	-29.01	341.43	19806.15	-1.49	1.66		
SPN23 TP	raw gases	246.03	32.97	-82.75	-32.71	-5.24	48.43	-19.49
SPN23 Eff		-0.13	52.27	81.67	0.01	8.46		
SPN23 TP	CVS							
SPN10 EO	raw gases	-24.87	260.43	4915.88	-1.03	-16.25		
SPN10 TP	raw gases	221.25	26.94	-82.21	-30.74	-6.34		
SPN10 Eff		-0.12	7.36	12.12	0.01	-1.02		
SPN10 TP	CVS	219.23	26.66	-82.22	-31.07	-5.76		
PM	soot filter weight	177.10	-30.78	-66.77	-9.97	-36.55		
CH ₄ EO	raw gases	-26.16	31.11	-94.57	-8.70	-1.01		
CH ₄ TP	raw gases	17.69	96.64	-15.93	106.46	-12.99		
CH ₄ Eff		-24.70	-1.08	-33.02	-61.07	0.25		
CH ₄ TP	CVS	-40.19	29.11	-5.18	63.54	10.20		
CH ₄ TP (CO ₂ eq)	raw gases	17.69	96.64	-15.93	106.46	-12.99		
	CVS	-40.19	29.11	-5.18	63.54	10.20		
NH ₃ EO	raw gases	-96.34	19.98	-52.80	-42.47	-39.12		

		Gaps**						
		B7 to HVO (CS mode)	E10 to E20 (CS mode)	E10 to B7 (CS mode)	PHEV to HEV (B7)	PHEV to HEV (E10)	Lab to road (B7 CS)	Lab to road (E10 CS)
		rel [%]	rel [%]	rel [%]	rel [%]	rel [%]	rel [%]	rel [%]
NH ₃ TP	raw gases	8.99	-31.78	2611.66	-6.48	-6.50		
NH ₃ Eff								
NH ₃ TP	CVS							
N ₂ O EO	raw gases	6.50	1.20	-68.45	5.77	-1.39		
N ₂ O TP	raw gases	0.74	-21.04	223.44	-0.83	-2.35		
N ₂ O Eff								
N ₂ O TP	CVS							
N ₂ O TP (CO ₂ eq)	raw gases	0.74	-21.04	223.44	-0.83	-2.35		
	CVS							
Urea	calculation for command signal	-6.08			-2.53		13.88	

8. APPENDIX - ANALYTICAL MODEL COEFFICIENTS

8.1. ENERGY CONSUMPTION

Cycles	C300e Consumptions regressions							
	Electricity CD			Fuel CD		Fuel CS		
	kWh/100km	kWh/100km /°C Δ Bat+Cab	kWh/100km /°C Δ Env	L/100km	L/100km /°C Δ Eng	L/100km	L/100km /°C Δ Cab+Eng	L/100km /°C Δ Env
'roadType1-roadConditions1'	29.9	1.51	1.138	0.0	0.000	7.0	-0.010	0.257
'roadType1-roadConditions5'	22.4	0.61	0.451	0.0	0.000	5.8	0.013	0.140
'roadType1-roadConditions7'	22.3	0.45	0.282	0.0	0.017	5.8	0.015	0.108
'roadType2-roadConditions1'	24.9	0.76	0.553	0.0	0.000	6.1	0.012	0.161
'roadType2-roadConditions5'	23.3	0.40	0.221	0.0	0.018	5.8	0.018	0.108
'roadType2-roadConditions6'	24.0	0.53	0.278	1.8	0.064	7.6	0.016	0.099
'roadType2-roadConditions7'	19.6	0.22	0.126	0.4	0.013	5.7	0.020	0.054
'roadType3-roadConditions1'	24.2	0.48	0.416	0.0	0.008	6.0	0.006	0.097
'roadType3-roadConditions2'	20.8	0.23	0.107	0.5	0.008	5.8	0.021	0.061
'roadType3-roadConditions3'	23.1	0.18	0.105	0.1	0.011	5.7	0.020	0.045
'roadType3-roadConditions4'	20.8	0.15	0.073	0.5	0.011	6.0	0.022	0.029
'roadType3-roadConditions6'	21.9	0.09	0.191	2.0	0.098	7.3	0.030	0.037
'roadType3-roadConditions7'	22.6	0.12	0.101	1.5	0.029	7.4	0.029	0.026
'roadType4-roadConditions1'	23.7	0.30	0.153	0.0	0.013	5.9	0.016	0.059
'roadType4-roadConditions2'	21.8	0.16	0.136	0.0	0.003	5.7	0.021	0.037
'roadType4-roadConditions3'	22.6	0.13	0.064	1.0	0.021	6.9	0.025	0.023
'roadType4-roadConditions4'	26.2	0.11	0.065	0.2	0.027	7.2	0.026	0.020
'roadType4-roadConditions5'	26.6	0.12	0.069	1.4	0.026	8.4	0.028	0.016
'roadType4-roadConditions7'	32.5	0.12	0.026	2.2	0.035	10.5	0.042	0.013

Cycles	C300de Consumptions regressions							
	Electricity CD			Fuel CD		Fuel CS		
	kWh/100km	kWh/100km /°C Δ Bat+Cab	kWh/100km /°C Δ Env	L/100km	L/100km /°C Δ Eng	L/100km	L/100km /°C Δ Cab+Eng	L/100km /°C Δ Env
'roadType1-roadConditions1'	29.8	1.51	1.137	0.0	0.000	5.6	0.004	0.293
'roadType1-roadConditions5'	22.1	0.61	0.449	0.0	0.001	4.6	0.024	0.162
'roadType1-roadConditions7'	21.8	0.45	0.288	0.0	0.023	4.4	0.027	0.134
'roadType2-roadConditions1'	24.6	0.76	0.553	0.0	0.000	4.8	0.024	0.190
'roadType2-roadConditions5'	22.7	0.40	0.226	0.1	0.029	4.5	0.027	0.122
'roadType2-roadConditions6'	23.2	0.54	0.304	1.6	0.047	5.8	0.030	0.117
'roadType2-roadConditions7'	19.2	0.23	0.130	0.3	0.017	4.3	0.029	0.069
'roadType3-roadConditions1'	23.7	0.51	0.404	0.0	0.011	4.4	0.028	0.132
'roadType3-roadConditions2'	20.3	0.24	0.114	0.5	0.012	4.4	0.028	0.070
'roadType3-roadConditions3'	22.9	0.21	0.069	0.1	0.009	4.5	0.027	0.056
'roadType3-roadConditions4'	20.5	0.15	0.090	0.4	0.011	4.7	0.027	0.039
'roadType3-roadConditions6'	20.9	0.37	0.113	1.8	0.058	5.7	0.030	0.041
'roadType3-roadConditions7'	21.6	0.45	-0.019	1.3	0.026	5.9	0.033	0.021
'roadType4-roadConditions1'	23.2	0.29	0.172	0.0	0.019	4.5	0.030	0.085
'roadType4-roadConditions2'	22.0	0.18	0.093	0.0	0.005	4.6	0.025	0.043
'roadType4-roadConditions3'	22.2	0.12	0.078	1.0	0.025	5.5	0.028	0.026
'roadType4-roadConditions4'	26.8	0.07	0.073	0.0	0.043	5.8	0.030	0.021
'roadType4-roadConditions5'	25.6	0.12	0.085	1.4	0.026	6.9	0.033	0.016
'roadType4-roadConditions7'	62.8	-0.39	0.394	0.9	0.007	9.8	0.140	-0.027

8.2. UTILITY FACTORS

Cycles	C300e Utility Factors regressions					
	CD			CS		
	%	%/°C ΔBat +Cab+Eng	%°C ΔEnv	%	%/°C ΔBat +Cab+Eng	%°C ΔEnv
'roadType1-roadConditions1'	100%	2.1E-18	-6.7E-18	89%	2.9E-04	-4.3E-03
'roadType1-roadConditions5'	100%	-1.5E-05	2.8E-06	82%	-1.6E-04	-4.1E-03
'roadType1-roadConditions7'	102%	-2.9E-04	-8.3E-04	79%	-3.1E-04	-4.0E-03
'roadType2-roadConditions1'	100%	8.4E-18	-5.5E-18	80%	-4.6E-05	-4.1E-03
'roadType2-roadConditions5'	102%	-2.5E-04	-1.1E-03	70%	-1.6E-04	-4.9E-03
'roadType2-roadConditions6'	97%	-1.7E-04	-7.8E-04	79%	-1.9E-04	-4.1E-03
'roadType2-roadConditions7'	99%	3.1E-05	-1.4E-03	49%	-1.3E-04	-2.7E-03
'roadType3-roadConditions1'	103%	-3.9E-04	2.7E-05	61%	-5.5E-05	-3.7E-03
'roadType3-roadConditions2'	97%	9.8E-05	-1.3E-03	49%	-2.5E-04	-3.0E-03
'roadType3-roadConditions3'	102%	-2.4E-04	-1.8E-03	35%	-3.6E-04	-2.1E-03
'roadType3-roadConditions4'	97%	-3.1E-05	-1.2E-03	17%	-1.1E-04	-1.5E-03
'roadType3-roadConditions6'	94%	-5.7E-04	-1.9E-03	42%	4.2E-05	-1.7E-03
'roadType3-roadConditions7'	92%	-2.5E-04	-6.6E-04	19%	-2.7E-04	-7.1E-04
'roadType4-roadConditions1'	105%	-6.0E-04	-2.3E-03	43%	2.3E-04	-2.9E-03
'roadType4-roadConditions2'	102%	-1.9E-04	-2.2E-04	15%	-2.3E-04	-3.5E-04
'roadType4-roadConditions3'	89%	1.9E-04	-1.6E-03	20%	-3.9E-04	-6.7E-04
'roadType4-roadConditions4'	99%	-1.4E-04	-3.3E-03	13%	-3.7E-05	-3.8E-04
'roadType4-roadConditions5'	85%	-1.5E-04	-2.6E-04	10%	-1.1E-04	-1.1E-04
'roadType4-roadConditions7'	85%	-4.7E-04	-1.5E-04	5%	3.6E-08	-1.6E-08

Cycles	C300de Utility Factors regressions					
	CD			CS		
	%	%/°C ΔBat +Cab+Eng	%°C ΔEnv	%	%/°C ΔBat +Cab+Eng	%°C ΔEnv
'roadType1-roadConditions1'	100%	-3.9E-18	-1.3E-17	89%	1.3E-04	-5.0E-03
'roadType1-roadConditions5'	100%	-2.1E-05	3.7E-06	81%	-3.2E-04	-5.1E-03
'roadType1-roadConditions7'	103%	-3.9E-04	-6.9E-04	77%	-3.8E-04	-5.4E-03
'roadType2-roadConditions1'	100%	7.4E-18	-6.6E-18	78%	-2.0E-04	-5.2E-03
'roadType2-roadConditions5'	104%	-4.9E-04	-1.1E-03	68%	-4.6E-04	-5.9E-03
'roadType2-roadConditions6'	96%	-1.1E-04	-8.8E-04	73%	2.0E-04	-8.7E-03
'roadType2-roadConditions7'	100%	-2.1E-04	-1.1E-03	42%	-6.5E-04	-2.7E-03
'roadType3-roadConditions1'	103%	-3.9E-04	-1.0E-04	56%	-2.3E-04	-4.1E-03
'roadType3-roadConditions2'	98%	-7.1E-05	-1.1E-03	46%	-7.3E-04	-4.3E-03
'roadType3-roadConditions3'	102%	-1.7E-04	-1.9E-03	33%	-7.3E-04	-2.2E-03
'roadType3-roadConditions4'	98%	-1.2E-04	-6.7E-04	14%	-4.2E-04	-8.1E-04
'roadType3-roadConditions6'	94%	-8.2E-04	-2.3E-03	42%	-5.5E-04	-1.8E-03
'roadType3-roadConditions7'	94%	-7.4E-04	-1.4E-03	19%	-3.5E-04	-5.9E-04
'roadType4-roadConditions1'	107%	-1.0E-03	-1.7E-03	38%	-6.1E-04	-2.8E-03
'roadType4-roadConditions2'	102%	-3.3E-04	-3.4E-04	14%	-3.0E-04	-2.0E-04
'roadType4-roadConditions3'	87%	2.2E-04	-1.9E-03	20%	-3.4E-04	-6.9E-04
'roadType4-roadConditions4'	113%	-1.8E-03	-3.6E-03	13%	-4.9E-05	-3.9E-04
'roadType4-roadConditions5'	83%	-1.3E-04	-2.7E-04	10%	-8.9E-05	-1.0E-04
'roadType4-roadConditions7'	68%	-1.0E-02	1.2E-02	5%	-6.5E-04	2.8E-04

8.3. TEMPERATURE DEVIATION PROGRESSION

Cycles	C300e temperature deviations regressions					
	Δ Cabin	Δ Battery	Δ Engine CD	Δ Engine CS		
	$^{\circ}\text{C}/\text{km}$	$^{\circ}\text{C.kWh}/\text{km}$	$^{\circ}\text{C}/\text{km}$	$^{\circ}\text{C}/\text{km}$	$^{\circ}\text{C}/\text{km} / ^{\circ}\text{C } \Delta\text{Eng}$	$^{\circ}\text{C}/\text{km} / ^{\circ}\text{C } \Delta\text{Env}$
'roadType1-roadConditions1'	5.0E-01	5.8E+00	0.0E+00	3.2	0.080	0.202
'roadType1-roadConditions5'	2.0E-01	2.4E+00	3.7E-03	1.8	0.143	0.160
'roadType1-roadConditions7'	1.5E-01	1.8E+00	1.9E-01	1.5	0.166	0.122
'roadType2-roadConditions1'	2.5E-01	2.9E+00	0.0E+00	0.9	0.165	0.176
'roadType2-roadConditions5'	1.4E-01	1.7E+00	2.3E-01	1.3	0.180	0.115
'roadType2-roadConditions6'	1.8E-01	2.2E+00	1.6E+00	2.1	0.229	0.095
'roadType2-roadConditions7'	8.1E-02	1.0E+00	6.2E-01	3.1	0.163	0.049
'roadType3-roadConditions1'	1.9E-01	2.2E+00	5.3E-02	3.5	0.187	0.063
'roadType3-roadConditions2'	7.8E-02	1.0E+00	7.4E-01	1.6	0.184	0.061
'roadType3-roadConditions3'	6.4E-02	9.2E-01	2.0E-01	2.7	0.156	0.037
'roadType3-roadConditions4'	4.8E-02	7.1E-01	7.0E-01	3.2	0.178	0.019
'roadType3-roadConditions6'	6.8E-02	1.1E+00	1.6E+00	3.2	0.221	0.022
'roadType3-roadConditions7'	4.5E-02	7.9E-01	1.4E+00	3.5	0.216	0.017
'roadType4-roadConditions1'	1.0E-01	1.3E+00	1.8E-01	4.0	0.179	0.032
'roadType4-roadConditions2'	5.3E-02	7.6E-01	3.7E-02	2.6	0.179	0.018
'roadType4-roadConditions3'	3.9E-02	6.7E-01	1.2E+00	3.2	0.209	0.006
'roadType4-roadConditions4'	3.9E-02	6.9E-01	5.8E-01	3.3	0.237	0.005
'roadType4-roadConditions5'	3.5E-02	6.7E-01	1.5E+00	3.0	0.259	0.003
'roadType4-roadConditions7'	3.1E-02	1.0E+00	2.0E+00	7.7	-0.002	-0.100

Cycles	C300de temperature deviations regressions					
	Δ Cabin	Δ Battery	Δ Engine CD	Δ Engine CS		
	$^{\circ}\text{C}/\text{km}$	$^{\circ}\text{C.kWh}/\text{km}$	$^{\circ}\text{C}/\text{km}$	$^{\circ}\text{C}/\text{km}$	$^{\circ}\text{C}/\text{km} / ^{\circ}\text{C } \Delta\text{Eng}$	$^{\circ}\text{C}/\text{km} / ^{\circ}\text{C } \Delta\text{Env}$
'roadType1-roadConditions1'	4.9E-01	5.8E+00	0.0E+00	1.7	0.061	0.234
'roadType1-roadConditions5'	2.0E-01	2.4E+00	3.3E-03	2.8	0.040	0.148
'roadType1-roadConditions7'	1.5E-01	1.8E+00	1.1E-01	3.1	0.036	0.128
'roadType2-roadConditions1'	2.5E-01	2.9E+00	0.0E+00	1.7	0.071	0.178
'roadType2-roadConditions5'	1.4E-01	1.7E+00	1.5E-01	3.3	0.032	0.117
'roadType2-roadConditions6'	1.8E-01	2.2E+00	1.2E+00	2.8	0.089	0.094
'roadType2-roadConditions7'	8.1E-02	1.0E+00	3.3E-01	3.7	0.028	0.071
'roadType3-roadConditions1'	1.9E-01	2.2E+00	4.3E-02	3.6	0.022	0.112
'roadType3-roadConditions2'	7.8E-02	1.0E+00	4.3E-01	3.7	0.034	0.071
'roadType3-roadConditions3'	6.4E-02	9.1E-01	1.2E-01	4.0	0.032	0.054
'roadType3-roadConditions4'	4.8E-02	7.1E-01	3.8E-01	4.3	0.033	0.036
'roadType3-roadConditions6'	6.9E-02	1.3E+00	1.2E+00	4.0	0.070	0.012
'roadType3-roadConditions7'	4.7E-02	1.3E+00	1.0E+00	9.6	-0.111	-0.167
'roadType4-roadConditions1'	1.0E-01	1.3E+00	1.0E-01	3.8	0.032	0.080
'roadType4-roadConditions2'	5.3E-02	7.6E-01	2.9E-02	4.2	0.025	0.042
'roadType4-roadConditions3'	3.9E-02	6.6E-01	8.4E-01	4.3	0.057	0.008
'roadType4-roadConditions4'	3.9E-02	6.8E-01	2.4E-01	4.4	0.069	-0.003
'roadType4-roadConditions5'	3.5E-02	6.6E-01	1.1E+00	3.5	0.129	-0.010
'roadType4-roadConditions7'	3.7E-02	2.0E+00	8.2E-01	7.2	0.019	-0.125

Concawe
Boulevard du Souverain 165
B-1160 Brussels
Belgium

Tel: +32-2-566 91 60
Fax: +32-2-566 91 81
e-mail: info@concawe.org
<http://www.concawe.eu>

ISBN 978-2-87567-157-8



9 782875 671578 >